

GEOLOGICAL AND STRUCTURAL  
INTERPRETATION OF SOUTH–EAST VOLTAIAN BASIN,  
GHANA, USING AIRBORNE GRAVITY AND  
MAGNETIC DATASETS

By  
KNUST

VICTOR MENSAH

(BSc. Geomatic Engineering)

A Thesis Submitted to the Department of Physics, Kwame Nkrumah University of  
Science and Technology in partial fulfillment of the requirements for the  
degree of

MASTER OF PHILOSOPHY (GEOPHYSICS)

College of Science

Supervisor: Dr. Kwasi Preko

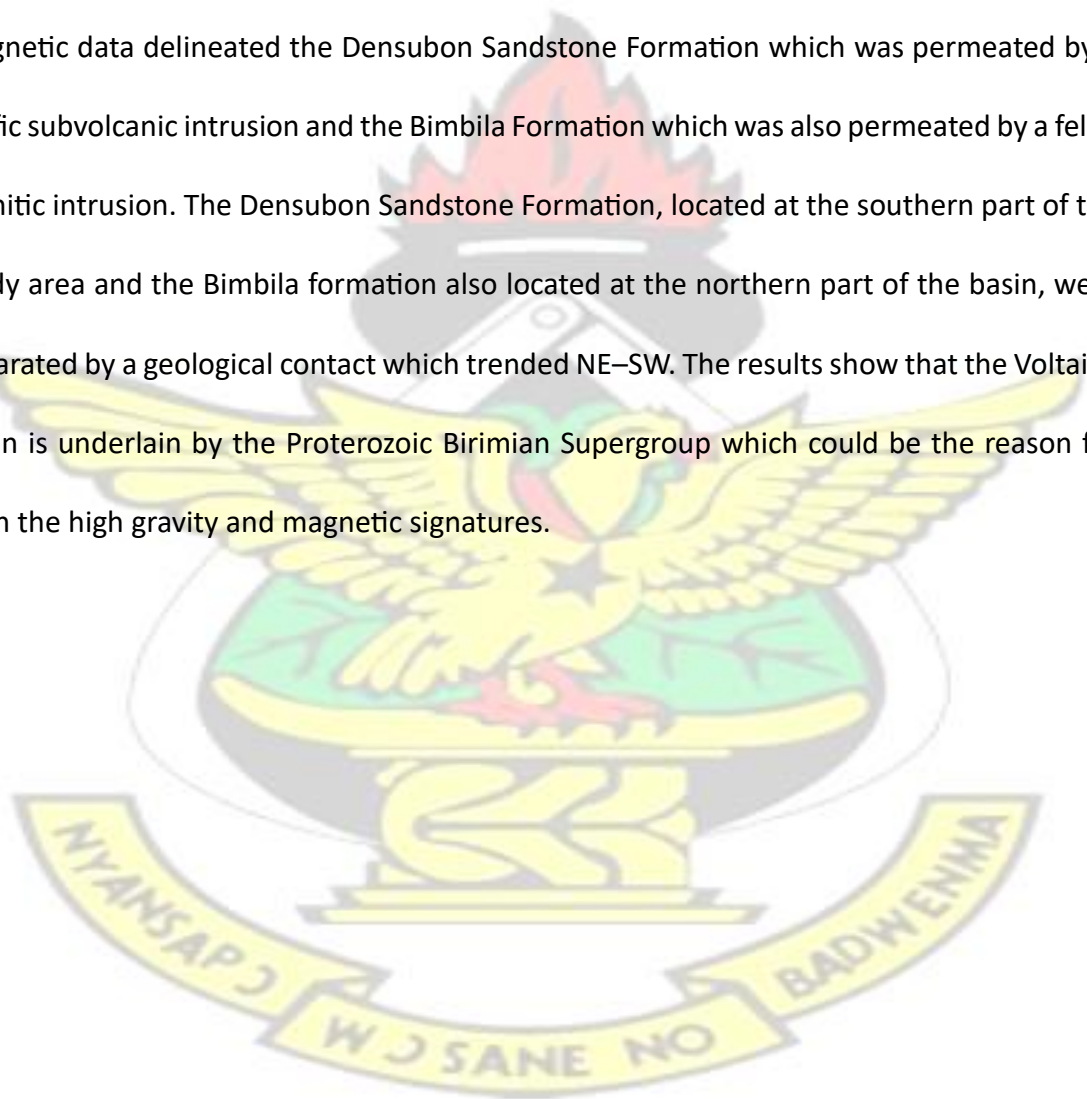
© Department of Physics

September 27, 2015



# Abstract

Airborne gravity and magnetic methods were used to interpret the geology of the south eastern Voltaian, Ghana. The study was aimed at mapping lithologies and geological structures responsible for any observed anomaly in the Area. The enhancement filters applied were used to reduce signal-to-noise ratio. The high-resolution airborne gravity and magnetic data delineated the Densubon Sandstone Formation which was permeated by a Mafic subvolcanic intrusion and the Bimbila Formation which was also permeated by a felsic granitic intrusion. The Densubon Sandstone Formation, located at the southern part of the study area and the Bimbila formation also located at the northern part of the basin, were separated by a geological contact which trended NE-SW. The results show that the Voltaian Basin is underlain by the Proterozoic Birimian Supergroup which could be the reason for both the high gravity and magnetic signatures.



# Contents

Declaration		i
Abstract		ii
List of Tables		vii
List of Figures		viii
List of Symbols and Acronyms		viii
Acknowledgements		xi
1 INTRODUCTION	1	
1.1 Introduction	1	
1.2 Literature Review	4	
1.3 Research Problem Definition	7	
1.4 Objectives of the Research	9	
1.5 Thesis Layout	9	
2 GEOLOGICAL SETTING OF STUDY AREA	11	
2.1 Birimian Supergroup	13	
2.2 The Tarkwaian Formation System	15	
2.3 Voltaian Basin	16	
2.3.1 Bombouaka Supergroup	17	
2.3.2 Pendjari–Oti Supergroup	18	
2.3.3 Obosum or Tamale Supergroup	18	
2.3.4 The Togo Series	20	
2.3.5 Buem Structural Unit	21	
2.3.6 The Dahomeyide System	22	

3 THEORETICAL BACKGROUND OF GEOPHYSICAL METHODS USED	24
3.1 Gravity	24
3.1.1 The Earth's Gravity Field	25
3.1.2 Basic Theory	26
3.1.3 Basis of the Gravity Method	27
3.1.4 Measurement of Gravity	28
3.1.4.1 Absolute Measurement	29
3.1.4.2 Relative Measurement	29
3.1.5 Variations of Gravity with Latitude	30
3.1.6 The International Gravity Standardisation Net 1971	31
3.1.7 Densities of Rocks and Minerals	31
3.1.8 Airborne Gravity Survey	33
3.1.9 Data Filtering and Enhancement	34
3.1.9.1 Bouguer Anomaly Map	35
3.1.9.2 Regional-Residual Separation	35
3.1.9.3 Upward and Downward Continuation (UC and DC)	37
3.1.9.4 Vertical Derivatives	39
3.2 Magnetism of the Earth	39
3.2.1 Nature of the Geomagnetic Field	40
3.2.2 The Earth's Magnetic Field	41
3.2.3 The International Geomagnetic Reference Field (IGRF)	43
3.2.4 Magnetic Susceptibility	44
3.2.5 Magnetism of Rocks and Minerals	46

3.2.6	Aeromagnetic Survey .....	47
3.2.7	Lithology, Structure and Magnetism .....	48
3.2.8	Data Enhancement Techniques .....	50
3.2.8.1	Fourier Transform Filters .....	50
3.2.8.2	Reduction-to-the-Pole .....	51
3.2.8.3	Analytic Signal .....	51
3.2.8.4	Vertical Derivative Filter .....	52
3.2.8.5	Total Horizontal Derivative .....	52
3.2.8.6	Upward and Downward Continuation .....	53
4 MATERIALS AND METHODS .....		54
4.1	Description of Study Area .....	54
4.1.1	Location .....	54
4.1.2	Physiography and Drainage .....	55
4.1.3	Vegetation .....	56
4.1.4	Climate Conditions and Occupation of Inhabitants .....	56
4.2	Data Acquisition .....	57
4.2.1	Metadata .....	59
4.3	Data Processing .....	60
4.3.1	Processing of Gravity Data .....	61
4.3.2	Complete Bouguer Anomaly (CBA) .....	62
4.3.3	Processing of Aeromagnetic Data .....	62
4.3.3.1	Diurnal Variation Removal .....	63
4.3.3.2	Geomagnetic Reference Field Removal .....	63

4.3.3.3	Effect of Height Variations .....	64
4.3.3.4	Leveling Data .....	64
4.3.3.5	Tie Line Leveling .....	65
4.3.3.6	Interpolation .....	65
4.3.4	Gridding .....	66
4.3.5	Regional–Residual Separation .....	68
4.3.6	Enhancement of Gravity and Magnetic Datasets .....	68
4.3.7	Reduced–to–Pole .....	70
4.3.8	Vertical and Horizontal Derivative Filter .....	70
4.3.9	Downward and Upward Continuation (DC and UC) .....	71
4.3.10	Low–Pass Filter .....	72
4.3.11	Analytic Signal Amplitude .....	73
5	RESULTS AND DISCUSSIONS .....	74
5.1	Digitized Elevation Map (DEM) .....	74
5.2	Maps generated from Airborne Gravity Survey .....	76
5.2.1	Complete Bouguer Anomaly (CBA) Map .....	76
5.2.2	Residual Map .....	77
5.2.3	Summary of Geology of the area .....	79
5.3	Maps generated from Aeromagnetic Survey .....	81
5.3.1	Total Magnetic Intensity Map .....	81
5.3.2	Reduction–to–Pole Map .....	83
5.3.3	Analytic Signal Map .....	86
5.3.4	First Vertical Derivative (1VD) Map .....	88

5.4	Summary .....	90
5.5	Proposed Geological Map of the Study Area from Airborne Gravity and Magnetic Datasets .....	91
5.6	Proposed Geological Map compared with Existing Geological Map of the Study Area .....	93
<b>6 CONCLUSION AND RECOMMENDATIONS</b>		<b>96</b>
6.1	Conclusion .....	96
6.2	Recommendations .....	97
<b>REFERENCES</b>		<b>99</b>
A	Used Softwares .....	111
A.1	Used Softwares .....	111

## List of Tables

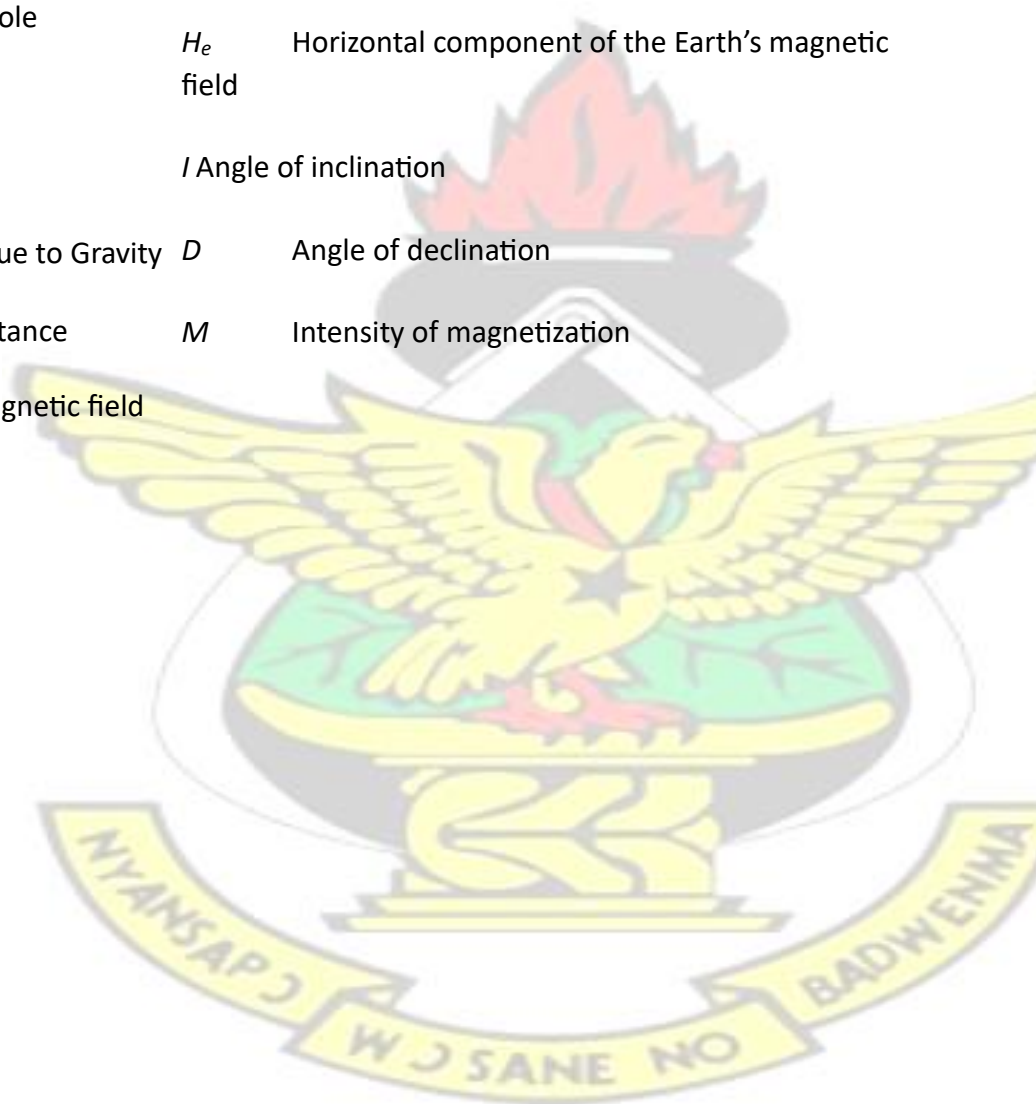
2.1	Comparison of lithostratigraphical scheme proposed by Affaton et al. (1991) and Affaton (2008) .....	20
4.1	Parameters for Airborne Geophysical Survey (Geological Survey of Ghana, 1998) .....	60

# List of Figures

2.1	Geological map of Ghana, with the Voltaian Basin highlighted.(Ghana, Geological Survey, 2009) .....	13
3.1	Earth's Magnetic Field Elements (Whitham, 1960) .....	43
4.1	Location and accessibility of the study area (modified from Ghana Shapefiles)	55
4.2	Diagram showing flight line path during data acquisition .....	59
5.1	Digitized Elevation Map (DEM) of Study Area .....	75
5.2	Complete Bouguer Anomaly (CBA) Map of Study Area .....	77
5.3	Residual Map of Study Area .....	78
5.4	Interpreted Geological Map from Airborne Gravity Data .....	80
5.5	Total Magnetic Intensity (TMI) Map of Study Area .....	83
5.6	Reduced-to-Pole (RTP) Map of Study Area .....	85
5.7	Analytic Signal Map of Study Area .....	87
5.8	First Vertical Derivative of RTP Map of Study Area .....	89
5.9	Interpreted Geological Map from Aeromagnetic Dataset .....	91
5.10	Proposed Geological and Structural Map of the Study Area .....	92
5.11	Proposed Geological Map of Study Area .....	94
5.12	Existing Geological Map of the Study Area .....	94

# List of Symbols and Acronyms

$\kappa$	Magnetic susceptibility	$h$	Applied external field
	Continuation Height	$\pi$	pi
$F$	Force	$mGal$	MilliGal
$G$	Gravity	c.g.s	centi gram second
$CBA$	Complete Bouguer Anomaly	$J_r$	Remanent magnetization
$1VD$	First Vertical Derivative	$J_i$	Induced magnetization
$DEM$	Digital Elevation Map	WGS84	World Geodetic System 1984
$UP$	Upward Continuation	$UTM$	Universal Transverse Mercator
$TMI$	Total Magnetic Intensity	$Z_e$	Vertical component of the Earth's magnetic field
$RTP$	Reduced-to-Pole	$H_e$	Horizontal component of the Earth's magnetic field
$m_1$	Mass	$I$	Angle of inclination
$m_2$	Mass	$D$	Angle of declination
$g$	Acceleration due to Gravity	$M$	Intensity of magnetization
$r$	Separation Distance		
$F_e$	The Earth's magnetic field		



# Acknowledgments

My first thanks and heartfelt gratitude goes to the Almighty God for His unprecedented mercies and grace towards me throughout the duration of this work. I honestly thank my supervisor Dr. Kwasi Preko for his encouragement, motivation, technical advice and criticism that helped me to the end of this project. To Dr. M. K. E. Donkor I say God richly bless you for the support in Linux and Latex platform I used. I appreciate all the lecturers who took me through the geophysics programme and to Emmanuel H. Tetteh, Issahaku Jakalia Sontaa and Benjamin Boadi who shared their knowledge and time on this project I say God bless you. This work would not have been possible without the supports of Mr. Nana Takyie Kyeremeh (Production Geophysicist, Newmont Ghana Limited) who gave me the Oasis Montaj (Geosoft) training and some technical advice; Mr. Nana Takyie Kyeremeh, I say God richly bless you. I am also grateful to the administration of Geological Survey Department, Accra, for granting the datasets. I would also like to thank all the MPhil. students of Physics Department for their support. My final thanks go to my family members, especially my parents, Mr. Victor Mensah and Mrs. Ethel Mensah who understand and had hope in me; I really appreciate your supports in diverse ways.

# CHAPTER 1

## INTRODUCTION

### 1.1 Introduction

Exploration geophysics, in the past few decades, has played a very significant role in trying to understand the structure of tectonic movements, regions of platforms and geosynclinal areas as well as for the identification of structures capable of oil and gas accumulation. Geophysics extensively applies physical principles, estimations and theories for the investigations of the earth's properties. Geophysical methods, sometimes called indirect observation methods, does not give a "photo" of what is beneath the surface of the Earth but instead proposes a sub-surface model derived from the interpretation of the distribution of different physical parameters. There are several geophysical methods which include gravity, magnetics, seismics and radiometric and these give data on the distribution of certain physical parameters such as density, magnetic susceptibility, electrical conductivity and radioactivity in the sub-surface which can be used to provide various solutions to several geological problems as well as structural mapping. These physical properties and formation of diverse rock types driven by distinctive physical and chemical compositions of the Earth differ from one area to another (Roy, 1966). Controlled by the prevalent physical properties of the distinctive rock types, suitable geophysical methods can possibly help in the identification of the geology as well as mapping geological structures liable to have advanced in a specific area (Afenya, 1982). Despite the fact that all these

methods are ground-based, airborne surveys can also be achieved using some of these geophysical methods.

The Earth Scientists use airborne geophysics as a powerful technique for rapidly carrying out investigations over very vast areas. The Earth's expansive view from the perspective of the airborne geophysics has been very much perceived subsequent to the beginning of military reconnaissance and balloon photography (Dobrin and Savit, 1988). Airborne methods, contrasted with ground-based techniques, has the advantage to remotely survey very large areas and difficult terrains in very short periods of time hence, making it very cost effective.

According to Murphy (2007), three principal airborne geophysical techniques exist utilizing magnetic, electromagnetic, and radiometric procedures while airborne gravity, which is the fourth technique, has likewise been accepted from the past decade or so. Airborne gravity and aeromagnetic surveys are used extensively as reconnaissance tools in hydrocarbon and mineral exploration. Thus, both survey methods have surficial discontinuities perceived by the regular correspondence of linear anomalies to surficial evidence of faulting across the area. The resolution of geophysical datasets have further improved due to advances in data analysis, processing and image enhancement techniques and therefore exceptionally unobtrusive variations in the geophysical responses can be distinguished.

Airborne Gravity survey is a very regular type of geophysical method which employs the use of a gravity sensor installed on a moving platform and measures the sum of the gravity and inertial acceleration of the system in the aircraft. This can be employed in areas where density contrasts exist in a geological structure, and the standard methodology is to measure differences in gravity from place to place. Airborne gravity prospecting usually

deals with lateral differences in Earth structure, since these include lateral contrasts in density.

Gravity was initially carried out in the Gulf of Mexico for the prospecting of salt domes, ([www.earthsci.unimelb.edu.au/ES304/](http://www.earthsci.unimelb.edu.au/ES304/)) and later for looking for anticlines in continental areas. Gravity anomalies can result from Anticlines since they produce high or low densities, conveyed closer to the surface. Sedimentary rocks have lower densities than basement rocks and therefore Gravity prospecting helps locate thick enough sedimentary basin for further exploration. Gravity prospecting can only be used for mineral exploration if one expects substantial density variations, e.g., very high densities are attributed to chromite bodies. Also, relatively low densities are attributed to gold or uranium which may be contained within buried channels.

An aeromagnetic survey makes use of a magnetometer attached to an aircraft (airplane or helicopter) which is flown over the area on interest and most common aircraft magnetometers measure the total intensity of the magnetic field, but not its direction, along continuous flight lines with fixed distances apart. Koulomzine et al. (1970), indicates that the resulting magnetic map shows the Earth's magnetic field strength variations which are caused by magnetic minerals (most regularly, magnetite) in the upper crust of the Earth. Magnetic maps permit a visualisation of the geology as well as geological structures of the Earth's upper crust. This is especially very supportive in places where the bedrock is masked by water, surface sand or soil. The apparent contrasts in the magnetic value's intensity (hills, ridges and valleys) perceived on the interpreted data are attributed to magnetic anomalies for which a mathematical modelling can be used to ascertain the shape, depth and properties of the rock bodies responsible for these anomalies. The Earth's magnetic field,

particularly considering the percentage of magnetite in the rocks, is directly affected by geological structures, geological composition and magnetic minerals. It has been made feasible to map sedimentary basin structures and lithologies, fracture systems and lineaments, geological faults and magnetic anomaly targets because of the advancements in instrumentation as well as data processing techniques.

## 1.2 Literature Review

According to Kesse (1985), Airborne geophysical surveys in Ghana to prospect for radioactive minerals was first carried out in 1952. However, continuous developments were made to the techniques used in airborne geophysical methods in the 1980s and 1990s, including an evolution to digital technology and refinement of the survey procedures. Major applications of airborne geophysics in the previous decade have seen an increase in prominence for environmental, and engineering applications, including hazard mapping (Murphy, 2007). Furthermore, Reeves (1989) indicates that it was just within recent decades that airborne geophysical datasets were accepted as an effective tool in geological mapping. Direen et al. (2001) indicates that airborne geophysical data, on a regional scale, have frequently been used to determine various distinctive attributes, such as: limits of geologic regions, fold belts, sedimentary basin as well as tectonic and structural details of shear zones and overprinted structural trends.

Integrating gravity data together with magnetic, gamma-ray or seismic datasets in interpretation has demonstrated to be exceptionally helpful in geological and structural mapping (Chandler, 1990; Gunn et al., 1997). The analytic signal of the total magnetic

intensity was applied by Asadi and Hale (1999) to define the intermediate composition of magmatic rocks in the Takab area of Iran. Chandler (1990) utilized the second vertical derivative enhanced–aeromagnetic data together with gravity data to carry out an interpretation of the geology of the central region of the poorly exposed Duluth Complex.

Geological controls were established from secluded outcrops and the well–mapped surrounding areas. Gunn et al. (1997) affirmed that correlating magnetic data with seismic reflection data has revealed that geological structures mapped in sedimentary rocks in northern Australia are indeed present. Evidence from Finland likewise demonstrates high level of correlation between the outcome from aeromagnetic data and bedrock structure (Airo and Karell, 2001). Kesse (1985) reported that outcomes from the 1960 magnetic survey by Hunting Survey Limited over the Ashanti belt were very gratifying. Geological interpretation which was frequently based on the magnetic maps was confirmed fruitful in characterizing lithologies, faults and fracture zones.

Silva et al. (2003) investigated more on airborne geophysical data processing and the application of several enhancement techniques for exact positioning of geological boundaries. The principal goal was to decree that geophysical anomalies ought not be what we ought to be searching for, but instead the responses identified with mineralisation, lithology, and structures that may have economic significance. Silva et al. (2003) likewise demonstrated that aeromagnetic survey have the capability to distinguish magnetic greestone units; important structures identified with mineralisation and permitted a better understanding of structural geophysical pattern.

Mahanta and Billiton (2003) reported the mapping of coal seam in the Latrobe Valley at the south-eastern part of Australia utilizing airborne gravity gradiometry. The outcomes demonstrated a shallow dip of the seam toward the north-western region under gravel cover, which brought about a gradual decrease in the amplitude of the gravel signal with ordinal thicknesses of this seam around 30–50 m at dips a little below 10°. Greater seam thickness and dip will generally support the detectability of coal seams. Castro et al. (2002) report that a gravity survey was used to determine the three-dimensional geometry and constrain the emplacement mode of the Quixadá granite at depth in the central Ceará domain of the Borborema Province (NE Brazil).

According to Pesonen et al. (2003), a high-resolution airborne geophysical study was carried out over the Lake Bosumtwi impact crater, Ghana. This survey was completed in 1997 by the Geological Survey of Finland in partnership with the University of Vienna, Austria, and the Geological Survey Department of Ghana. A contemporary model of the structure was produced from the magnetic data which showed several magnetic rims, providing indications of the presence of a central uplift. The electromagnetic data also delineated several circular features around the structure. The gamma ray data additionally ended up being shockingly important and obviously pinpointed two ring features, one coinciding with the actual crater rim and the other one marking an outer ring feature (Pesonen et al., 2003)

Metelka (2012) reported that the litho-structural framework in an inadequately unmasked Paleoproterozoic granite-greenstone terrane of Burkina Faso in the West African Craton was created using an integrated interpretation of airborne geophysical data with field structural and lithological observations. Details of the lithological units and structural

features present were sufficiently portrayed by the geophysical data. The results suggested that, the granitoid domains are formed by various small to medium-sized plutons. The presence of cogent formations of magmatic episodes has a critical effect on the advancement of a regional tectonic model. The magnetic data provided a superior definition of the real pluton shapes furthermore reliably distinguished various highly magnetic late-orogenic plutons (Metelka, 2012).

Christensen et al. (2001) indicated that the Cannington silver-lead-zinc deposit would have been identified via airborne gravity gradiometry whilst Lane (2006), established, in a detailed assessment of a Falcon survey over the Broken Hill lead-zinc mine, that the original deposit would have been identified by the survey. Anderson et al. (2006) reported that the same study led to cogent zinc intersections at the Goldfinger target. Bayat (2006), used gravity gradiometry to conduct a model investigation of gold deposits in the greenstone belts of Western Australia's Yilgarn craton and he indicates that airborne gravity gradiometry assumed an extremely valuable role in detecting the low density weathered zones connected with these deposits. According to Nelson et al. (2004) airborne gravity gradiometry was successfully applied in structural mapping in the Papua New Guinea fold belt which is an area where exploration on the surface is difficult and expensive due to "jungle cover rugged topography and paucity of roads" make. Rose et al. (2006) also reported the fruitful mapping of an Eocene channel in a Falcon survey over a part of the Gippsland Basin which is Australia's main domestic oil source. O'Brien et al. (2005) also investigated the successful use of Full Tensor Gradiometer (FTG) data in a 3D inversion constrained by seismic data to compute the base of the K2 salt body in the Gulf of Mexico down to depths of 20,000 feet.

### 1.3 Research Problem Definition

Airborne gravity and magnetic datasets have, in the past, been used widely in the survey of extensive areas, as a means to map out the basins including basement structures. These methods have frequently been used as a forerunner to seismic surveys and as a means to highlight possible target areas for oil traps which are controlled stratigraphically or structurally. In Ghana, various airborne geophysical studies have been carried out including gravity and magnetics to delineate the various distinctive geological attributes over the entire country.

The oil and gas industry contributes significantly to the development of Ghana in so many important ways. Basically, it provides the country with foreign exchange as well as increasing the rate of employment. It also contributes to the build up of the internal economy of the country through payment of taxes and duties by the investors (Kesse, 1985). Earlier research within the research area has described the Voltaian basin as the largest onshore sedimentary basin in Ghana with high prospects for oil and gas accumulation. From the known stratigraphy of the basin, it is envisaged that the Variegated and Lower Greenish grey shales of the Oti Group (Bozhko, 2008) may constitute potential source rocks. The Lower Voltaian sandstones and limestones could serve as reservoirs and Middle Voltaian shales as potential seals. Compressional features, faults and stratigraphic features could serve as traps to complete the petroleum system elements required for commercial accumulation of hydrocarbons. Identifying structures hosting hydrocarbons will help demarcate the best areas to carry out further studies for oil and gas exploration. Just a little endeavour has so far been made to comprehend the correlation between structural features observed on the ground and those that extend into the subsurface.

The purpose of this research is therefore to undertake a geophysical interpretation of the study area using airborne gravity and aeromagnetic datasets to identify and delineate the subsurface structures associated with the basin, which are capable of holding oil and gas. A new and detailed geological map would be produced depicting magnetic units as well as dense structures.

## 1.4 Objectives of the Research

The primary goal of this research is to undertake a geological interpretation of the study area utilizing airborne geophysical datasets, specifically, gravity and magnetic data. Specific objectives are in twofold, namely;

- Map the lithology of the study area.
- Map geological structures responsible for any observed anomalies.

## 1.5 Thesis Layout

This Thesis has six (6) chapters with each chapter attempting to address a major heading. Chapter one introduces the field of research and the geophysical techniques that are applied in the research, it further deal with the objectives of the research, importance and the justification fo the research objectives. Furthermore, this chapter contains the literature review and the structure of the complete thesis work.

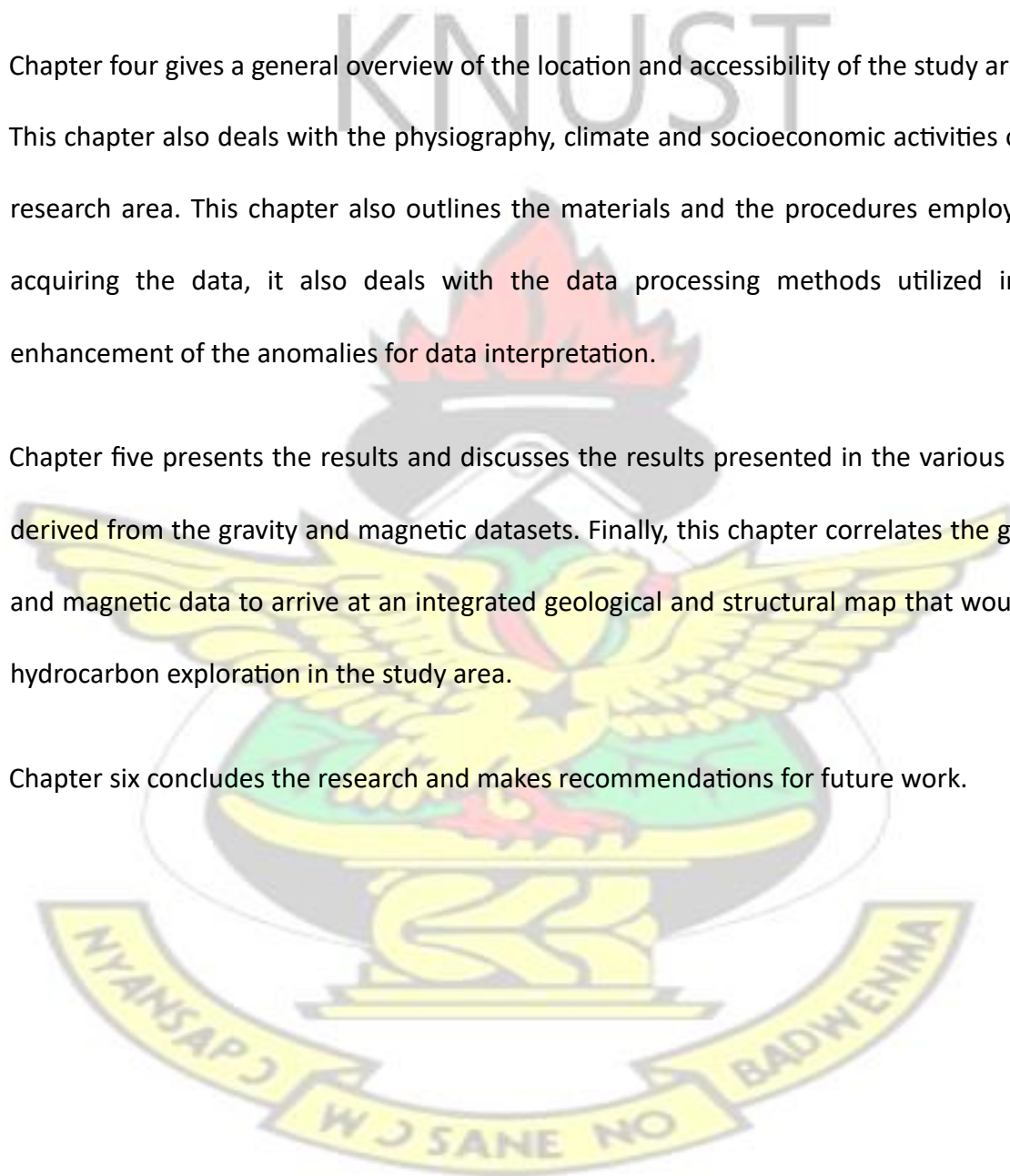
Chapter two gives a general overview of the regional and local geological settings of the study area.

Chapter three outlines the theoretical background of gravity and magnetic methods, taking into consideration some enhancement techniques that can be applied to gravity and magnetic data.

Chapter four gives a general overview of the location and accessibility of the study area. This chapter also deals with the physiography, climate and socioeconomic activities of the research area. This chapter also outlines the materials and the procedures employed in acquiring the data, it also deals with the data processing methods utilized in the enhancement of the anomalies for data interpretation.

Chapter five presents the results and discusses the results presented in the various maps derived from the gravity and magnetic datasets. Finally, this chapter correlates the gravity and magnetic data to arrive at an integrated geological and structural map that would aid hydrocarbon exploration in the study area.

Chapter six concludes the research and makes recommendations for future work.



## CHAPTER 2

### GEOLOGICAL SETTING OF STUDY AREA

Most part of Ghana lies within the West African Craton which was preserved in the proterozoic (2000 Ma) amid the Eburnean Orogeny. This structural deformation further strengthened the Zaire Craton and affected enormous parts of Western Africa and neighbouring regions in South America that were coextensive with the Eburnean tectono-thermal province. Apart from South Africa, the West African Craton is actually the second largest region in Africa where, predominantly, lower Proterozoic rocks are widely preserved. These early Proterozoic rocks encompasses broad belts of metamorphosed volcanic and sedimentary rocks that can be located in Ghana, Niger, Burkina Faso and Cote d'Ivoire. The Craton is bordered on the eastern and western sides by the late Proterozoic mobile belts (700 to 500 Ma) and is also called the Pan African mobile belts (Kesse, 1985; Wright, 1985; Leube et al., 1990). Key (1992) indicates that about 40% of Sub-Saharan Africa is dominated by Precambrian basement rocks which supports about 235 million rural inhabitants. The rocks predominantly comprise of crystalline igneous and metamorphic rocks. The study area falls within the Sene-Obosom River Basin and the Lake Volta. The Obosum group is the dominant rock formation prevalent with the neighbourhood (Deynoux et al., 2006). Crowe and Jackson-Hicks (2008), indicate that the faults and fractures in the area are associated with iron oxide alteration, that is very magnetic, and silicification. Majority of the structures trend east-west, along the south-western part of the District and rotate to a NNE-SSW trend locally connecting with and reactivating basement structures along the Sefwi Belt, for instance, the Pru fault (Crowe and Jackson-Hicks, 2008).

The geology of Ghana (Fig.2.1) is controlled predominantly by metavolcanic Paleoproterozoic Birimian sequences and the clastic Tarkwaian in the central west and northern parts of the country. The eastern part of the country is covered by clastic shallow water sediments of the Neoproterozoic Voltaian basin. Along the coast, a small strip of Paleozoic and Cretaceous to Tertiary sediments exist likewise at the extreme south-eastern part of the country. According to Hastings (1983), Ghana can be divided into three main geological terranes which are:

1. an early Proterozoic terrane (Birimian System) and the Tarkwaian system of the main West African shield which hosts majority of the the mineral deposits in the country and occupies the west and north of the country;
2. a pan African mobile belt which covers the Togo, Dahomeyan and Buem Formations, distinguished from the Birimian terrane by a famous topographic feature known as the Akwapim–Togo range and occupies the eastern and south-eastern parts of the country; and
3. the Voltaian Basin, in which the late precambrian to Paleozoic sediments that mantle the craton are preserved and are situated at the east and central parts of the country.

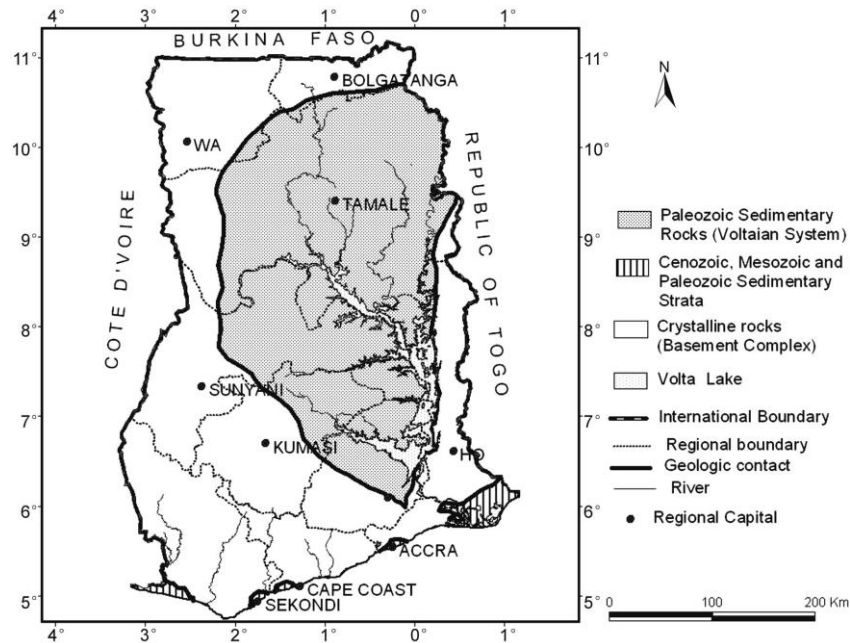


Figure 2.1: Geological map of Ghana, with the Voltaian Basin highlighted. (Ghana, Geological Survey, 2009)

## 2.1 Birimian Supergroup

The most important Paleoproterozoic units are extensive sediments and volcanics, which are generally referred to as the Birimian Supergroup. Most of the northern, southern and western Ghana are underlain by rocks of the Birimian System. Junner (1940), indicates that the Birimian Series in Ghana was long ago divided into two which are:

1. an Upper series of the greenstone, mainly consisting of metamorphosed basic and intermediate lavas and pyroclastic rocks, and
2. a Lower series of mainly sedimentary origin.

Junner (1940) also believed that the Lower Birimian sedimentary packages constitutes classical miogeosynclinal basin sediments, however, the rich volcanic units were believed

to represent eugeosynclinal units. Recent studies by Leube et al. (1990), however, indicates that the sediments and volcanics constituted lateral facies equivalents. This was supported by the interbedding of the two units, their similar depositional environment and similar geochemistry.

According to Griffis et al. (2002), the Birimian Meta-volcanic formations were divided into:

1. an upper Basic Volcanic Subseries,
2. a middle Acid Volcanic Subseries, and
3. a lower Sedimentary-Volcanic Subseries that included tuffaceous greywackes, quartzite, conglomerates and grits.

Hirdes et al. (1988), indicate that the the type of rocks occurring in the Birimian Meta-sedimentary Belts are greywackes with turbidite features, phyllites, slates, schists, weakly metamorphosed tuffs and sandstones. Some of the phyllites contain pyrite, and finely divided carbonaceous matter is present in most of them. Silicification is common in the phyllites, particularly towards the boundary with the Upper Birimian. The Birimian Meta-volcanics consists of lava flows and dyke rocks composed of basalts and andesine. There has been a metamorphoses of most of these rocks to hornblende actinolite-schists, calcareous chlorite schists and amphibolites (the greenstones). Felsic volcanic rocks also occur in the Meta-volcanic belts and mainly in sedimentary sections. The felsic units include dacitic pyroclastic rocks, minor andesitic and rhyolite flows, and undifferentiated volcanogenic sediments. The volcanics are permeated by minor intrusions of mafic and ultramafic rocks cut in some places. Leube et al. (1990) indicate that volcanoclastic sediments transpires

within the basaltic flows of all volcanic belts. Metamorphism in most volcanic rocks is limited to the chlorite zone of the green–schist facies. Amphibolite–facies assemblage occurs intermittently but along, especially, the margins of granitoid units.

## 2.2 The Tarkwaian Formation System

According to Kesse (1985), the Tarkwaian Formation consists of rocks that are concentrated mainly at the south–western part of Ghana in the Tarkwa area where they outcrop in a north–east to south–west trending belt. The Birimian is overlain by the Tarkwaian which is a Proterozoic supracrustal system. It is mainly made up of shallow water sediments which exist in all the Birimian Meta–volcanic belts Junner (1940). It is composed of coarse clastic sedimentary rocks with conglomerates, arkoses, sandstones and minor amounts of shale. Eisenlohr and Hirdes (1992), indicate that the Tarkwaian is mostly considered as the detritus of Birimian rocks that were uplifted and eroded following the Eburnean tecto–thermal event. Economically, the Banket series is the most vital unit of the Tarkwaian, which encompasses economic concentrations of gold in various area.

The age of the Tarkwaian Formation has been the focus of recent research by Davis et al. (1994) and Hirdes and Nunoo (1994). The age of deposition of the Tarkwaian Formation can be classified by:

- the youngest zircon grain from the lowermost Kawere series and;
- the age of the authigenic rutile formed after the deposition.

These dates give a time range of 2096 to 2132 Ma.

## 2.3 Voltaian Basin

The Voltaian basin is a structural basin which represents a sedimentary series of stable shelf deposits of a late Precambrian geosynclinal system, which prior to the break-up of the African and South American continents in pre-Cretaceous time, probably extended across present day northwest Africa and Ghana into Brazil. The Voltaian basin forms a Neoproterozoic to Early Palaeozoic, largely clastic sedimentary fill in an intracontinental basin. In Ghana, approximately one third of the landmass is covered by sediments of the inland Voltaian basin, which correlates to an area of approximately 103,600 km<sup>2</sup> and comprises of sediments that are mostly level lying or very gently dipping, and rest on a dominant Precambrian unconformity (Griffis et al., 2002). This unconformity denotes an erosional surface, which seemingly covered the whole Man Shield. The Voltaian basin Formation underlies the northern part of the Volta Region, central and eastern sections of both Northern and Brong-Ahafo Regions and the north-eastern parts of the Ashanti and Eastern Regions. The heterogeneous Voltaian basin is made up of mudstone, limestones, shales, conglomerate, sandy and pebbly beds and sandstones. As indicated by Hoffman (1999), the Voltaian basin area looks as if it was the eastern margin of a massive West African cratonic block which had split away from the previous supercontinent Rodinia. This block merged with other cratonic blocks and resulted in a new supercontinent, Gondwana, during the Pan-African thermo-tectonic event (approximately 600–550 Ma). Kennedy (1964), indicates that along the eastern margin, the sedimentary rocks were folded at the time of orogenic activity associated with a late Precambrian to early Paleozoic thermal event, the Pan-African Thermo-Tectonic Episode.

Several geological researches have been undertaken in the Voltaian basin beginning from the early days of the preceding Gold Coast Geological Survey. Only limited areas were ultimately covered, but Junner (1940) offered a more comprehensive assessment of the stratigraphy on a regional basis and established an Upper, Middle and Lower series of units. The Lower series is eclipsed by shallow marine, quartz-rich sediments and a basal conglomerate. The Middle Voltaian involves a large diversity of sandstones and shales with some conglomerate interbeds, a few carbonate sequences and clastic units predominantly classified as glacial tillites. The Upper series is almost constrained to the central and eastern regions of the basin and it is prevailed by massive, quartz-rich sandstones.

According to Kesse (1985), more comprehensive stratigraphic studies have revised the division of the Voltaian basin sediments unobtrusively and endeavoured to more appropriately define the regional tectonic setting and stratigraphic correlations. The Voltaian basin constitutes three main disconformable lithostratigraphic units defined as megasequences or supergroups (Deynoux et al., 2006) : They are the Bombouaka (or Gambaga), Oti (or Pendjari), and Tamale (or Obosum) megasequences.

### 2.3.1 Bombouaka Supergroup

The current stratigraphy includes the lower Bombouaka (or Gambaga) Supergroup and shows detrital and epicontinental characteristics. Its thickness is in the vicinity of about 1000 m and is eclipsed by matured sandstones and a central part of siliceous and clay-units. The Bombouaka and Kwahu groups were deposited during a post-Kibaran phase of crustal downwarping within the supercontinental of Rodinia. Though separated geographically,

they are considered to be equivalent in age. Both groups form prominent scarp and dip slope features which are particularly well seen along the north and south margins of the basin. The Bombouaka Group commences with quartz arenites.

### 2.3.2 Pendjari–Oti Supergroup

The succeeding Pendjari (or Oti) Megasequence is unconformable with the underlying Gambaga sediments and is also considerably thicker (average is about 2500 m). The Pendjari sediments encompass a peculiar lower sequence with tillite and sandstones, carbonate, and silexite which are fine-grained cherty sediments. The Pendjari also comprises thick sequences of less matured clastic sediments exhibitiv of a deeper marine depositional environment, apparently on a passive continental margin. The unconformity marking the base of the Pendjari-Oti Group represents a time-gap of some 350 million years duration. In reality, the tillites rests on the Birimian basement at certain places and signify extensive local erosion and gouging by Neoproterozoic glaciers that apparently correlate with similar events in several other regions of Africa and probably signify a dominant, worldwide glacial event (Hoffman, 1999).

### 2.3.3 Obosum or Tamale Supergroup

According to Affaton et al. (1991), the Obosum Megasequence is the youngest group of sediments in the Voltaian basin which are evident only in Ghana. The thickness of this series is approximately 500 m and features a basal portion of sediments that as well comprise glacial tillites. Affaton et al. (1991) indicate that these are dominated on the top by cross-

bedded quartz with shale and mudstones below that are interpreted to signify a foreland molassic basin developed along the western margins of a major, Pan–African mountain chain (the Dahomeyides). The early and middle sequences in the Volta Basin records a transition from epicontinental seas to deeper marine sedimentary environments along a passive continental margin (Kesse, 1985). This was followed by eastward subduction of oceanic crust beneath a central African crustal block and eventual collision, which led to the Pan–African Dahomeyide orogenic fold belt (approximately 600 Ma) and the build–up of Tamale Supergroup molassic sediments derived from the fold belt. Faulting and folding has divided the group into two separate outcrops, each containing different facies associations. North of the Pru Fault, the group is largely undivided and mainly made up of variegated mudstones and siltstones interbedded with micaceous sandstones; an association perhaps representing overbank or lacustrine environments located at a distance from the main distributary systems and thus only able to receive sediment sporadically. Below is a table showing a comparison of litho–stratigraphical scheme proposed by Affaton et al. (1991) and Affaton (2008).

Table 2.1: Comparison of lithostratigraphical scheme proposed by Affaton et al. (1991) and Affaton (2008)

Affaton et al. 1991		Affaton, 2008		
Obosum Group		Tamale Supergroup	Kebia Group	Kebia Formation
				Salaga Formation
				Sang Formation
		Yendi Group		
Pendjari Group	Pendjari Formation	Pendjari-Oti Supergroup	Oti–Pendjari Formation	
	Kodjari		Sud-Banboli	Barkoissi Formation

	Formation	('Afram Supergroup')	Group	Sud-Banboli Formation
Dapango- Bombouaka Group	Panabako Formation	Bombouaka Supergroup	Bombouaka	Panabako Formation
	Poubougo Formation		Group	Bogou Formation
			Fosse-aux-Lions Group	Kotiare Formation
	Tossiegou Formation			Dapaong Group
			Group	Korbongou Formation

#### 2.3.4 The Togo Series

The southeastern part of Ghana is dominated by a series of largely North-East trending units, more or less in fault contact with Voltaian basin sediments, Birimian metamorphics, and Eburnean granitoids. The Togo Series is a fault-bounded, irregular belt of metamorphic units that encompass the Akwapim hill and ridges which begins from just the northern and western parts of Accra and stretches along the Ghana-Togo border and into the Atacora Range which is at the northern part of Benin. The Togo Series is mostly dominated by metamorphosed sediments (phyllite, chlorite schist, marble, and quartzite) but meta-volcanics are as well present.

#### 2.3.5 Buem Structural Unit

As defined by Affaton (2008), the Buem Structural Unit contains rocks that crop out within the northerly extension of the Akwapim mountain range. This strongly folded and thrust-

imbricated topography forms part of the Pan–African 'Dahomeyide' orogenic belt. Affaton et al. (1991), indicates that it constitutes the westernmost part of the Dahomeyide, which includes quartzitic rocks that have long been thought to represent the highly faulted and folded equivalents of the older Volta Basin strata exposed in the Kwahu Plateau area. Although this correlation was mainly based on lithological characteristics, it is supported by comparisons between detrital zircon and spectra of sandstones from the Volta Basin and Buem Structural Unit (Kalsbeek et al., 2008). Kesse (1985), further indicates that the Buem Formation is composed of a thick lower series of clastic sediments at the western part, with some carbonate and tillite units preceding the clastics and volcanics that comprise mafic flow units and pyroclastics. Although unmetamorphosed, the sequences are highly folded and faulted so as to obscure their relationships with the nearby Voltaian sediments and the more highly metamorphosed Togo Formation. According to Dapaah-Siakwan and Gyau-Boakye (2000), the upper part of the Buem Formation are formed from rocks of volcanic origin and comprises tuff, lava, and agglomerate interbedded with shale, sandstone, and limestone. Kesse (1985) states that the rocks of the Buem Formation are strongly folded with several faults and therefore estimating the average thicknesses for the various series becomes very difficult. However, the volcanics and closely related clastics have an estimated thickness of approximately 5000 m and the basal clastic series are of the same order. The folds are expressed as chevron folds but are not properly developed and in the finest grained material (Kesse, 1985). Towards the west, large–scale thrusting is included in the deformation in the Buem Formation. Several events of serpentinized ultramafic bodies are closely related with the thrust sheets (Wright, 1985). The Buem Formation was widely believed to be older than the Voltaian basin sediments by early workers in the region (Kesse, 1985). As indicated further by Affaton et al. (1991), the Buem

Formation is apparently a lateral equivalent to the Pendjari Megasequence of the Voltaian basin. The mafic and ultramafic units apparently denotes tectonically emplaced slices of paleo–oceanic crust involved in the suturing of adjacent continental blocks during the Pan–African orogeny (Griffis et al., 2002).

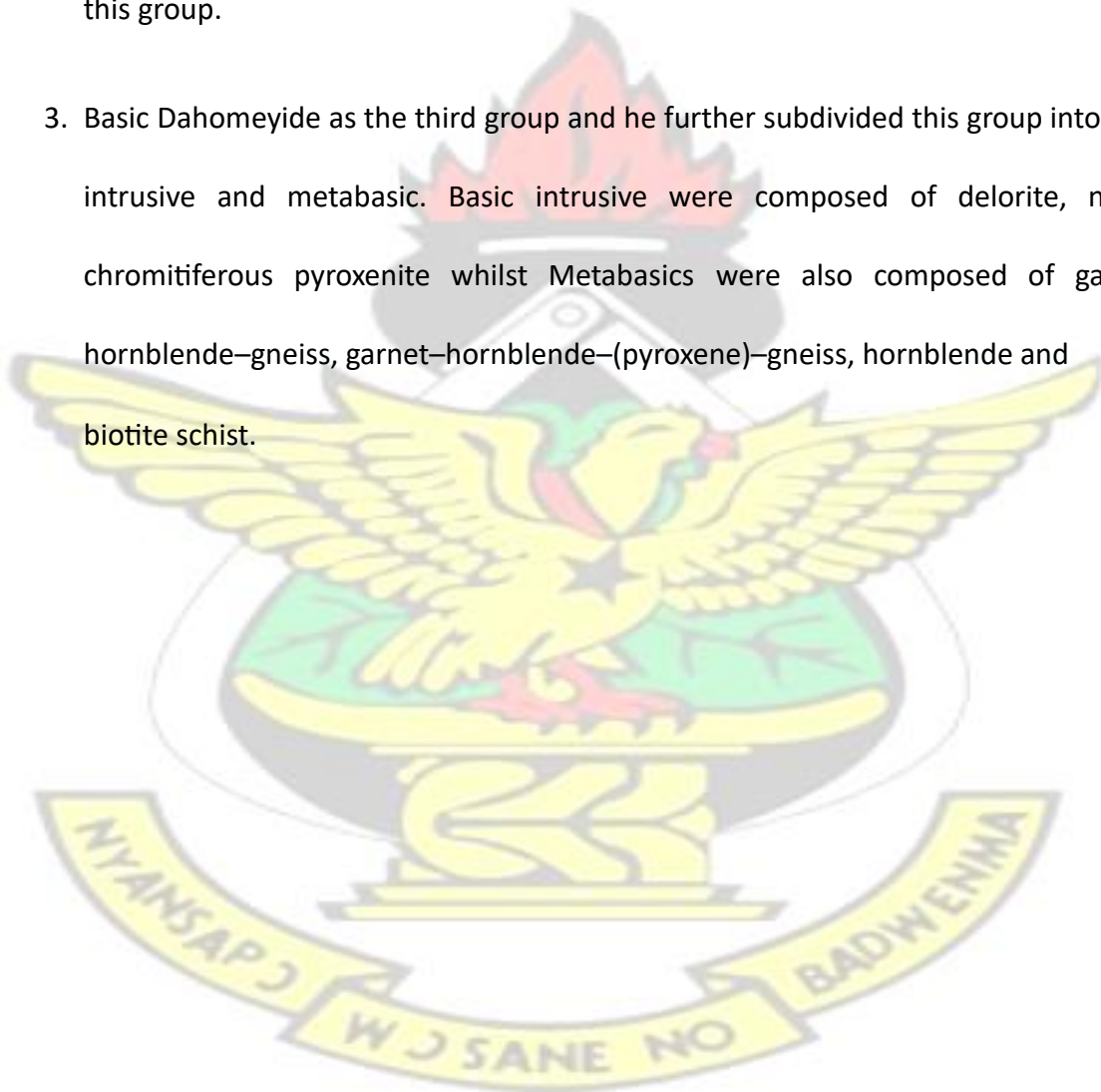
### 2.3.6 The Dahomeyide System

The Dahomeyide System underlies the eastern and south–eastern part of Ghana and also forms a section of the second major tectono–stratigraphic terrane. Kennedy (1964), indicates that the Dahomeyide system transpires as four alternate belts of acid and basic gneiss which trends SSW to NNE from the coastal plains and extends into Togo. The Dahomeyide system has a strongly bimodal lithological layering defined at regional scale by alternating outcrops of mesocratic and leucocratic gneiss. In Ghana, the easternmost rock unit is the Dahomeyan and it can considerably be distinguished from other rocks in that it is comprised of high grade metamorphic rocks. Four lithologic belts of granitic and mafic gneiss makes up the Dahomeyide system. According to Holm (1974), the mafic gneisses are comparatively uniform oligoclase, hornblende, andesine, salite and garnet gneisses of igneous origin and predominantly of tholeiitic composition. Intruded in the Dahomeyide are granites, nephelinesyenite and dikes of several compositions (Kennedy, 1964). The age and nature of the Dahomeyide metamorphics have always been a mystery. The high degree of metamorphism led early workers in the region to quite reasonably suggest the Dahomeyide to be old Archean basement. However, with the advent of isotopic age–dating and a better understanding of plate–tectonics, it was understood that the Dahomeyides were largely the

product of the Pan–African orogeny with most age–dates within the range 600 – 500 Ma.

Mani (1978), classified the Dahomeyide Stratigraphy into threefolds which are:

1. Acid Dahomeyide with pegmatite, aplite, quartz veins, Cape Coast granite, granitic gneiss and migmatite, granite, and gneiss as rocks of this type.
2. Alkalic Gneiss with Kpong conglomerate and nepheline gneiss as some rock types in this group.
3. Basic Dahomeyide as the third group and he further subdivided this group into basic intrusive and metabasic. Basic intrusive were composed of delorite, norite, chromitiferous pyroxenite whilst Metabasics were also composed of garnet–hornblende–gneiss, garnet–hornblende–(pyroxene)–gneiss, hornblende and biotite schist.



## CHAPTER 3

### THEORETICAL BACKGROUND OF GEOPHYSICAL

#### METHODS USED

#### 3.1 Gravity

Gravity was actually the very first geophysical method to be used in hydrocarbon exploration. The gravity method, even though being marred by seismology, has continued to a vital and sometimes very crucial constraint in many areas of exploration. The principle underlying gravity surveying is based on the fact that it estimates the variations in the gravitational field of the Earth generated by differences in the density of sub-surface rocks and despite colloquially known as the 'gravity method', the variations of acceleration due to gravity is what is actually measured. Minor changes in the gravity field of the Earth originate due to the distinctions in rock density and these minor changes can be measured using a very portable instruments known as gravimeters or gravity meter. Gravity has also historically, played a principal role in the studies of dynamic processes in the Earth's interior and is also important in exploration geophysics.

Gravity measurements have been successfully used for an extensive variety of purposes and at an extensive variety of scales. To mention just a few, understanding the details of the gravity field on a global scale, are very important in military operations which, since World War II, has encouraged interest in much of the research and development in the areas of gravity instrumentation and building of global data bases. Gravity has also been extensively

used on an exploration scale, for both hydrocarbon and mineral exploration, and even at the reservoir scale for the development of hydrocarbons. In exploration, the use of gravity has actually involved all kinds of targets, originating with the use of the torsion balance in exploring for salt domes, particularly in the U.S. Gulf Coast. Gravity is still extensively used as an exploration tool in the mining industry to both map the geology of the subsurface and also help in the estimation of ore reserves for some massive sulfide orebodies. In the oil industry, gravity is also generally used in relatively remote areas such as under-explored basins and foothills and to provide a critical limitation for imaging the bottom of allochthonous salt bodies imaged with very long offset seismic ray paths and prestack depth migration which also requires very excellent velocity models. Opfer et al. (1989), also indicate that there is a limited use of gravity measurements as an alternate means of evaluating static corrections for seismic data.

### 3.1.1 The Earth's Gravity Field

The gravity field of Earth is almost similar to that of a sphere with same average radius and total mass but slight increasing in the direction of the poles. Between the polar and equatorial fields, the difference is approximately 0.5% or 50,000 g.u. with the rate of change being zero at the poles and equator and reaching a maximum of about 8 g.u. per kilometer north or south at 45 degrees latitude (Milsom, 2003). The gravity method is based on a natural and ever-present gravitational force field as such, it is said to be a passive method since no active energy source is required as is necessary with seismic and most electrical exploration methods. Obviously, this is an advantage but can also be a disadvantage because the field cannot be modified to suit the particular application. The gravity field of

the Earth varies both spatially and temporally to distort the changes in the anomaly fields caused by local subsurface conditions of interest in gravity surveying although the Earth's gravity field is ever-present. Thus, these variations must be removed from the observed data to produce interpretable measurements.

### 3.1.2 Basic Theory

The gravity force field is caused by the fundamental phenomenon of gravitation that attracts bodies towards each other. Specifically, a mass in the presence of another body, like the Earth, has energy due to the gravitational attraction which is called gravitational potential (Hinze et al., 2013). This energy results in the acceleration of objects towards each other if they are free to move. Hinze et al. (2013), indicate that the force of gravity between objects on the surface of the Earth is not observed because their mass is so much smaller than the Earth's, and thus their attractive effect on each other is negligible. Gravity surveying may be conducted on many scales such as small scale prospecting, regional marine surveys and global satellite surveys. The fundamental equation used for mathematical treatment of the data and results is Newton's Law of Gravitation which states that "The force between two particles of masses  $m_1$  and  $m_2$  is directly proportional to the square of the distance between the centers of mass":

$$F = \frac{Gm_1m_2}{r^2} \quad (3.1)$$

where;  $G = 6.67 \times 10^{-11} \text{Nm}^2/\text{kg}^2(\text{m}^3/\text{kg}\cdot\text{s}^2)$   $F$

= force  $m_1$  and  $m_2$  = mass

$r$  = separation distance

If the Earth were to be a perfect sphere with no lateral inhomogeneities and did not rotate, acceleration due to gravity,  $g$  would be the same everywhere and would obey the formula:

$$g = \frac{GM}{r^2} \quad (3.2)$$

This is however not the case, since the Earth is inhomogeneous and it rotates. The rotation accounts for the Earth to assume the shape of an oblate spheroid with an eccentricity of 1/298. The Earth's polar radius is approximately 20 km less than the equatorial radius, which implies that acceleration due to gravity;  $g$  is approximately 0.4% less at the equator than at the pole. At the equator,  $g$  is approximately 5300 mGal (milliGals).

### 3.1.3 Basis of the Gravity Method

Gravity is measured in N/kg or  $m/s^2$  in SI units but in geophysical exploration, the gal is used in gravity and is equivalent to  $0.01 m/s^2$  in SI units or  $1 cm/s^2$  in CGS units. The gal is however, a large unit compared with the changes in gravity which is as a result of the variations in the subsurface masses of the Earth and as a result, the unit milligal (mGal) is used in geophysical exploration, while in engineering geophysics and other high-sensitivity studies, the microgal is normally used because of the very small magnitude of many of the noteworthy anomalies. The gravity unit (g.u.) is another unit sometimes used in gravity exploration in the petroleum industry but the use of the g.u. should be avoided due to

possible confusion with the unit milligal commonly used in gravity exploration. According to Hinze et al. (2013), the gravity method is focused on measuring and analysing perturbations or anomalies in the terrestrial field which is as a result of lateral variations in density within the subsurface. The gravity field of the Earth also includes spatial variations due to the size, shape, and rotational properties of the Earth and temporal variations related to the differential gravity effects of the Moon and Sun on the Earth. Algermissen (1961), also makes it known that every gravity observation at or near the Earth's surface includes these normal gravity effects, which in the case of spatial variations and some temporal variation are large compared with many geological gravity effects and must be removed from gravity measurements to isolate the gravity effects of subsurface targets for analysis.

#### 3.1.4 Measurement of Gravity

Geodesists measure gravity to determine the shape of the Earth, and geophysicists use the measurements to predict changes in the subsurface Earth and study geophysical phenomena. The requirements in the accuracy of gravity measurements are generally in the milligal range, but an accuracy of one microgal or better has been the target of an increasing number of measurements for near-surface studies, geodetic measurements, and drillhole gravity surveys (Hinze et al., 2013). The measurement of gravity should simply involve determining length and time since gravity is acceleration. Such seemingly simple measurements, however, are not conveniently achieved at the precision and accuracy required in gravity surveying (Keary and Brooks, 1992). Hinze et al. (2013), indicate that obtaining these levels of precision is a remarkable achievement considering that the Earth's

gravity field is roughly 1000 gal, which means the measurement of one part in a billion of the total field is obtainable.

Gravity measurements may either be absolute or relative.

#### 3.1.4.1 Absolute Measurement

The computation of an absolute gravity value is strenuous and depends on complex apparatus and long periods of observation. Such computation is traditionally done employing large pendulums or galling body techniques which can be made with a precision of 0.01 g.u.(Nettleton, 1976). Absolute measurements have been made only on a restricted basis because they are not necessary for exploration purposes and until recently have been more difficult and time-consuming to make and have had a lower accuracy than relative measurements (Hinze et al., 2013). According to Sakuma (1986), absolute gravity measuring instruments in the field were initially cumbersome, expensive and slow to read. Modern absolute measuring instruments have been developed which are devoid of these disadvantages and are expected to be extensively used in years to come (Brown et al., 1999). Absolute gravity measurements provide the exact value of gravity without reference to a station that initially has been observed with an absolute gravimeter. Absolute values are functional in geodetic work, in establishing gravity benchmarks for use with and calibration of relative gravimeters, and in measurements for temporal studies of the Earth's field because they are free of intrinsic drift effects (Hinze et al., 2013). At survey stations, absolute gravity values can be obtained by referring to the International Gravity Standardisation Network (IGSN) of 1971, which is a network of stations whose absolute gravity values have been determined by reference to sites of gravity measurements (Morelli et al., 1972).

#### 3.1.4.2 Relative Measurement

The computation of relative gravity values is easier and is the standard procedure in gravity surveying, which implies differences of gravity between locations. For most purposes, relative gravity measurements are quite satisfactory. Most relative gravimeters today are based on the principle of the inclined zero-length spring sensor in which the lever arm provides mechanical advantage to amplify small relative displacements of the mass (Hinze et al., 2013). According to Keary and Brooks (1992), a relative reading instrument is used to determine the absolute value of gravity at a particular location by simply determining the difference in gravity between a field location and an IGSN station. Relative gravity measurements have been made over much of the attainable land surface of the Earth with gravimeters and over vast areas of the oceans with a combination of satellite-derived measurements and gravimeters mounted in surface ships.

#### 3.1.5 Variations of Gravity with Latitude

The shape of the Earth is one of the many reasons why the value of acceleration due to gravity differs over the Earth's surface. The polar radius (6357 km) is 21 km shorter than the equatorial radius (6378 km). According to Hinze et al. (2013), at the poles, points are nearer to the Earth's centre of mass and consequently, the value of gravity at the poles is greater than at the equator. There is another aspect which is the fact that there is a centrifugal acceleration acting greatest where the rotational velocity is largest, namely at the equator and decreases to zero at the poles and this is due to the fact that the Earth rotates once per sidereal day around its north-south axis. The factors that affect density must be appreciated

in order to aid in the interpretation of gravity dataset since gravity surveying is sensitive to variations in density of rocks.

### 3.1.6 The International Gravity Standardisation Net 1971

According to Morelli et al. (1972) intense efforts were made in the late 1950s and 1960s to develop new global pendulum and spring-based gravimeter ties and to include the new choleric absolute gravimeter measurements in the adjustment. These data were combined and solved synchronously and published as the International Gravity Standardization Net 1971, IGSN-71. Approximately 1,900 global sites were in this network and each site had an approximated standard error of less than  $\pm 50$  microGals, with a correction of  $-14.0$  milliGals at the Potsdam site, nevertheless, corrections at other sites varied (Woollard and Rose, 1963). The IGSN-71 remains the official worldwide gravity datum today eventhough several countries have re-observed the sections of IGSN-71 in their jurisdictions. Apart from finding some errors, various temporal changes resulting from local geologic changes have been determined. Moose and Rockville (1987) indicate that the Potsdam and IGSN-71 datums each have a corresponding formula for the calculation of theoretical gravity which are used in the calculations of Bouguer and other gravity anomalies.

### 3.1.7 Densities of Rocks and Minerals

Gravity prospecting requires the use of density contrasts, that is, the local lateral variations in density in interpretations so appreciating the factors that influence density will greatly help in the interpretation of gravity data. Rock densities vary very little, the least of all

geophysical properties. Density is generally, not measured in situ, however it can be measured by borehole logging tools. Emphasis is made on the fact that the determination of densities in gravity prospecting depends on rocks that are accessible either at the surface, where they may be weathered or dehydrated, or from boreholes, where they may have been subjected to some form of stress relaxation. Density is also a scalar property and is most readily measured to first-order accuracy without sophisticated instruments. However, measurements of the density of many Earth materials are not easy to make accurately, as a result, there is a limited base of high-quality measurements reported in sufficient detail to allow their evaluation and general use (Hinze et al., 2013).

Beneath the water table of the Earth is a saturated zone and all void space is assumed to be filled with liquids, but locally gases may be entrapped or occur in their migration from generation within the Earth to the surface. There are several types of densities which have been identified and are regularly used in reporting on measurements and the various types acknowledge that all terrestrial materials are made up of three phases to a greater or lesser degree: the solid mineral grains, the void spaces, and the void filling material, either liquids or gases or both. The True density of a material is the mass of a unit volume of solid material where the volume excludes the voids in the rock. The Bulk density is the density of a thoroughly dry rock including both the solid material and the void space. The Natural density is the density of a rock with all the pore space, both flow and diffusion, filled with water.

Hinze et al. (2013), indicate that the primary controls on the density of subsurface materials are mineral composition and void space, which are largely dependent on the rock types and the chemical and physical effects of secondary processes including rock fracturing,

solutioning, and chemical alteration of minerals. However, the density of minerals varies from  $1,990\text{kg/m}^3$  for sylvite, the potassium salt, to about  $20,000\text{kg/m}^3$  for gold, but the greater majority of commonly occurring minerals range from  $2,500$  to  $3,500\text{kg/m}^3$ , although ore minerals of metals are in the range of  $4,000$ – $6,000\text{kg/m}^3$ .

Earth materials, for the purpose of considering density, are conveniently classified into crystalline rocks, sedimentary rocks, and unconsolidated sediments. Crystalline rocks comprise both plutonic and volcanic igneous rocks that originate from magma that has solidified respectively within the Earth and at the surface. More so, they include metamorphic rocks derived from both igneous and sedimentary rocks that have been altered deep in the crust by increased lithostatic pressure, tectonic stress and enhanced temperatures. However, unconsolidated sediments comprise fragments derived from erosion of pre-existing rocks that are commonly deposited in water or less commonly in air and by chemical precipitants. Sedimentary rocks are also made up of sediments that have been lithified by lithostatic pressure and chemical precipitants (Johnson and Olhoeft, 1984). In sedimentary rocks, density increases with depth and age, that is, compaction and cementation. More so, in igneous rocks, density increases with basicity, however, granites tend to have low densities and basalts high densities. The density of exposed rocks is often less than that of the same rock at depth, because of weathering and open cracks and because often it is not fully saturated with water; this needs to be appreciated when collecting samples for density measurements for the purpose of interpretation in gravity surveys (Mussett and Khan, 2000).

### 3.1.8 Airborne Gravity Survey

An airborne gravity survey is a common type of airborne geophysical survey that is performed using a gravimeter on board an aircraft. It has a similar principle to a gravity survey performed on land, but allows regional coverage of the Earth's surface for reconnaissance. The airplane flies typically in a grid-like pattern with the resolution of the data being determined by the height and line spacing as well as the cost of the survey for each unit area.

The variations in the in the gravitational field of the Earth are measured by the gravimeter, as the airplane flies, which is influenced by density contrasts of the sub-surface rocks. The idea is based on a "Causative Body", which produces a gravity anomaly. It is possible for geologists to make inferences about the distribution of strata due to a great variation in density among rock types. Changes in the force of gravity at the surface is caused by lateral changes in the subsurface and the intensity of the force of gravity due to a buried mass difference is superimposed on the larger gravitational force due to the total mass of the Earth. This produces a gravity map. Eventhough results may differ between systems, superior gravity data is predominantly acquired at night when survey airplanes can fly in less turbulent conditions. By very precise measurements of gravity and by carefully correcting for the variations in the larger component due to the whole Earth, an airborne gravity survey can sometimes detect man-made or natural voids, variations in the depth to bedrock, and geologic structures which are of interest in engineering. Airborne gravity surveys are also widely used in petroleum and natural gas exploration as well as mineral exploration.

### 3.1.9 Data Filtering and Enhancement

Before interpretation of the datasets, the observed data must be rendered into an alternate structure by filtering or enhancement methods, which is a common first step. A range of linear and non-linear filtering algorithms can be used to enhance airborne geophysical datasets which scrupulously complements the anomalies due to one group of geological sources with respect to anomalies due to other groups of geological sources (Gunn et al., 1997). The aim can be to facilitate the subsequent application of other techniques or data integration. The aim is often to isolate or enhance gravity anomalies of interest in the observed data. Because gravity and magnetic fields are mathematically related, filtering and enhancement techniques are often transferable between them. The effects of selected geological sources can be visually complemented with mathematical enhancement methods which are augmented by a range of imaging procedures. The Fourier transforms serve as a very useful tool in transforming from the frequency domain to the wave number domain and for the computation of derivatives as well (Telford and Sheriff, 1990). Contrarily, few enhancement techniques alter the data, and one ought be mindful so as to guarantee that enhanced datasets are not erroneously used.

#### 3.1.9.1 Bouguer Anomaly Map

According to Hinze et al. (2013) information about the sub-surface density alone will be revealed by the Bouguer anomaly, once the corrections for Free Air and Bouguer have been made and the effect of latitude and elevation have been eliminated. A Bouguer anomaly map depicts a good impression about the density of sub-surface. Low (negative) values of

Bouguer anomaly indicate lower density underneath the measurement point on the surface of the Earth and high (positive) values of Bouguer anomaly also indicate higher density underneath the measurement point.

### 3.1.9.2 Regional–Residual Separation

Anomalies that are of significance are usually superimposed on a regional field due to source being too deep to be of relevance or larger than the scale of study. It is important in this case, as a crucial initial step in data interpretation, to carry out a regional–residual separation. Historically, this problem was approached along two lines by either using a simple graphical approach or by the use of several mathematical methods to be able to arrive at the regional field and many of these classical methods are still commonly used today. The gravity field recorded at the surface of the Earth is the combined effect of the sources at diverse levels. The effect of gravity on sources from the surface downward, at least up to the Moho, is mostly recorded in these surveys. It is essential however, to isolate the observed field originating from various levels (Reeves, 1989). They are generally separated into two broad groups, which are the regional field and the residual field, which originates from deep–seated and shallow–seated sources, respectively. Wellman and Hinze (1985) report that, generally, the regional field is characteristic of the whole region and is sourced from deep–seated bodies, while the residual field is contained to a localised area and originates from shallow–seated sources. Smoothing the fluctuations based on visual inspection is the easiest approach used to separate the regional field from the residual component of the observed field and this method assumes that the values outside the anomalous zone signify a regional field that differs smoothly in the region, while the

residual component demonstrates sharp fluctuations. This approach is most appropriately used along profiles. The graphical method is another method of regional–residual separation, and this method is appropriate for data recorded over a grid. The average of the observed gravity field encompassing a specific grid point is determined and subtracted from the central value, which provides the residual field at that point. Consequently, a new grid is generated at all grid points, which is contoured to obtain the residual anomaly mainly representing shallow sources.

According to Reeves (1989), regional–residual separation can be accomplished by applying a bandpass wavelength filter, but the residual filter, in practical cases, would predominantly be designed to roll-off again at wave numbers relating to noise so that noise could be simultaneously removed. Information from a range of wave numbers which are considered as imperative for the study of the residual anomalies at hand will only be retained by the band-pass filter (Gupta and Grant, 1985). Generally, the better the separation between straight-line branches of the radially averaged power spectrum, the more fruitful the consequent separation into regional and residual components is prone to be. This separation, however, is never impeccable since sources at any depth have a tendency to contribute to all smaller wave numbers in the spectrum to a greater or lesser extent (Hinze et al., 2013). There are still some unresolved problems in the area of regional–residual separation since so many techniques are in exist for regional–residual separation. As such, there is no single “right” answer for how one can highlight the target of interest.

### 3.1.9.3 Upward and Downward Continuation (UC and DC)

A potential field observed in one plane and at a consistent elevation can be recalculated as if the observations were made on an alternate plane, with higher (upward continuation) or lower (downward continuation) altitudes. Upward continuation methods are used in the interpretation of gravity data to investigate the form of the regional gravity variation over a survey area, since the regional field is assumed to originate from generally deep-seated structures. Upwards continuation attenuates the higher wavenumber anomalies related with such features and relatively complements the anomalies of the deeper-seated structures (Keary and Brooks, 1992). Upward continuation utilizes wavelength filtering to simulate the appearance of potential-field maps if the data were recorded at a higher height. Shorter wavelength anomalies are suppressed conversely. Upward continuation is intuitive, as it is easy to understand and avoids the bandpass filtering pitfalls. The bulk structure of the upper crust, where the brittle faults reside, above the brittle-ductile transitions regularly exposed by upward continuing potential field data. According to Reeves (1989), the equation of the wavenumber domain filter which results in upward continuation is simply:

$$F(\omega) = e^{-h\omega} \quad (3.3)$$

where  $h$  is define as the continuation height. This function decays consistently with increasing wavenumber, attenuating the higher wavenumber more extremely, thus producing a map in which the more regional features are predominant.

Downward continuation of potential fields is of more restricted application. The method could be used in the resolution of the separate anomalies introduced by nearby structures whose effects overlap at the level of observation. Higher wavenumber fields are relatively enhanced and the anomalies depict extreme fluctuations if the field is continued to a depth which is greater than that of its causative body. The levels at which these fluctuations begin gives an evaluation of the constraining depth of the anomalous body (Keary and Brooks, 1992). The equation of the wavenumber domain filter to produce downward continuation is

also:

$$F(\omega) = e^{h\omega} \quad (3.4)$$

This is a curve which is zero at zero wavenumber and increases exponentially at higher wavenumbers, thus emphasizing the effect of shallow sources and noise. The viability of this method is diminishing if the potential field is contaminated with noise, since the noise is accentuated on downward continuation (Reeves, 1989). Noise removal is therefore a crucial first step before downward continuation, and continuation depths should not exceed real source depths. In order to obtain acceptable results, some careful experimentation is usually necessary.

#### 3.1.9.4 Vertical Derivatives

Nabighian (1972) indicate that derivatives of the gravity field enhances high frequency fields at the expense of the low frequency components, therefore delineating shallow structures and this technique has been well known with geophysicists. Vertical derivative maps also known as vertical gradient maps emphasize shorter-wavelength components of the

anomaly field at the expense of the longer-wavelengths. The vertical derivative can be considered as the rate of change of anomaly values as the potential field data are continued upward. Such maps are not intuitive, and they may be much difficult than horizontal derivative maps to compare with the original anomaly shapes. However, vertical derivative maps help highlight the details, discontinuities and breaks in anomaly texture (Nabighian, 1972).

### 3.2 Magnetism of the Earth

The application of the magnetic method is underlain by the principle that when the Earth's magnetic field has a ferrous material placed inside it, the ferrous material establishes an induced magnetic field which is superimposed on the field of the Earth at that location which creates a magnetic anomaly. The quantity of magnetic material that exist and its distance from the sensor determines its detection; however, the anomalies are often presented as contour maps or as profiles.

According to Herndon (1996), the Earth's magnetic field is mainly due to the internal and external fields. The internal field which is also referred to as the main field (90%) is global and of internal origin deep within the Earth's interior. The Earth's outer core is assumed to consist of a mixture of iron and nickel which are both good electrical conductors. The inner core of the Earth, according to seismic studies, is of solid form whilst the Earth's outer core comprises a metallic liquid material. Modern theories proposes that the magnetic field of the Earth is due to the of flow of material in the outer core which generates an electrical current which effectively results in a massive electromagnet. The inner core cannot make

any contributions to the Earth's magnetic field since it is above Curie temperature (Clark and Emerson, 1991).

### 3.2.1 Nature of the Geomagnetic Field

The Earth's geomagnetic field, prior to exploration geophysics, consists of three parts (Telford and Sheriff, 1990);

- The main field, which originates from within the Earth and differs relatively slowly.
- The small field (contrasted with the main field), which is of external origin and differs rather rapidly.
- The spatial variation of the main field which are most often lesser than the main field, are almost constant in time and place, and are due to local magnetic anomalies in the near-surface crust of the Earth. These are the targets of interest in magnetic prospecting.

(Telford and Sheriff, 1990) indicates that the geomagnetic field resembles that of a dipole whose north and south magnetic poles are located approximately at  $75^{\circ}\text{N}$ ,  $101^{\circ}\text{W}$  and  $69^{\circ}\text{S}$ ,  $145^{\circ}\text{E}$ . The dipole is displaced about 300 km from the center of Earth toward Indonesia and is inclined some  $11.5^{\circ}$  to the Earth's axis. However, the geomagnetic field is more complicated than the field of a simple dipole. The points where a dip needle is vertical, the dip poles, are at  $75^{\circ}\text{N}$ ,  $101^{\circ}\text{W}$  and  $67^{\circ}\text{S}$ ,  $143^{\circ}\text{E}$ .

### 3.2.2 The Earth's Magnetic Field

The terrestrial magnetic field is the summation of several magnetic components, derived from both within and outside the Earth, which vary spatially and temporally over and above the Earth (Hinze et al., 2013).

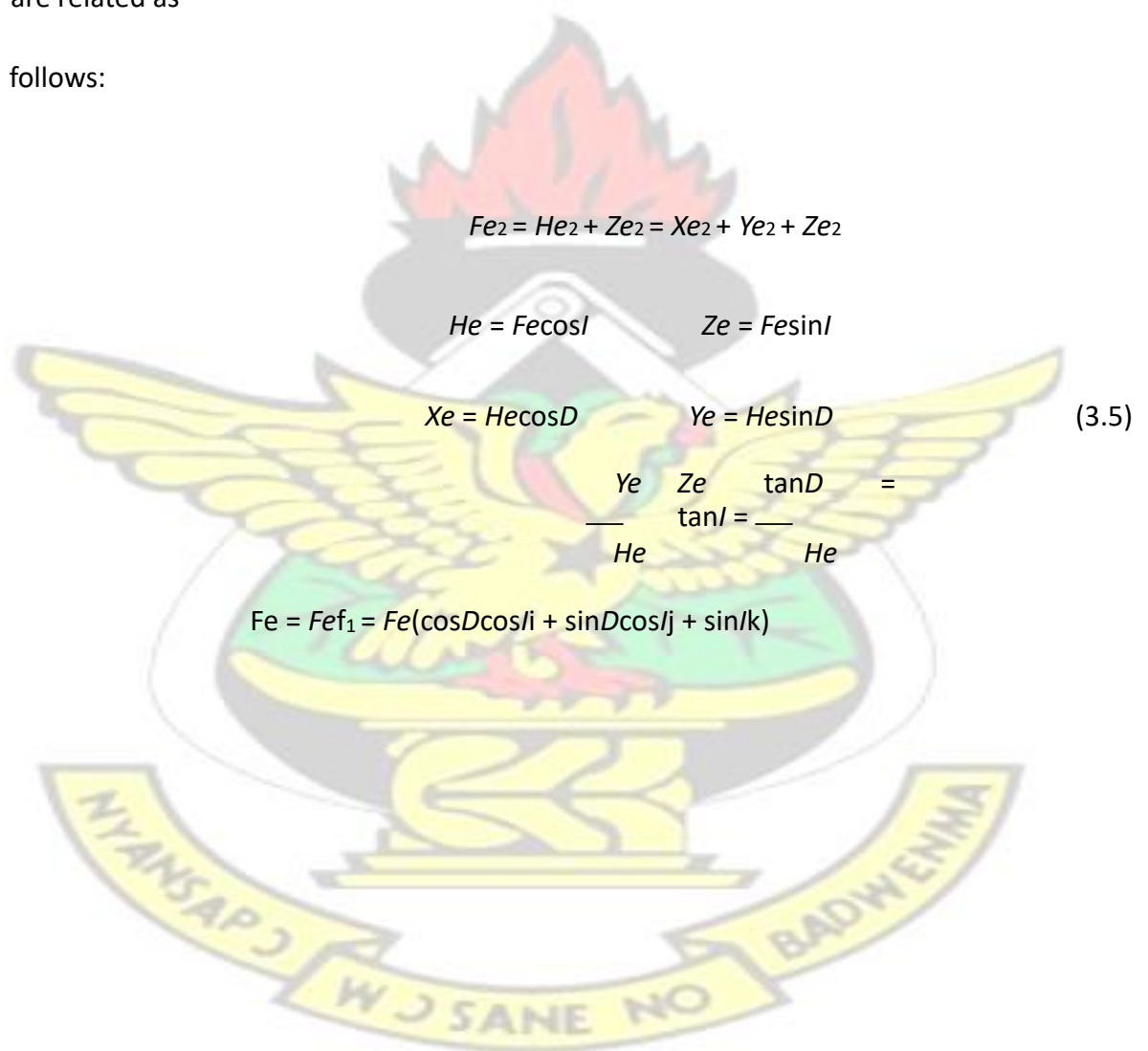
Reeves (1989) report that the Earth, from the geomagnetism point of view, may be considered to comprise of three sections namely: the core, mantle and crust. A dipolar geomagnetic field results due to convection processes in the liquid iron core. The mantle however, is not greatly involved in the magnetism of the Earth, as such, the magnetic anomalies results from the geomagnetic field's (past and present) interaction with the rocks.

According to Telford and Sheriff (1990), an unmagnetized steel needle would ascertain a direction that is most often neither horizontal nor in-line with the geographic meridian (direction of the total magnetic field of the Earth) if it could be hung at its centre of gravity to freely orient itself in any direction, in the absence of other magnetic field. The magnitude of this field  $F_e$ , the dip (or inclination) of the needle from the horizontal  $I$ , and the angle it makes with the geographic north (the declination)  $D$ , completely define the main magnetic field.

The magnetic element (Whitham, 1960) are illustrated in Fig 3.1. One can as well describe the field with regards to the vertical component,  $Z_e$ , reckoned positive downward, and the horizontal component  $H_e$ , which is always positive.  $X_e$  and  $Y_e$  are the components of  $H_e$ , which are considered positive to the north and east, respectively (Telford and Sheriff, 1990).

(Reeves, 1989) indicate that Weber/m<sup>2</sup> or volt–seconds per square metre or Teslas (T) are the units of measurement. It is very convenient to use the nanoTesla (nT = 10<sup>-9</sup> T) as the SI unit of measurement in geophysics considering the fact that the magnitude of the Earth's magnetic field is just about 5 × 10<sup>-5</sup> T. Moreover, at the magnetic equator, the vertical component of the magnetic intensity of the Earth's magnetic field differs with latitude from a minimum of about 30,000 nT to about 60,000 nT at the magnetic poles. These elements are related as

follows:



$$\begin{aligned}
 F_e &= H_e + Z_e = X_e + Y_e + Z_e \\
 H_e &= F_e \cos I & Z_e &= F_e \sin I \\
 X_e &= H_e \cos D & Y_e &= H_e \sin D \\
 \frac{Y_e}{H_e} &= \frac{Z_e}{H_e} \tan D = \tan I
 \end{aligned} \tag{3.5}$$

$$F_e = F_{e1} = F_e (\cos D \cos I + \sin D \cos J + \sin K)$$

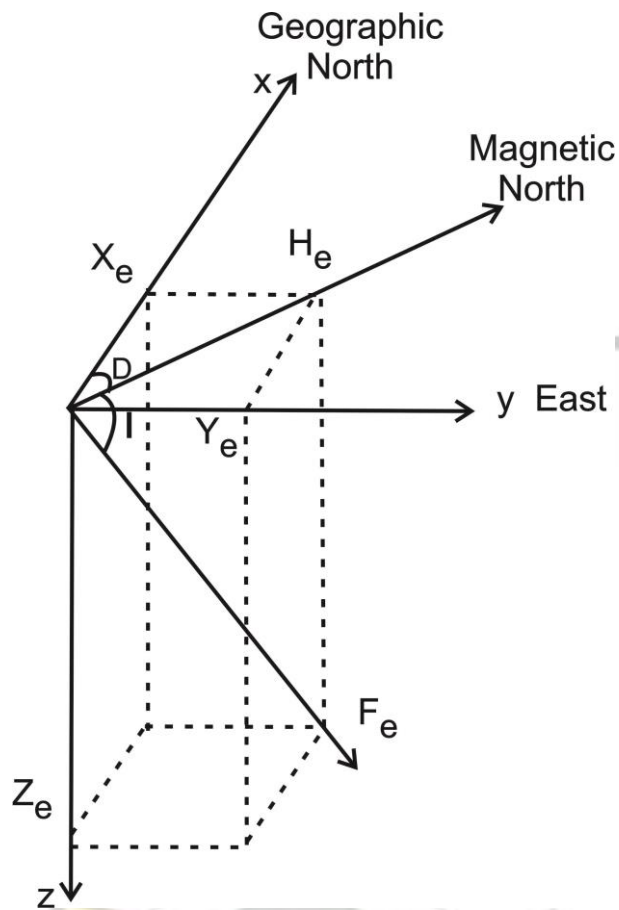


Figure 3.1: Earth's Magnetic Field Elements (Whitham, 1960)

### 3.2.3 The International Geomagnetic Reference Field (IGRF)

The IGRF is a series of mathematical models describing the Earth's main field and its secular variations. Recording  $X$  and  $Y$  with the variations in the Total Field,  $F$  over a survey area and eliminating all time-based variations is the aim of airborne magnetic surveys. The magnitude of the total field,  $F$ , will therefore lie between 20,000 and 70,000 nT throughout and it is possibly anticipated to have local variations of several hundred nT and rarely several thousand nT. Generally, the 'anomalies' are usually two orders of magnitude slightly less than the value of the total field. On an analytical basis, the IGRF provides the means of subtracting the expected variation in the main field, leave anomalies that may be compared

between surveys, even when surveys are carried out several decades apart and when, as a result, the main field may have been prone to be affected by considerable secular variation. The IGRF removal involves the subtraction of about 99% of the measured value, however, if the remainder is to retain accuracy and credibility, then the IGRF needs to be defined with precision.

According to Reeves (1989), the IGRF is published, on a five-yearly basis, by the International Association of Geomagnetism and Aeronomy (IAGA). The working group develops a mathematical model that best fits all absolute observational data from geomagnetic observatories, satellites and other endorsed sources for a given epoch. The model is however, characterised by a set of spherical harmonic coefficients to degree and order 13. The IGRF values are calculated which an available software which allows application of these coefficients, over any chosen survey area. Reeves (1989) indicates that once all other corrections to the data have been made, it is normal practice to remove the appropriate IGRF in the reduction of airborne magnetic surveys. Retrospectively, when re-examining older surveys, one may need to consider departures of the deducted IGRF from an eventual definitive IGRF. From the exploration geophysics point of view, the IGRF is freely available and universally accepted and certainly, it offers an advantage of consistency in magnetic survey procedures.

#### 3.2.4 Magnetic Susceptibility

Magnetic susceptibility is the quantitative measure of the degree to which a material may be magnetised relative to a given applied magnetic field. Wemegah et al. (2009) also defines

magnetic susceptibility as a measure of the ease with which specific sediments are magnetised when magnetic field is applied. The ease of magnetisation is primarily identified the concentration and composition (size, shape and mineralogy) of material within the sample that can be magnetised. It plays the same role as density does in gravity interpretation. Ferromagnetic minerals (strongly magnetisable) and any of the paramagnetic (moderately magnetisable) minerals as well as other substances are examples of minerals that have the ability of being magnetised (Wemegah et al., 2009; Reynolds, 1997).

In terms of unit volume, volume susceptibility ( $\kappa$ ) is defined as the ratio between the induced magnetisation and the inducing field, which is represented mathematically as  $\kappa = M/H$ , or  $\kappa = J/H$  where  $M$  or  $J$  (also termed as the intensity of magnetisation) is the volume magnetisation induced in a material of susceptibility  $\kappa$ , by the applied external field  $H$  (Clark, 1999). Despite the fact that susceptibility is dimensionless, the value in c.g.s. equivalent units should be multiplied by  $4\pi$  in order to make compatible with the SI or rationalised system of unit its numerical value.

According to Telford and Sheriff (1990), despite the fact that there is great contrast, even for a specific rock type, and vast overlap between different types, basic igneous rocks are highest in average susceptibility while sedimentary rocks are the lowest. The susceptibility in each situation is dependent only on the quantity of ferrimagnetic minerals present, predominantly magnetite, sometimes titanomagnetite or pyrrhotite. The values of chalcopyrite and pyrite are usually of many sulfide minerals that are fundamentally non-magnetic.

### 3.2.5 Magnetism of Rocks and Minerals

Various rocks containing iron-bearing minerals behave as tiny magnets. These minerals start forming as magma cools. Since the molten rocks have not totally solidified at this point, the magnetic minerals align themselves to the magnetic field as they float in the molten mass. These minerals attain the magnetic field present when the rocks finally solidifies (Reeves, 1989). Sedimentary rocks likewise, have a magnetic record. Iron-bearing sedimentary minerals likewise, align themselves with the existing magnetic field as they are deposited from the water column. The magnetism is constrained in the rock except the rock is subsequently heated above the Curie point, which is the temperature at which all magnetisation is lost (Reeves, 1989). The heated rock will record the magnetic field at this later time when it cools again below the Curie point, and the old magnetic field will be lost. It can therefore be established that a rock's magnetism is primary and has not been re-set at a later time (Petersen, 1990). Contrasts in the magnetic mineral content (mainly magnetic and pyrrhotite) of the near surface rocks produces local changes in the main field which results in magnetic anomalies. are caused by magnetic minerals (Rajagopalan, 2003). Substances are divided based on their responses to an external field (Telford and Sheriff, 1990).

There are no unpaired electrons in diamagnetic materials, since all the electron shells are complete. The electrons orbit are such that they create a magnetic field which opposes the applied field which results in a weak, negative susceptibility (Telford and Sheriff, 1990). Graphite, salt, marble and quartz are the Earth's most common diamagnetic materials (Reynolds, 1997). Incomplete electron shells contain unpaired electrons that create a spin of unbalanced magnetic moments and weak magnetic interactions amongst atoms in

paramagnetic materials such as fayerite, amphiboles, pyroxenes, garnets, biotite and olivine (Reeves, 1989). Paramagnetic materials posses a weak positive susceptibility, eventhough they decrease inversely with the absolute temperature as indicated by the Curie-Weiss Law (Reynolds, 1997). Ferromagnetic materials decrease with an increase in temperature and vanishes completely at the Curie temperature. Genuinely, ferromagnetism occurs only exceptionally in nature but encompass substances such as cobalt, nickel and iron, all of which are aligned in a parallel manner. In anti-ferromagnetic materials, hematite for example, the moments have an anti-parallel alignment (Nagata, 1961).

The sub-lattices in ferrimagnetic materials (of which magnetite, titanomagnetite and ilmentite are prime examples) are unequal and anti-parallel. Larger susceptibility and spontaneous magnetization are distinctive of ferrimagnetic materials, for example, in the case of pyrrhotite (Reynolds, 1997). The greater part of naturally occuring magnetic minerals portrays either ferrimagnetic or imperfectly anti-ferromagnetic qualities (Telford and Sheriff, 1990).

### 3.2.6 Aeromagnetic Survey

Magnetic surveying is one of the few geophysical techniques that can be effectively carried out from the air. The magnetometer sensor is either mounted on a boom extending from the plane or put in a 'bird' towed behind on a cable to reduce the effect of any magnetism of the plane. The principle which permits very large areas of the Earth's surface to be quickly surveyed for regional reconnaissance is correlative to a magnetic survey executed with a hand-held magnetometer. The aircraft usually flies along parallel lines at constant height

above the ground surface, so far as this is feasible, with occasional tie lines at right angles to check for errors by comparing readings where lines cross.

Tiny contrasts in the intensity of the ambient magnetic field are recorded by the magnetometer, as the aircraft flies, which are caused by the temporal effects of the continually varying solar wind and spatial variations in the Earth's magnetic field, the latter which is as a result of both the regional magnetic field, and the local effect of magnetic minerals in the Earth's crust. The resulting aeromagnetic map, by deducting the solar and regional effects, will represent the spatial distribution and relative abundance of magnetic minerals (commonly the iron oxide mineral magnetite) in the upper layers of the crust. The aeromagnetic map permits a visualisation of the geological features of the upper part of the crust in the sub-surface and since different rock types have different magnetic minerals content, it particularly helps visualise the spatial geometry of rock bodies and the existence of structures such as faults and folds. Aeromagnetic surveys are generally used to support in the generation of geological maps and are also usually used amid mineral exploration. It is particularly very useful in areas where the bedrock is concealed by surface sand, soil or water.

### 3.2.7 Lithology, Structure and Magnetism

According to Plummer et al. (2001), structures may be simply subdivided into two categories

specifically:

- Brittle structures – Faults and Joints are classified in this category. The brittle–elastic failure of rocks are recorded.
- Ductile structures – Folds and metamorphic foliations fall in this category. The permanent visco–plastic deformation of rock are preserved throughout geologic time.

Confined magnetic anomalies, usually circular or oval in plan and several hundred meters across, and with amplitude of tens to hundreds of nanoteslas, may emerge from amassing of magnetite and pyrrhotite, which may be correlated with economic grades of copper, lead, silver, zinc, and gold deposits (Plummer et al., 2001). The Abra deposit in the Bangemall Basin of Australia, for example, which precipitated from mineral bearing solutions are frequently located within the rocks adjacent to major faults.

Sedimentary rocks are generally non–magnetic. However, Grant (1985) indicate that the analysis of survey data postulates that the base of the sedimentary sequence may lie above the magnetic sources. This allows hidden sedimentary basins in petroleum exploration to be rapidly identified. By estimating the depths to the magnetic sources (also known as the 'Magnetic Basement') systematically, across the survey area, the sedimentary layer may be delineated to ascertain.

The greatest part of the Earth's crust is probably composed of metamorphic rocks which have an extensive range of magnetic susceptibility. In practice, these usually amalgamate to produce complicated patterns of magnetic anomalies across areas of apparent metamorphic terrain. The largest anomalies are produced by itabiritic rocks, succeeded by meta–basic bodies, while felsic areas of granitic/gneissic terrain generally depicts an

abundance of low amplitude anomalies which are imposed on a comparably smooth background (Grant, 1985).

Igneous and plutonic rocks depict a extensive range of magnetic properties. Homogeneous granitic plutons are most often evidently featureless when compared with the magnetic signature of their surrounding rocks; they may exhibit a weak magnetic nature but it is by no means universal (Plummer et al., 2001). Banded iron formation (Itabirites) could also be very highly magnetic that they could be unambiguously distinguished on airborne magnetic maps. Less magnetic examples in an area where the Earth's total field is just 23000 nT, however, could be confused with mafic or ultramafic complexes (Grant, 1985). Typical causes of magnetic anomalies, moreover, encompass dykes, fault, truncated or folded sills and lava flows, massive basic intrusions, metamorphic basement rocks and magnetite ore bodies.

### 3.2.8 Data Enhancement Techniques

It is usually visually challenging to observe and interpret the distinctive structures on the original total magnetic intensity grid. One can visually enhance the effects of selected geologic sources by specifying a range of image procedures using mathematical enhancement techniques. In order to enhance near-surface magnetic sources, it is very important to use end results such as reduced-to-pole, residual and vertical derivative fields, but the limitations of the end results depend on the quality of the data and additional factors such as magnetic inclination and declination (Nicolet and Erdi-Krausz, 2003).

### 3.2.8.1 Fourier Transform Filters

In magnetics, Fourier transforms are particularly essential for (Telford and Sheriff, 1990):

- Improving the resolution of specific anomalies by upward or downward continuation method,
- Alternating the effective field inclination (reduction-to-pole) or transforming total-field data to vertical-component data,
- Calculate derivatives and
- Filtering-separating anomalies which is as a result of sources of different size and depth, as well as modelling.

Cooley and Tukey (1965) developed the Fast Fourier Transform (FFT) which is a much faster and an efficient algorithm used in the computation of the discrete Fourier transform (DFT) and its inverse.

### 3.2.8.2 Reduction-to-the-Pole

According to Mendonça and Silva (1993), when magnetisation occurs anywhere other than at the magnetic poles, an observed anomaly will have an asymmetric shape. A horizontal displacement between the measured anomaly and the exact location of the body occurs, due to the dipolar nature of the magnetic field. A very powerful and effective operation called the Reduction-to-Pole is designed to transform a total magnetic intensity (TMI) anomaly, which is influenced by an arbitrary source, into the anomaly that would be

produced by this same source if it were situated at the pole and magnetised by induction only (Li, 2008).

### 3.2.8.3 Analytic Signal

The combination of the horizontal gradient as well as the vertical gradient produces the analytic signal, which is also known as total gradient. The analytic signal has a form over causative body which is dependent on the locations of the body (horizontal coordinate and depth) but does not depend on the direction of magnetization. Analytic signal is a quantity that encompasses this property and has been extensively used in the detection of edges as well as the estimation of depth of magnetic bodies by several authors (Ansari and Alamdar, 2009).

### 3.2.8.4 Vertical Derivative Filter

According to Keating (1995), the calculation of the first vertical derivative considerably enhances the resolution of closely spaced and superimposed anomalies by removing long wavelength features from the magnetic field. Calculations can be directly made from the gridded residual magnetic intensity data to obtain values for the first vertical derivative by employing a fast Fourier transform, in combination with the transfer function of the first vertical derivative and a low-pass filter. The aim of the low-pass filter is attenuate high frequencies which are irrelevant and complemented by the derivative operator.

#### 3.2.8.5 Total Horizontal Derivative

A magnetic body is more involved spatially with the related magnetic response after the reduction-to-pole correction. The maximum horizontal gradient (more appropriately, the maxima of the total horizontal gradient) of the anomaly slope is later located near or over the edge of the body. Particularly in map form, maximum ridges over the edges of magnetic basement blocks as well as faults or other magnetic bodies are produced by the horizontal gradient operator. Furthermore, linear features, associated with contacts, are highlighted by the horizontal gradient in the dataset (Milligan and Gunn, 1997).

#### 3.2.8.6 Upward and Downward Continuation

Relative to low-frequency anomalies, upward continuation smoothens out anomalies produced by high frequencies. This serves as a very useful process for suppressing the effects caused by shallow anomalies when the details of interest are the deeper anomalies. The effects of the anomalies (enhances high frequencies) are sharpened by downward continuation and this is achieved by bringing them closer to the observation plane. It stimulates carrying out the airborne survey closer to the ground (Milligan and Gunn, 1997). Anomalies would however, possess less spatial overlap which makes them distinctive (Gunn, 1978).

# CHAPTER 4

## MATERIALS AND METHODS

### 4.1 Description of Study Area

#### 4.1.1 Location

The study area is located in the Sene District of Brong–Ahafo Region, Ghana, and at the North–Eastern corner of the regional capital, Sunyani. It is one of the 27 districts in the region with Kwame Danso as the district capital. The district lies within Longitudes  $0^{\circ}$  E and  $0^{\circ}30^0$  W, and Latitudes  $7^{\circ}30^0$  N and  $8^{\circ}30^0$  N (figure 4.1).

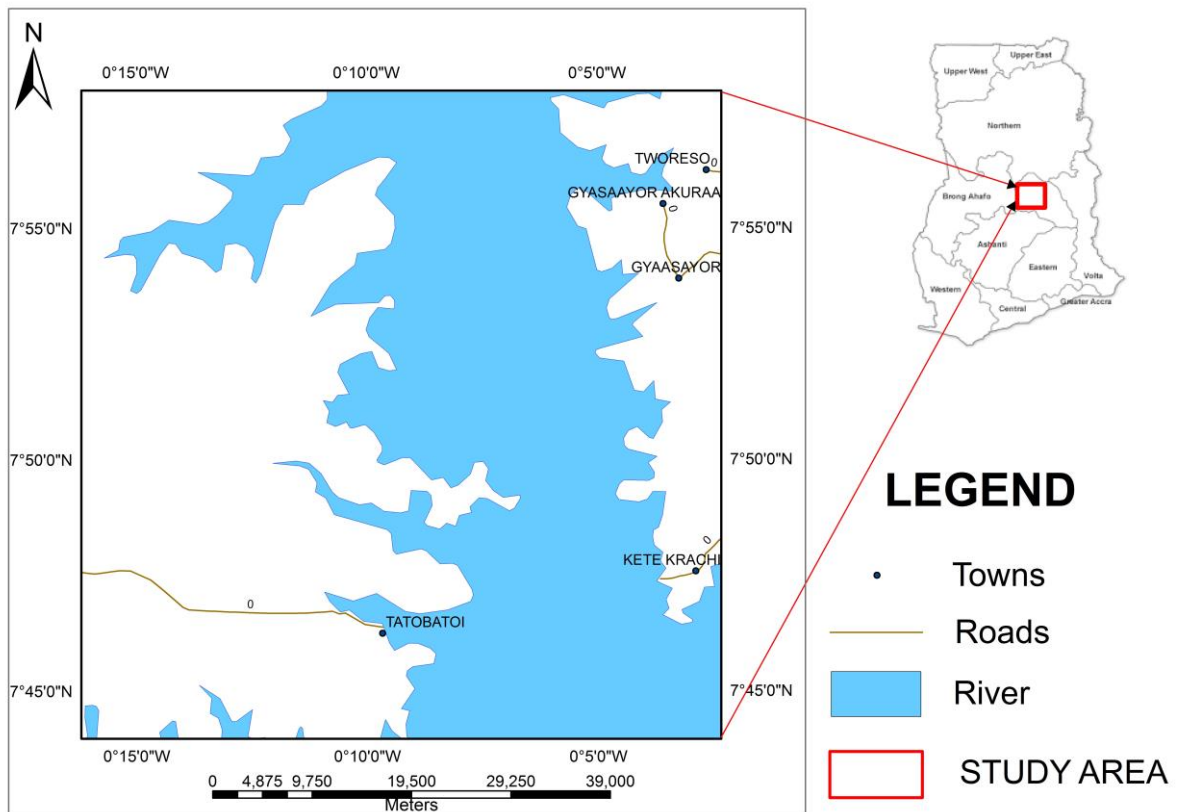


Figure 4.1: Location and accessibility of the study area (modified from Ghana Shapefiles)

#### 4.1.2 Physiography and Drainage

The district, whose topography is generally rolling and undulating, forms part of the Voltaian basin sandstones which is the largest physiographic region. The district has an average elevation of approximately 166 m above mean sea level (MSL). The district is underlain by the Middle and Lower Voltaian rock units. The Lake Volta, as well as the Sene and Pru rivers are the three main rivers that flows within the district. The formation of the Lake Volta, which occupies an extensive area within the district, has created various Islands in the district. Considering the district's low elevational nature, an extensive portion of the distict is prone to flooding during heavy rains due to its flood plain locations of Lake Volta, Sene and Pru rivers. The Lake Volta has to some extent, been supportive to water transportation in the district. The Sene river separatinds the south eastern part from other parts of the district since it has presently become an arm of the Lake Volta in the district. Development in that part of the district is a dominant problem since transportation is affected.([www.sene.ghanadistricts.gov.gh](http://www.sene.ghanadistricts.gov.gh)).

#### 4.1.3 Vegetation

The vegetation is predominantly Guinea Savanna woodland. The transitional nature of the interior wooded Savanna does not make it a typical one. Tall grasses such as the elephant grasses and varieties of anthropogenic species combined with savannah wood type of trees

such as Daniela Olivetti, Terminalia avocado, Dawadawa, Baobab, Acacia and the Shea butter can predominantly be identified. There are very few trees which are distributed along the margins of the moist deciduous forest and normally germinate and develop very close to each other. The grasses develop tussocks with a height of about 3 m and above. As one travels to the northern part of the district, the vegetation gradually opens up and the height of the trees reduce ([www.sene.ghanadistricts.gov.gh](http://www.sene.ghanadistricts.gov.gh)).

#### 4.1.4 Climate Conditions and Occupation of Inhabitants

The district lies between the tropical continental climatic region and wet semi-equatorial region of Ghana. Furthermore, the district occurs in the transitional zone between the two main climatic regions. The district is noted for high temperatures all year round with a mean annual temperature of approximately 27°C. The area has a high relative humidity, averaging over 75% all year round. However, it usually varies between the wet and dry seasons. The district has a bi-modal rainfall regime with major rainfall occurring between April and July while the minor period occurs between September to late October. The area records a mean annual rainfall of approximately 1191.2 mm ([www.sene.ghanadistricts.gov.gh](http://www.sene.ghanadistricts.gov.gh)).

Approximately 65% of the population in the district are occupied economically with agricultural activities such as poultry production/animal husbandry, vegetable/food production and fisheries. By virtue of the low elevation of the area, an extensive portion of the district is flood prone during heavy rains, combined with the existence of swamps, it has created opportunities for rice farming. It also provides a conducive environment for a variety of other agricultural produce, for example, yam, cassava, groundnuts, maize, okro,

garden eggs, tomatoes and pepper to be cultivated. Generally, agriculture in the area is rain fed and is greatly dependent on the weather. Fishing activities predominantly occur in the communities along the banks of the Volta lake, Sene and Pru rivers in the district ([www.sene.ghanadistricts.gov.gh](http://www.sene.ghanadistricts.gov.gh)).

# KNUST

## 4.2 Data Acquisition

The main dataset used in this study is based on aero-geophysical dataset collected in early 2008 by Fugro Airborne Surveys, Perth, over the Volta and Keta Basins in Ghana under the Mining Sector Support Program (MSSP) for the Ghanaian government and was funded by the European Union. The main aim of the project was to develop the mining sector in Ghana, however, one of the minor objectives was also to analyse the oil prospectivity of this deep sedimentary basin, Voltaian basin. High resolution airborne geophysical information was generated from the survey for the purposes geological mapping and mineral exploration. The new airborne geophysical survey provided gravity, magnetic, electromagnetic, radiometric data over the Voltaian and Keta basins. Fugro Airborne Surveys carried out the survey over the entire Voltaian basin using a fixed wing aircraft (Cessna 208B Caravan) with a GPS installed. A North-West survey line direction was chosen to perpendicularly intersect the main North-East geological strike direction.

A GT-1A vertical component gravimeter was used to acquire the gravity data at a 5 km flight line spacing and a 50 km tie line spacing at approximately 500 m above the ground. The output from the gravimeter was sampled at 0.1 s (10 Hz) and a nominal sensor terrain clearance of 859 m with a gentle drape flying at 160 knots. The airborne magnetic data was

acquired with a fixed-wing aircraft with a Scintrex Cesium CS-2 cesium vapour magnetometer. The result from the magnetometer was sampled at 0.05 s (20 Hz) with a nominal sensor terrain clearance of 75 m above ground level. The flight line spacing and tie line spacing for the aeromagnetic were respectively 500 m and 5000 m. A high-resolution aero-geophysical information was produced for the purpose of the objectives mentioned above. Figure 4.2 is a diagram to illustrate the flight lines during data acquisition.

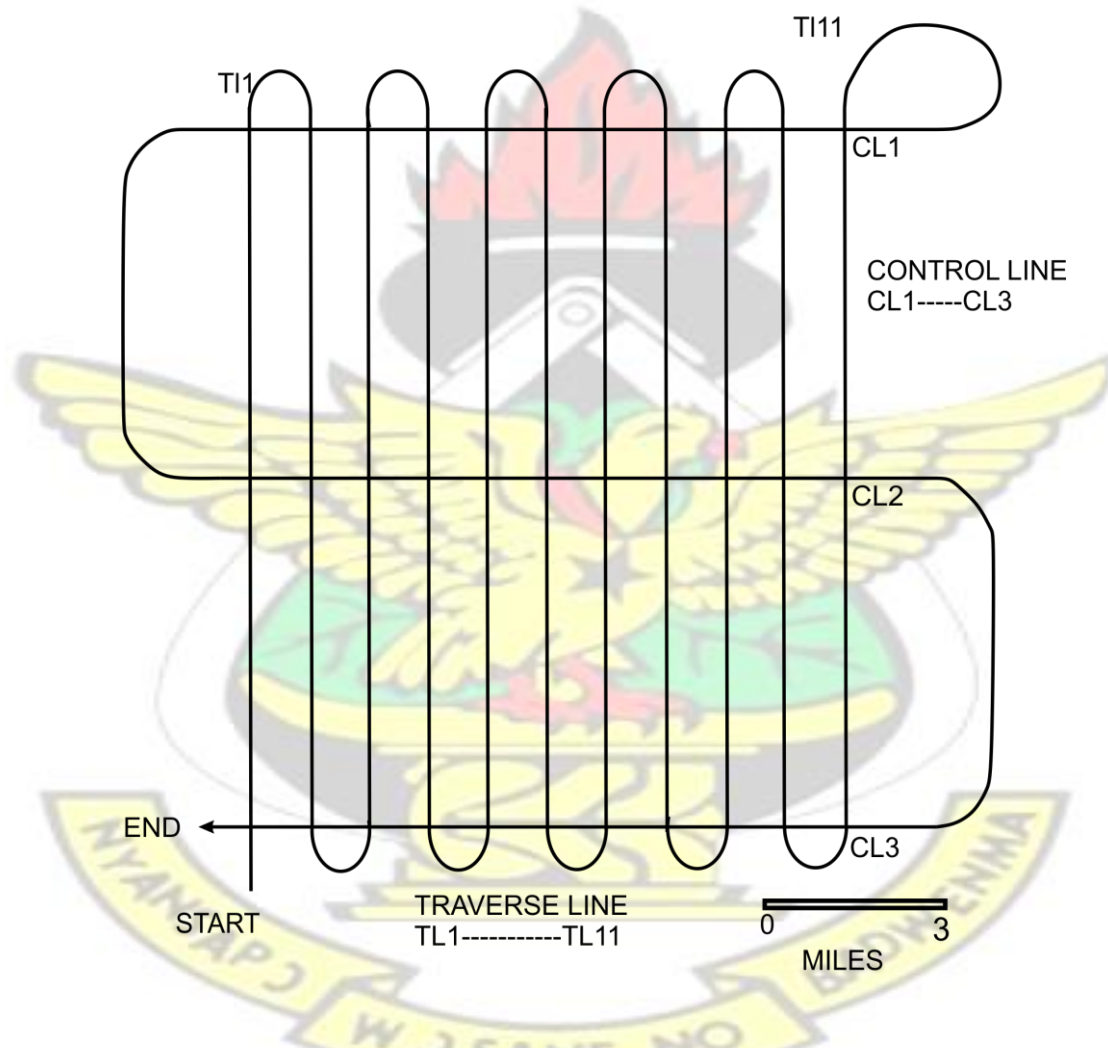


Figure 4.2: Diagram showing flight line path during data acquisition

### 4.2.1 Metadata

The geophysical information was acquired with the following survey parameters in figure 4.1 below.

Table 4.1: Parameters for Airborne Geophysical Survey (Geological Survey of Ghana, 1998)

Acquisition Type	Fixed–Wing Magnetic	Fixed–Wing Gravity
Flight line spacing	500 m	5000 m
Tie lie spacing	5000 m	50000 m
Flight line direction	135°	312°
Tie line direction	225°	042°
Sensor height	75 m AGL	450 m AGL (gentle drape flying)
Magnetometer along line sampling	0.05 sec (20 Hz) (4–5 m)	0.1 sec (10 Hz) <7.5 m at 160 knots
Survey height	75 m	859 m
Survey Area	6570 km <sup>2</sup>	6570 km <sup>2</sup>
Total line kilometres	18,801 km	1908 km

### 4.3 Data Processing

The processing and enhancement of the airborne geophysical datasets was primarily carried out with the Geosoft (Oasis Montaj). The interpreted results were integrated with GIS environment which was created using the ArcGIS. The airborne geophysical datasets namely gravity and magnetic was aquired courtesy of the Ghana Geological Survey Department (Accra) by the Physics Department (Kwame Nkrumah University of Science and Technology, Kumasi) on the 15<sup>th</sup> October, 2014. The geophysical dataset for the study area was georeferenced to Universal Transverse Mercator (UTM), Zone 30N of the Northern hemisphere.

Geosoft Oasis montaj software was used to process the gravity and magnetic. The processing of airborne datasets comprised the sequential application of enhancement

techniques, the application of a gridding routine, corrections such as Bouguer, terrain, isostatic corrections among other, and removal of the background magnetic field of the Earth. A few corrections such as background correction (Aircraft), stripping, levelling, micro-levelling, aircraft heading, diurnal variation removal from the Earth's magnetic field, instrumentation variation, decorrugation, theoretical gravity correction, free air, isostatic, bouguer, tidal corrections, lag error between aircraft and the sensor and irregularities between flight lines and tie lines were done by the British Geological Survey (BGS).

#### 4.3.1 Processing of Gravity Data

The observed gravity readings acquired from the gravity survey gives a reflection of the gravitational field as a result of all masses in the earth and the Earth's rotational effect. To interpret gravity data, all known gravitational effects which were not relative to the subsurface density changes were eliminated, which included latitudinal variations, elevation changes, topographic changes, building effects and earth tides (LaFehr, 1991). The field survey removed the earth tidal effects during the drift curve determination. A gravity reading on a flat ground surface was first considered in order to understand the corrections. To account for the deviations from this condition, the corrections were then applied. The gravitational pull decreased with an increase in the distance from the center of the earth. The correction which accounts for this is termed elevation correction. If the gravity reading was taken on top of a hill, then there was a deficit of mass on either side of the hill as compared to a horizontal ground surface. A topographic correction was applied to correct for this. It is important to note that mass higher than the reading site will also affect the data and therefore had to be accounted for. This may occur in areas of significant

topography or when surveys are conducted near large buildings. In a modern instrument such as the Scintrex, the tidal and drift corrections may be automatically applied by the meter.

According to LaFehr (1991), the Bouguer gravity anomaly or Bouguer gravity is the difference between the observed gravity ( $g_{obs}$ ) and theoretical gravity ( $g_{th}$ ) at any point on the surface of the Earth after the gravity readings have been reduced to the geoidal surface (i.e. making all the required corrections) which is as a result of lateral variations in density in the subsurface (assumed to be caused by geologic structure being sought) and is used for interpretations.

#### 4.3.2 Complete Bouguer Anomaly (CBA)

For a given station, the observed gravity field with corrections added in for instrument drift, tidal variation brought about by the Sun and the Moon, latitude (the oblateness of the Earth's surface), and density of the rock lying between the station and sea level represents the CBA. These factors in totality results in the Bouguer anomaly. The CBA is then obtained by adding corrections for topographic effects. A digital topographic model was used to calculate the effects of mass contributions (from nearby mountains) or lack thereof (from voids caused by nearby valleys) owing to the physical relief that encompasses the gravity station to obtain the corrections for topography (Blakely, 1995).

### 4.3.3 Processing of Aeromagnetic Data

Aeromagnetic survey is described as a supportive geophysical technique employed to map sub-surface bedrock geology (lithology) and structures caused by variations in magnetic susceptibility of rocks (Gunn et al., 1997).

#### 4.3.3.1 Diurnal Variation Removal

Time variations of magnetic field of the Earth can affect magnetic surveys. These variations are caused by the interaction of the solar wind activities with the Earth magnetic field. A most popular method to correct diurnal variations in magnetic surveys is to use data from one or a few fixed magnetometers in the survey area called base stations. To correct diurnal variations occurring during the survey, the magnetic data from the base station was subtracted from the collected data. The base station was located far away from any human activity to avoid cultural noise. According to Reeves (1989), the position of the base station should not be more than 50 km away from the most remote part of the survey area. In order to avoid bad diurnal correction some companies use two or three base stations located in different parts of the survey area. To minimise the effects of diurnal variations, tie and flight lines were flown over a short time periods.

#### 4.3.3.2 Geomagnetic Reference Field Removal

This removed from the survey, the strong influence of the main field of the Earth. This was done because dynamo action in the core which is not related to the geology of the (upper) crust greatly influences the main field. The Australian or International Geomagnetic

Reference Field (AGRF or IGRF) helped to achieve this by subtracting a model of the main field from the survey data since it is generally used for this purpose. This model accounts for both the spatial and long period (>3 years) temporal variation (secular variation) of the main field (Barton et al., 1990).

#### 4.3.3.3 Effect of Height Variations

Aeromagnetic surveys are generally planned with series of lines, flight lines and tie lines. Tie lines are normally perpendicular to flight lines. Generally tie line spacings are about 5 – 10 times larger than flight line spacing. Tie lines were applied to correct the recorded magnetic field on flight lines. The recorded magnetic fields on tie lines and flight lines differ by so called mis-ties. Sources of mis-ties are diurnal variations, navigational errors, flight height variations, and transient anomalies from aircraft, instrument drift and the random noise (Mauring et al., 2002). There are two different types of flights, draped flights with constant terrain clearance and barometric flights with constant height above the sea level. One of the advantages of barometric flights is a good coherence between adjacent lines but data resolution decreases over deep valleys (Roest and Pilkington, 1993). Therefore, for mountainous areas with sharp topography, draped flights are preferred. However, in practice draped flights always have derivations for a constant terrain clearance.

#### 4.3.3.4 Leveling Data

Aeromagnetic data usually suffer from data irregularities between adjacent flight lines called line level errors, (Mauring et al., 2002). Leveling is the process that is interested in removing short period magnetic variations from the data by minimizing mis-tie values.

Leveling is done without regarding the cause of the mis-ties. The leveling errors can be caused by different sources e.g., time variations of the magnetic field, navigational error, height variations, magnetometer drift and random noises.

There are three main categories for the correction of these discrepancies (Luyendyk, 1997).

These are:

- Minimizing intersection errors by adjusting navigation data.
- Loop closure methods.
- Polynomial leveling.

#### 4.3.3.5 Tie Line Leveling

Tie line leveling is a method that removes remaining errors e.g., Time variations, height variations effect, instrumental and systematic errors attributable to known sources of measurement error from the data. Mis-ties therefore can be used to level the data. However, it is seldom possible to remove all errors because of incomplete knowledge of the factors affecting the measurements or the lack of accurate values of the parameters used in calculating the error corrections. Various examples of tie line leveling methods have been published in the literature (Foster et al., 1970; Yarger et al., 1978; Bandy et al., 1978; Luyendyk, 1997). They used statistical methods to remove mis-ties. Afterwards, the micro-leveling procedures are recommended to eliminate the remaining leveling errors.

#### 4.3.3.6 Interpolation

In general, airborne geophysical survey data are collected along roughly parallel lines across the area of interest. The sampling interval along the flight lines usually are larger than and perpendicular to the flight line direction. Due to the higher density of samples along the flight lines in contrast with line spacing, we may miss some high frequency anomalies located between the flight lines (frequencies higher than the Nyquist frequency perpendicular to the flight line direction). Some interpolation techniques can be used to enhance the high frequency anomalies using measured magnetic field and horizontal gradient data.

#### 4.3.4 Gridding

According to Foss (2011), a new and essentially different form of the data is created since gridding interpolates of the data from the measurement locations to nodes of a regular mesh. Gridding was the initial step in the data processing and this interpolated the Bouguer anomaly values of the database into a square grid. Grid is a term that best describes files containing gravity locations (x,y) and data (z) observation values, which are interpolated to form a regular and smoothly sampled representation of the locations and data. The Geosoft Oasis montage software makes use of the following interpolation methods of (x, y, and z) data:

1. Bi-directional gridding.

This is designed to roughly interpolate parallel line-based datasets, and it is achieved in two steps

- Along each survey line, the data is interpolated to produce values at each intersection with the defined grid lines.
- Along each grid line, the interpolated values are extracted from the previous interpolated values then stored, and finally interpolated to produce the gridded value at each grid cell.

## 2. Minimum curvature random gridding.

The  $(x, y, z)$  data are actually interpolated by fitting a two dimensional surface to the  $(x, y, z)$  data in this case to minimise the curvature of surface. It is recommended for random distribution data.

## 3. Kriging.

The statistically most probable value, in simple terms, determined the at the node from the surrounding real data values.

In preparing for gridding the data, their geographical coordinates were transformed to Cartesian (X–Y) coordinates using Projection – Universal Transverse Mercator (UTM), Datum – World Geodetic System 1984 (WGS1984), Ellipsoid – World Geodetic System (WGS84) and Zone 30N which are the same parameters used for the local maps. Geosoft Oasis Montaj, a computer program, was used to transform Gravity and Magnetic datasets to the grid depending on the minimum curvature surface method (Briggs, 1974; Swain, 1978), with a grid cell size of 1250 m and 125 m for Gravity and Magnetic grids respectively and once a grid was created, it was displayed as an image to create final bouguer anomaly

and TMI maps. The gridded datasets were displayed as colour maps to produce both the gravity anomaly and TMI maps. It showed the distribution of the bouguer anomalies and magnetic anomalies within the region, which were predominantly caused by lateral variations in density and variations in magnetic susceptibilities respectively, within the sediments and basements, all through the Earth's crust. The images generated with the Geosoft software package and other associated files containing spatial reference information were exported in the GeoTIF format. Viewing the images was possible with any image viewing software and it was also possible to display images in a GIS environment since they were spatially referenced. Gridding the data made it possible for filters applied since equally spaced data points are required in filtering.

#### 4.3.5 Regional–Residual Separation

The gravity fields at the surface of the Earth comprise anomalies that are from sources of different sizes as well as various depths. Separating anomalies which are created by certain features from anomalies caused by others is often desirable in order to help in the interpretation of these fields. Shorter wavelength anomaly was correlated to the shallow-seated structures while the long wavelength anomaly was correlated to the deep-seated structures, that is, taking into consideration the wavelength of the gravity anomalies. According to Nettleton (1976), the smooth region is the regional field and is associated to effects which are too deep or too broad in relief to be a probable expression of structure or other disturbance of interest. After subtraction, the part left is called the residual field. The regional and residual images are generated based on the type of the study. The regional grid is mostly used to enhance the residual anomalies which are of fundamental interest in

hydrocarbon exploration, and is created by subtracting the regional anomaly grid from the original total field.

#### 4.3.6 Enhancement of Gravity and Magnetic Datasets

The first step before interpretation was to apply different filtering or enhancement techniques to the observed data. Because gravity and magnetic fields are mathematically related, the same filtering and enhancement techniques can be applied to both of them. A range of linear and non-linear filtering algorithms could be used to enhance airborne gravity and aeromagnetic datasets. Milligan and Gunn (1997) indicate that by using mathematical enhancement techniques, one can visually enhance the effects of selected geologic sources by specifying a range of imaging routines. Some enhancement methods which were applied and their results are described in the following discussion. Due to the fact that it is known that significant concentrations of mineral deposits are related to high frequency gravity and magnetic responses, high-pass and horizontal gradient filters were applied to the aero-geophysical datasets in order to define the edges of bodies as well as enhancing high frequencies. All the enhancement techniques were carried out using Geosoft Oasis montaj.

In Geosoft, the MagMap extension which provides various gravity and magnetic data processing utilities, was applied on both gravity-anomaly and magnetic-anomaly grid for the processing and applying filters. Gravity anomalies in the Earth's gravity field are caused by the variations in the density of rocks and the magnetic minerals in the rocks also influences the magnetic anomalies in the Earth's magnetic field. Thus, interpretation in

terms of geology can be made on these maps and images of these anomalies (Silva et al., 2003). An image was displayed with the aid of the GRID AND IMAGE tool after the generation of a grid and

the application of relevant filters.

Analytic signal and two-dimensional fast Fourier transformation (2D-FFT) filter were however, applied to help facilitate interpretation, by enhancing the quality of the datasets.

The 2D-FFT filters applied involved Reduction-to-Pole, First Vertical derivatives, Upward and downward continuations, and Analytic Signal. One of the dictums of the Fourier domain processing is that the signal must be periodic, however, in order to simulate periodicity in the preprocessing stage, the grid was continuously extended along both coordinates. Dummy values are used as a buffer along the edges of the grid. There was an expansion of the grid so as to permit adequate space for ensuring smooth periodicity. The substitute region was interpolated so as to render the filled grid periodic along both coordinates.

#### 4.3.7 Reduced-to-Pole

This is a data enhancement process carried out on only magnetic data. Reduced-to-Pole (RTP) filter, for low geomagnetic latitudes was applied on the magnetic anomaly data (Total Magnetic Intensity: TMI). This post-processing technique was performed on the gridded data so as to eliminate the asymmetry in the TMI data generated from the non-vertical inclination of the Earth's magnetic field. The images are simplified by this technique such that the induced magnetic anomalies from vertical sources are located over the causative geological body, instead of being skewed and offset to one side. By this approach, directional noise which is caused by the low geomagnetic latitude is minimised using an

azimuthal filter in the frequency domain (Phillips, 1998). The central coordinates of the area were used in the calculation of inclination and declination. It was realised that the study area had inclination of about  $-9.481^\circ$ , declination of about  $-3.932^\circ$  to an average total field strength of about 32459.7922 nT.

#### 4.3.8 Vertical and Horizontal Derivative Filter

This was a post-processing method applied on the gridded data that quantified the spatial rate of change of the potential fields in the vertical direction. It basically enhanced the high frequency anomalies relative to low frequencies. The First Vertical derivative filter (1VD) was applied on the RTP grid data and the Complete Bouguer Anomaly grid data for aeromagnetic and airborne gravity data. This filter permits a more equal representation of small and large amplitude responses. In an attempt to map linear features such as dikes and/ faults from the magnetic data, the First Horizontal derivative (1HD) filter was applied to enhance the RTP grid. At wider spacing, the filter provides horizontal resolution and better accuracy. The horizontal derivative filter helped in the identification of geologic boundaries of formations within the study area. However, the magnitude of the horizontal derivative, in gravity map form, can be gridded to display maximum ridges located relatively over each of the near-vertical lithological contacts and faults. Higher derivative images with different filter such as 2VD and 2HD produced intriguing results however, several distortions were noted to occur in the images which were as a result of the enhancement in the noise level introduced in the data by this process. These images were however, not employed in the interpretation but rather employed as a guide in the interpretation from the first vertical derivative images.

#### 4.3.9 Downward and Upward Continuation (DC and UC)

The interpretation of gravity anomaly data, in most cases, are performed on (or near) the surface where the observation was made. In some situations, it is however, appropriate to move (or continue) the data to another surface for interpretation or for comparison with other dataset. The gravity data set was upward continued by multiplying the flight line spacing by the number 10.

From deeper sources, the appropriation of the magnetic intensities led to the application of the UC filter to restrain the effects of shallow anomalies. DC and UC filter; 500, 800, 1000 and 1500 m were applied to each grid from the derivative filters (1VD and 1HD). This smoothed out the high frequency anomalies relative to low frequency anomalies. Responses of structures from shallow depths were enhanced with the DC filters by efficiently bringing the plane of measurement closer to the source. However, the data contained short wavelength noises that appeared as signals emanating from very shallow sources in the continuation ([www.geosoft.com](http://www.geosoft.com)).

In view of the fact that short-wavelength signals appear to be from shallow sources, they must be eliminated to avoid high magnitude and short-wavelength noises in the processed data. This was done by applying a low-pass filter to eliminate the short-wavelength noise (as determined by the radially averaged energy spectrum) before the downward continuation filter was applied. The energy spectrum produced from the MagMap was a method used to determine the depth to which the data could be continued downward.

#### 4.3.10 Low-Pass Filter

The long wavelength constituent of the Bouguer gravity field is regularly being caused by the density contrasts which are considered to be at deeper depths than the general interest of exploration for minerals and hydrocarbon.

The MAGMAP filter design in Geosoft Oasis Montaj makes it possible to select the appropriate filter to be applied on the original total field data. To produce a regional gravity anomaly map, the deep-seated structures from the gravity field data are enhanced by using a low-pass. In an attempt to generate a regional gravity anomaly map, different cut-off, e.g. 20, 30, 40 km were applied during the data processing. A 50 km cut-off was finally applied for the low-pass filter, which rejected wavelengths that were below 50 km. The residual gravity anomaly grid was generated from the regional gravity anomaly grid by simply subtracting the regional grid from the original total field grid. The anomalies of interest within the Voltaian basin which were related to the near-surface structures were enhanced and vanished on the regional gravity map.

#### 4.3.11 Analytic Signal Amplitude

The analytic signal, while greatly applied in magnetics, is less employed in gravity, predominantly due to the sparser nature of gravity data which makes it difficult to calculate the horizontal derivatives. In magnetics the analytic signal is defined as a complex function (or a quaternion) relating the vertical derivative to horizontal derivatives (Nabighian, 1972; 1974; 1984; Craig, 1996). The analytic signal amplitude was computed from the residual magnetic field. The analytic signal amplitude does not depend on the magnetisation

direction of the source but is dependent no the amplitude of magnetization (Silva et al., 2003). It is possible to extend the results acquired for magnetic data to gravity data if the horizontal derivative of the gravity field is used as input (Nabighian et al., 2005).

# KNUST



## CHAPTER 5

### RESULTS AND DISCUSSIONS

The results from the processed and filtered gravity and magnetic datasets were developed into different maps which are shown below in this chapter. These maps are interpreted below and major Lithological and structural features were mapped from the derivatives of the processed data. A detailed geological and structural Interpretation was carried out using the Airborne Gravity and Magnetic datasets in a GIS environment.

#### 5.1 Digitized Elevation Map (DEM)

The topography in the study area from the Digitized Elevation Map (DEM) is shown in Figure 5.1. The elevations range from 148 *m* to 229 *m* with a mean elevation of about 185 *m* above mean sea level. A larger part of the study area averagely, falls within highlands. The low land areas depicted by blue colour range from 148 *m* to 164 *m* above mean sea level. The low land regions are found in the north–eastern and south–western part of the study area and area noted to be the Volta lake and its river channels.

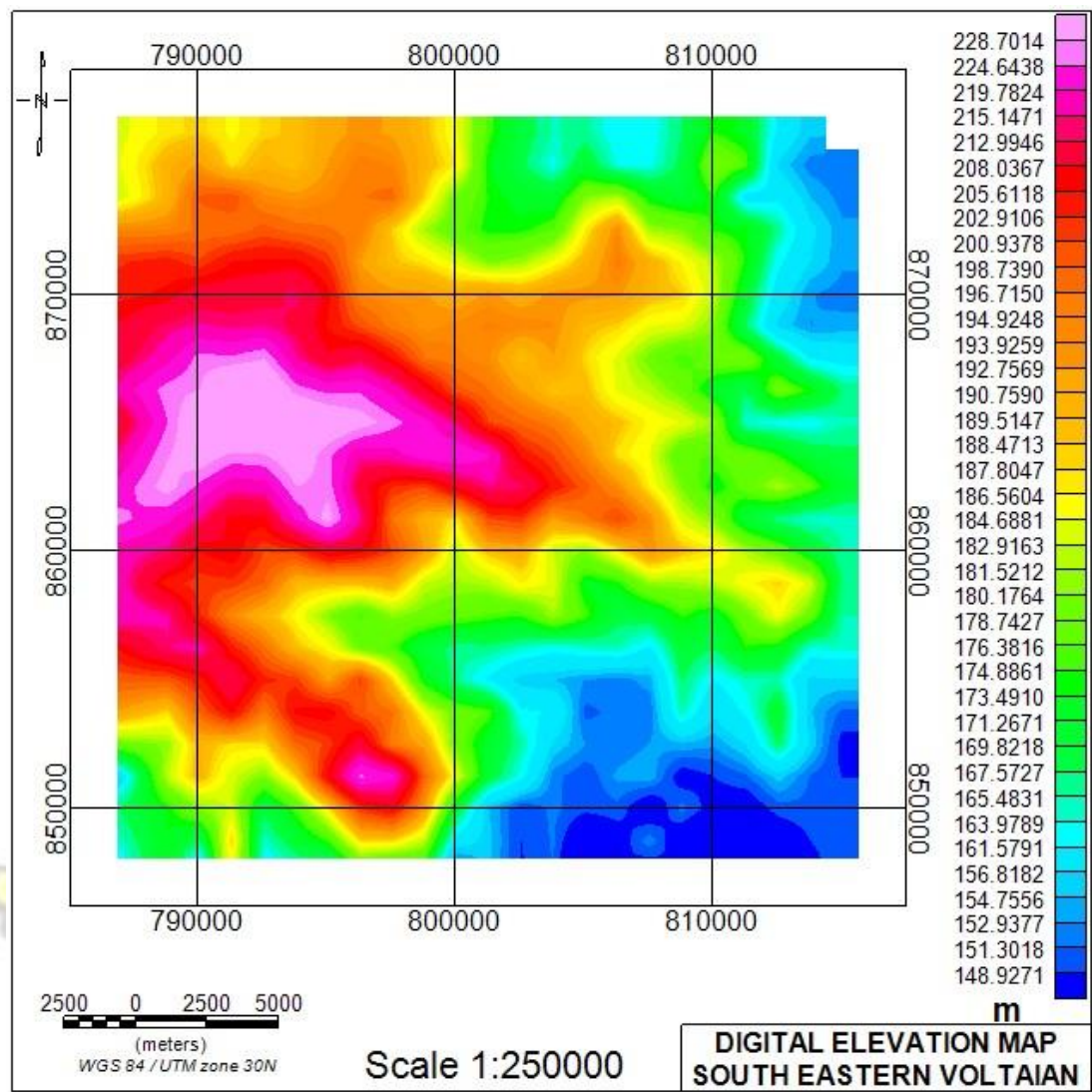


Figure 5.1: Digitized Elevation Map (DEM) of Study Area

The relatively low elevations (green in Fig. 5.1) correlates with the Voltaian sediments such as sandstones, shales, mudstones and siltstones delineated from the analytic signal image (Fig. 5.7). Comparing the analytic signal image (fig. 5.7) and the vertical derivative image (Fig. 5.8) with the DEM (Fig. 5.1), it is very evident that some major structures delineated corresponded with areas of high elevations.

## 5.2 Maps generated from Airborne Gravity Survey

Airborne gravity maps depict in different colours, the density contrast in different rock formations. The red colour is used to depict areas with high gravity signatures and the blue colour indicates areas with low gravity signatures. Airborne gravity maps also highlight structures such as lithological boundaries between different rock types as well as borders of intrusions. Airborne gravity survey can also be described as a supportive geophysical technique used to map subsurface lithologies and structures due to density variations or contrasts in different rock on a regional scale.

### 5.2.1 Complete Bouguer Anomaly (CBA) Map

Figure 5.2 shows the Complete Bouguer Anomaly (CBA) map of the study area. The study area was characterised by a low gravity signature to the north-western part. The gravity values increase to the south-eastern part towards the Lake Volta. There were relatively intermediate gravity signatures which trended from the north-eastern part to the south-western part which is mid-way of the gravity low and gravity high regions of the study area. Jones (1990) believes that the high gravity responses, indicated in pink, in the Voltaian basin were caused by mafic subvolcanic intrusives which are very dense below the Voltaian which were the feeders for the Buem volcanics. The area with high gravity signatures can be correlated to the Densubon Sandstone Formation which may be mafic-rich sandstone. The gravity highs may however, also be attributed to a relatively shallow sedimentary basin. Negative anomalies observed in the area may be due to a relatively deep sedimentary basin

or the presence of less dense sedimentary rocks (e.g. shale, siltstone, mudstone, sandstone) in the area.

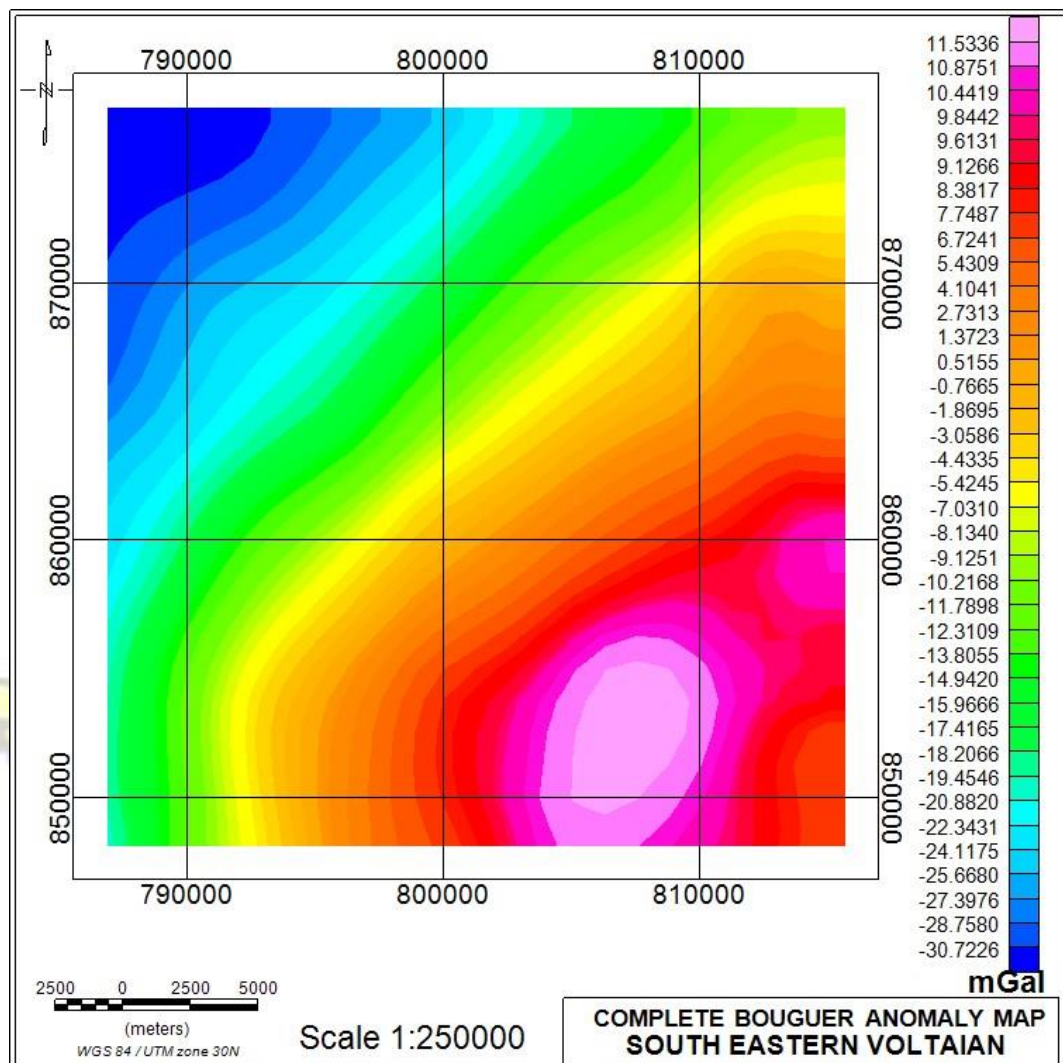


Figure 5.2: Complete Bouguer Anomaly (CBA) Map of Study Area

### 5.2.2 Residual Map

High and low pass filtering methods were employed for filtering the regional and local components using Geosoft Oasis Montaj software. The separation procedure was designed to get a good resolution of the effect of the broad deeper variations “i.e. regional” from

that of the sharper local ones “i.e. residual” gravity components as two distinct gravity maps. The residual map focused attention on weaker features, which were obscured by strong regional effects in the original map.

The high pass filter residual map (figure 5.3) reveals low frequency for the gravity anomalies at the south-eastern part while the north-western part reveals high gravity anomalies ranging from 36.9 *mGal* to over 52.9 *mGal*. The main low is separated from the high anomalies in the central part by an intermediate gravity signature which reflects a probable deep basin for the low anomaly region and shallow depth of the basement for the high anomaly region. The high-pass filter map (residual) suggests that the study area may have dense sedimentary structures.



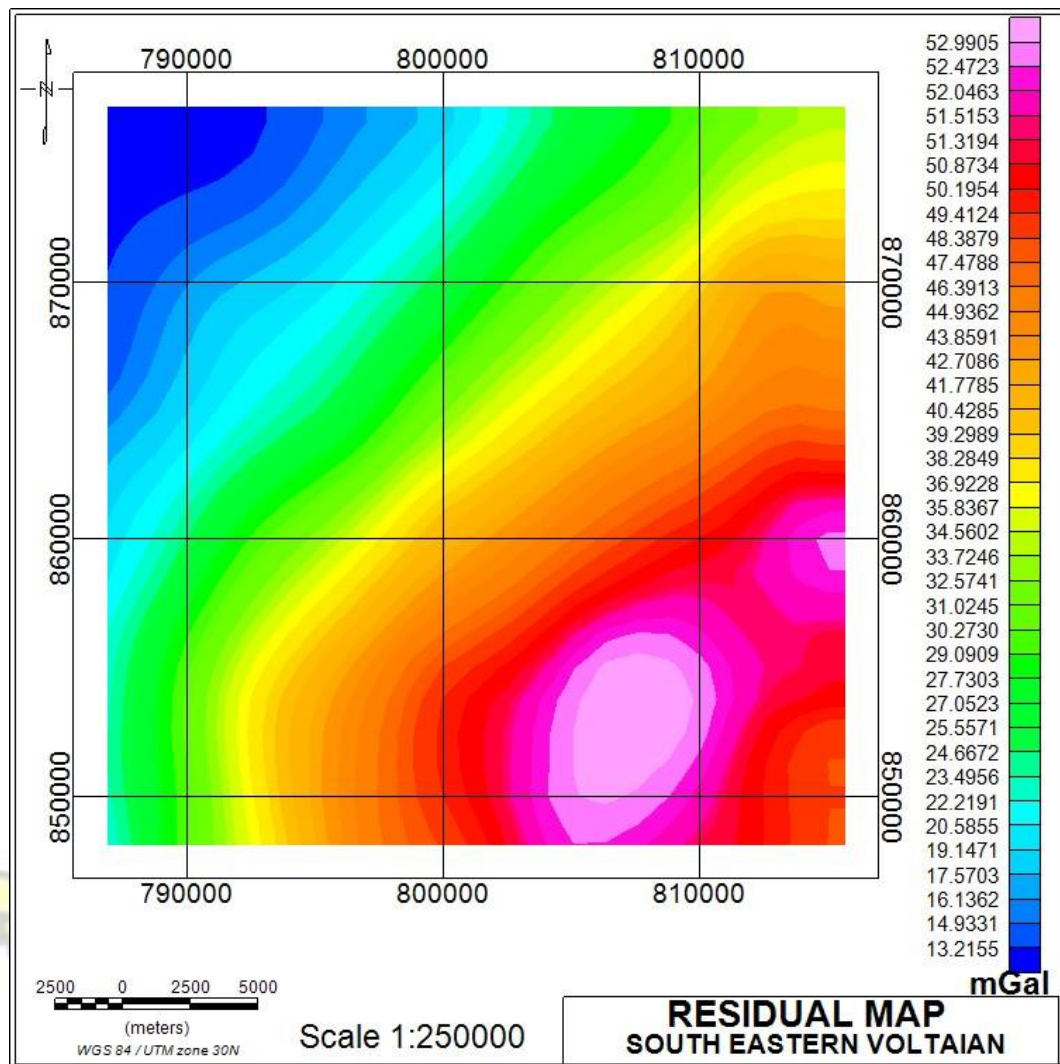


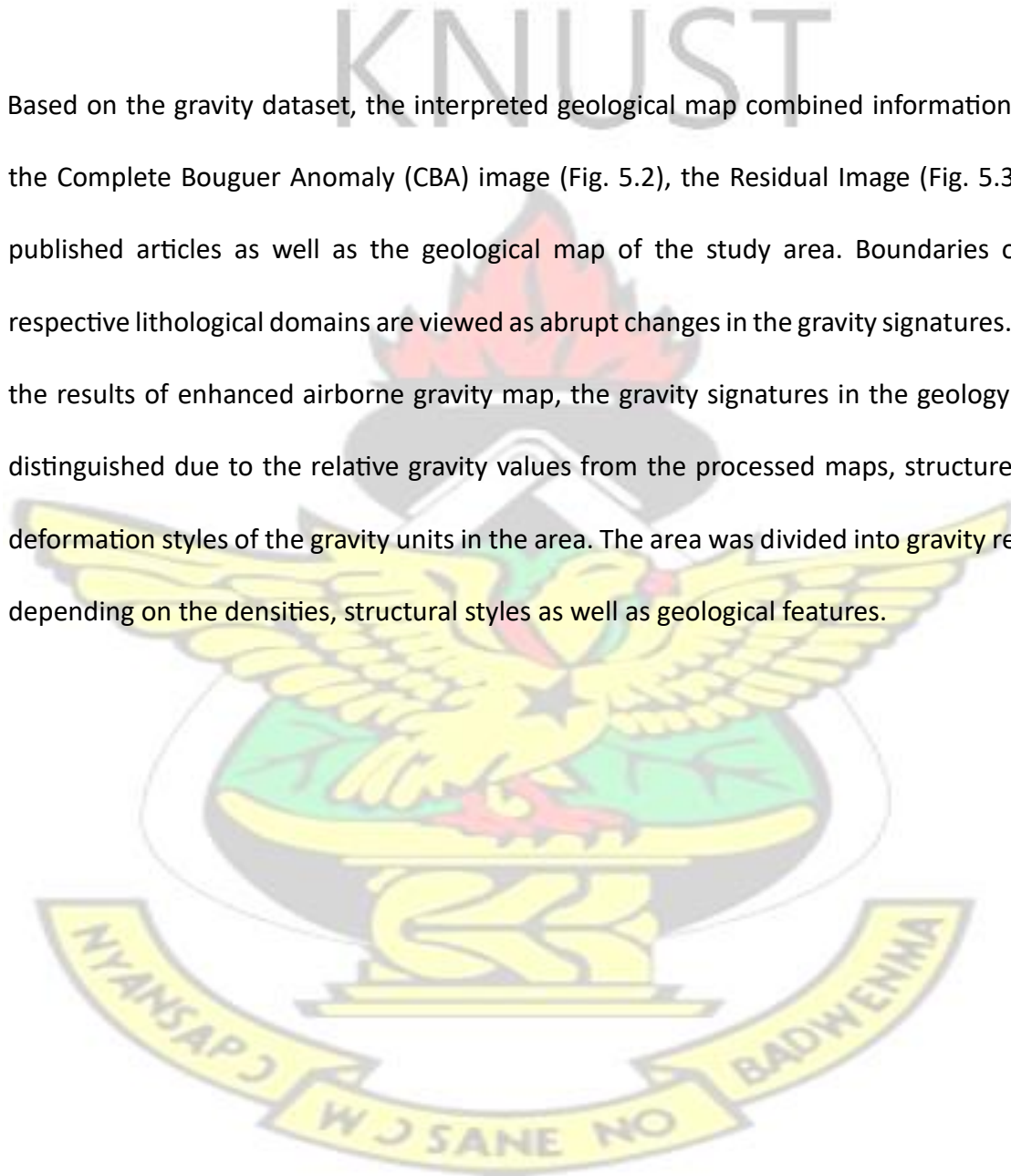
Figure 5.3: Residual Map of Study Area

Comparing the CBA map (Fig. 5.2) and the Residual map (Fig. 5.3), it is very clear that the regional gravity effect has been enhanced and the local gravity effect has been suppressed since the Residual map better revealed the very high gravity signatures (pink) which was hidden in the CBA map. Both the CBA map (Fig. 5.2) and Residual map (Fig. 5.3) when compared with the DEM (Fig. 5.1) indicated a very high gravity response which could be due to a shallow basin or a dense rock unit on the southern part of the study area to a low elevation on the DEM (Fig. 5.1). The northern part of the study area also showed a low gravity response on which could be as a result of a deep basin or less dense rock units on

both the CBA (Fig. 5.2) and Residual map (Fig. 5.3) to a high elevation on the north of the study area on the DEM (Fig. 5.1).

### 5.2.3 Summary of Geology of the area

Based on the gravity dataset, the interpreted geological map combined information from the Complete Bouguer Anomaly (CBA) image (Fig. 5.2), the Residual Image (Fig. 5.3) and published articles as well as the geological map of the study area. Boundaries of the respective lithological domains are viewed as abrupt changes in the gravity signatures. From the results of enhanced airborne gravity map, the gravity signatures in the geology were distinguished due to the relative gravity values from the processed maps, structures and deformation styles of the gravity units in the area. The area was divided into gravity regions depending on the densities, structural styles as well as geological features.



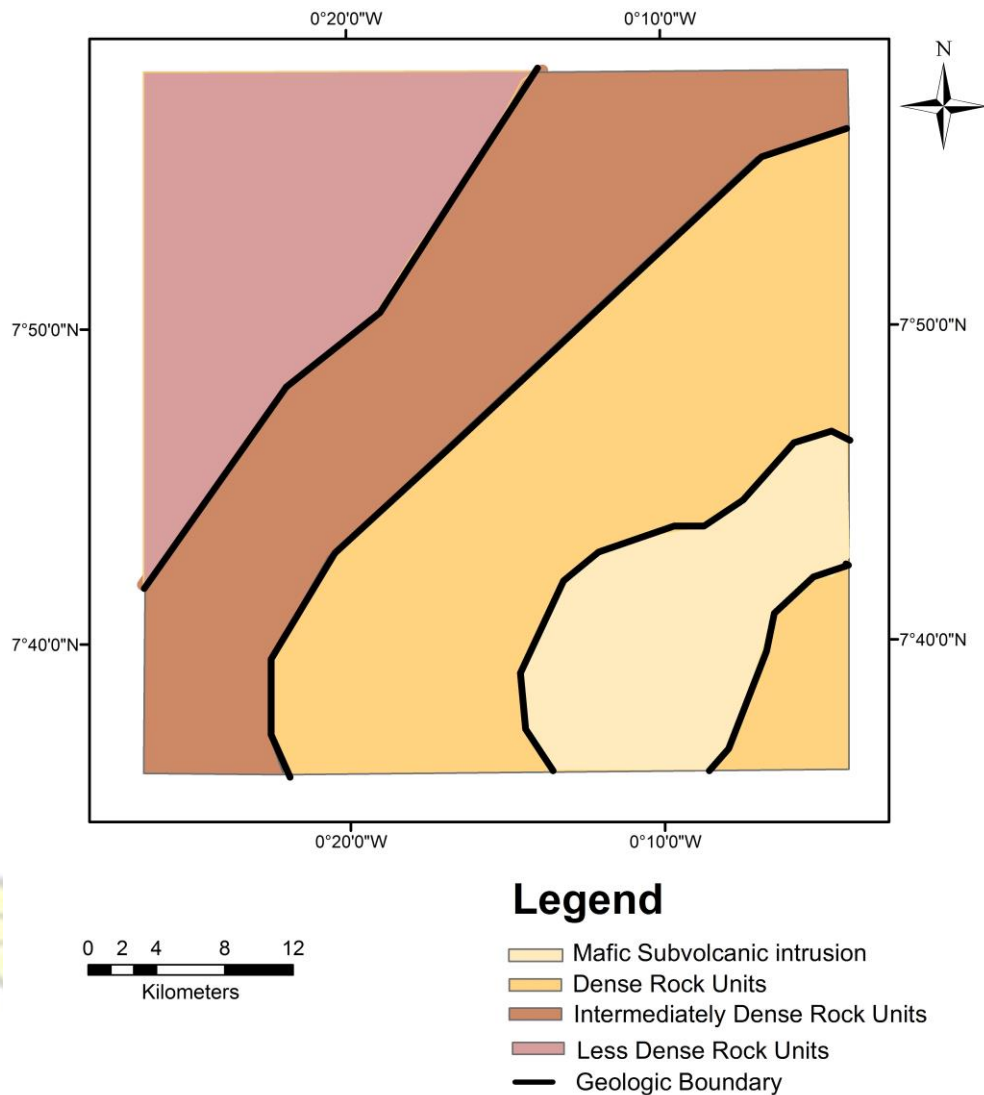


Figure 5.4: Interpreted Geological Map from Airborne Gravity Data

The interpreted geological map (Fig. 5.4) of the area from the gravity dataset showed mafic subvolcanic intrusives and geological boundaries. It was also evident that to the north-western part of the study area, the basin was relatively deep and increased in elevation towards the south-western part of the study area to give a shallow basin. It could also be that the high and low gravity signatures were as a result of dense and less dense rock units within the basin. This is so because the study area is known to rest unconformably on the lower Proterozoic Birimian Supergroup and related granitoids. This is supported by the

presence of abundant volcanic rocks in the lower sandstones cut by the Premuase well as described by Watt (1977) and Anan-York and Cudjoe (1971).

### 5.3 Maps generated from Aeromagnetic Survey

Aeromagnetic maps show in different colours the amount of magnetic minerals in different rock formations. The primary purpose for the use of magnetic data is to delineate geological structures. In areas where it is difficult to map the bedrock geology due to swamp, thick jungle, sand cover or deep weathering, aeromagnetic datasets makes it possible for information about the murked geology to be provided using methods of inference that are similar to those used in photo geological interpretation such as enhancement filters (Reeves, 1989). Aeromagnetic maps also highlights structures such as faults, folds, lithological contacts between different rock types and crosscutting features such as dykes. The pink colour is used to indicate areas of magnetic signatures and the deep blue colour indicates areas of low magnetic signatures.

#### 5.3.1 Total Magnetic Intensity Map

From the Total Magnetic Intensity (TMI) map of the study area in figure 5.5, three main anomaly regions were outlined. These regions named as, high magnetic anomaly region with amplitude greater than 360 nT, low regions with amplitude less than 233 nT and an intermediate region between the range of 233 and 360 nT were observed and distributed within different parts of the surveyed area. The total magnetic intensity is the magnetic

field observed in a particular location and it is a combination of the Earth's magnetic field and the magnetic field generated by the subsurface structures.

The positive anomaly region were classified as high magnetic anomaly that were possibly due to the responses from rocks which have low susceptibility. Since we are at minimum inclination (close to the equator) the response should be opposite. This misrepresentation is called directional noise that is observed in low magnetic latitude regions caused by the inclination of the Earth's magnetic field at these low latitudes. The high magnetic anomaly zone trended southwards and covered most of the southern part of the study area which was the area correlated to the Densubon Sandstone Formation. The second zone was of relatively low magnetic anomaly of less than 233 nT and trended South–West to North–East and this was possibly due to rocks of high magnetic susceptibility. This region covered most of the northern part of the study area which was the area correlated to the Bimbila Formation. The third region which had an intermediate value was observed at the center of the map which separated the region of high magnetic anomaly zone from the region of low magnetic anomaly zone. This region was also observed at the south–eastern part of the map. There was a sharp contrast between the boundary of the third region at the central region of the study area and the high magnetic region and it was correlated to the Pru fault which trends East to West and separates the Densubon Sandstone Formation from the Bimbila Formation.

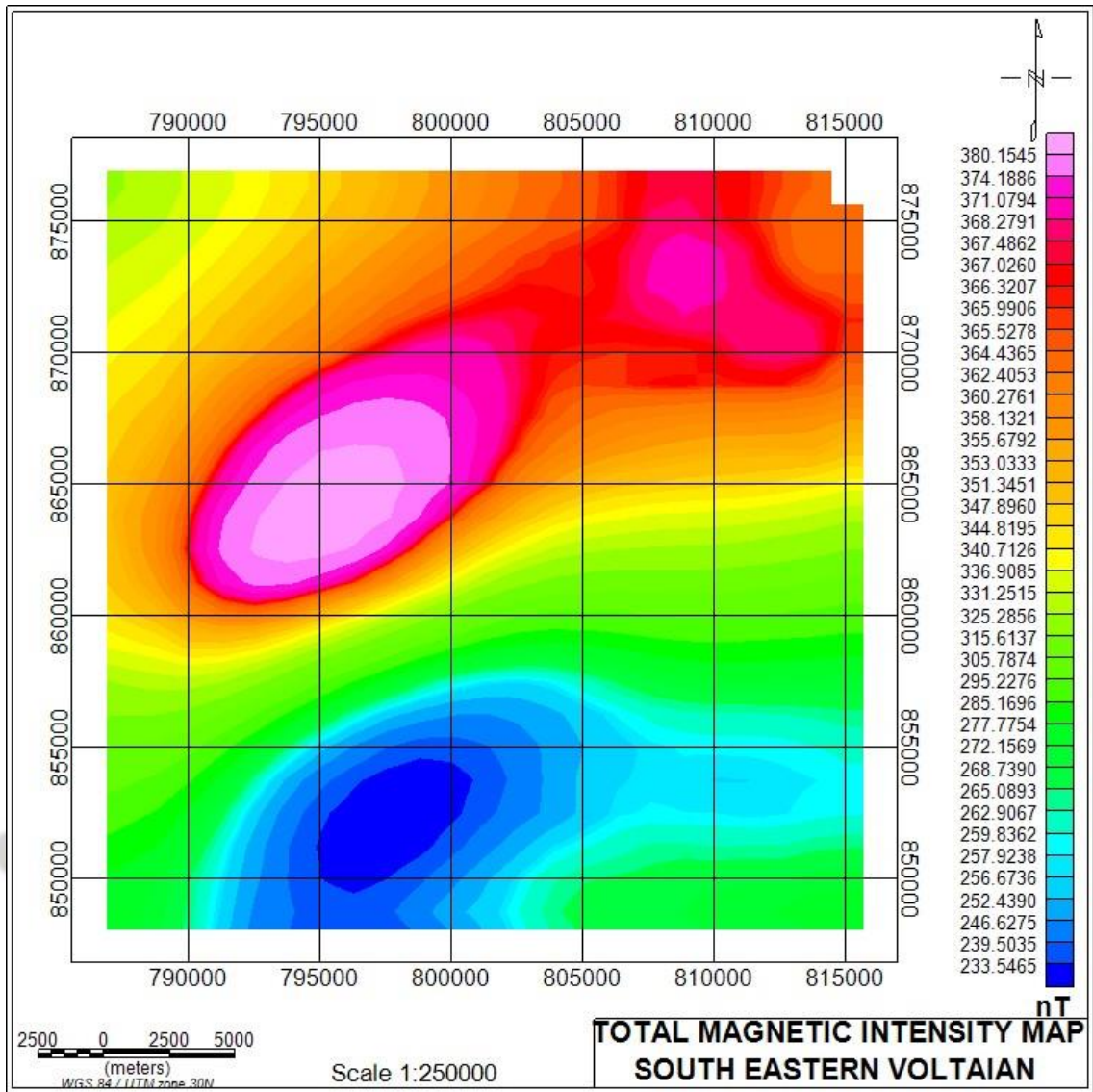


Figure 5.5: Total Magnetic Intensity (TMI) Map of Study Area

### 5.3.2 Reduction-to-Pole Map

According to Murphy (2007), the non-vertical inducing field generate asymmetric anomalies that are difficult to relate to the source structures or geometry which causes the anomalies in the magnetic survey. Reduced-to-Pole converts the magnetic field developed by magnetic bodies from the magnetic latitude where the Earth's field is inclined, to the field at the Earth's magnetic pole, where the inducing field is vertical. In figure 5.6, high

magnetic intensity regions were seen as low magnetic intensity regions and vice versa. However, the induced anomalies are directly over their sources when the inducing field is vertical. This can be identified by comparing the TMI (figure 5.5) and the RTP (figure 5.6) maps and it is clearly indicated that regions with high magnetic intensities in the TMI map are recording low magnetic intensities in the RTP map and vice versa. The same procedure can be applied in the conversion of magnetic fields between any two magnetic latitudes. A basic assumption of the reduced-to-pole method is that all bodies are magnetised by no remanent magnetisation.



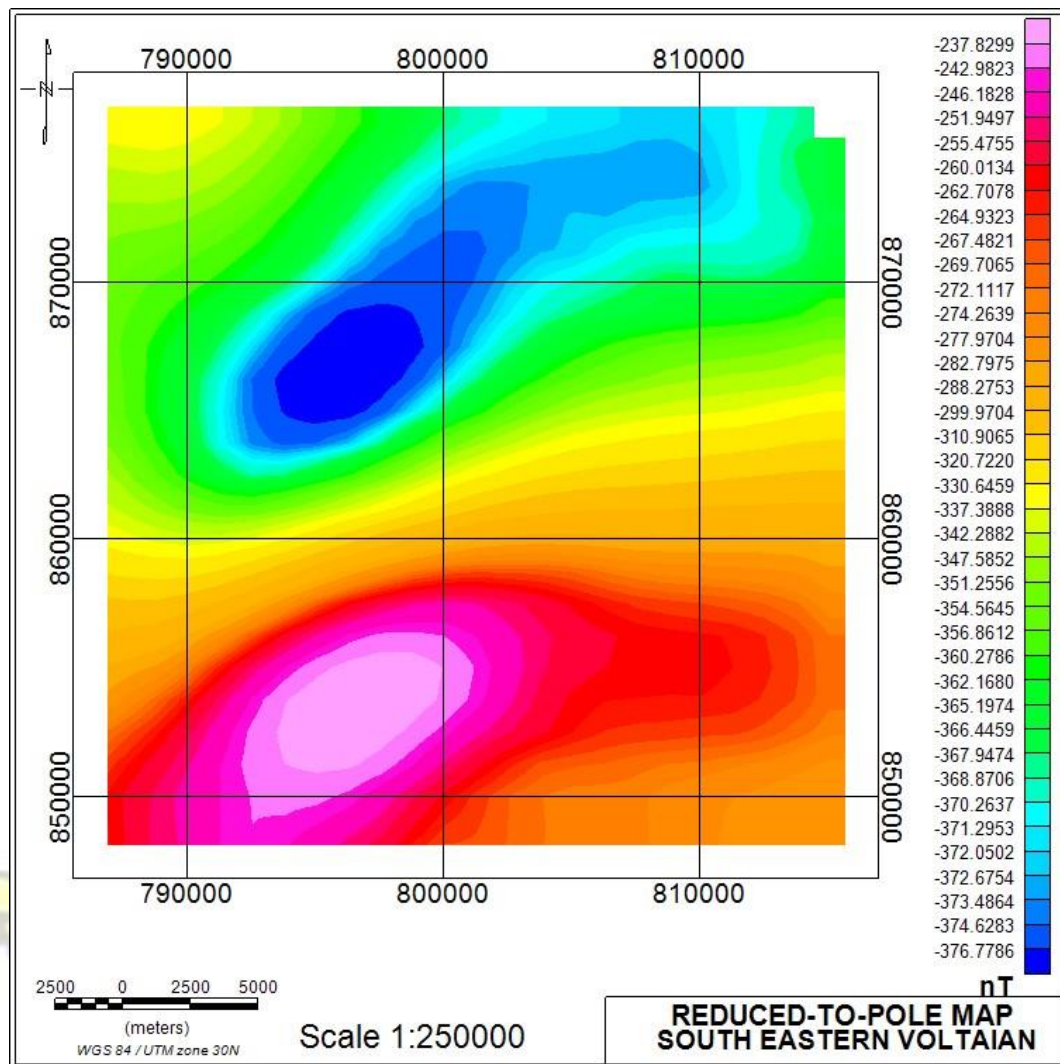


Figure 5.6: Reduced-to-Pole (RTP) Map of Study Area

The reduction-to-pole map (Fig. 5.6) indicates that both low and high frequencies were characterised by magnetic field in the area. The very high magnetic anomaly region (pink) can be interpreted as a mafic subvolcanic intrusive below the Voltaian and the high magnetic anomaly region (red–yellow) can also be interpreted as a mafic–rich sandstone which is resulting in high magnetic signatures. The very high (pink) and high (red–yellow) magnetic anomaly regions were correlated to the Densubon Sandstone Formation. The low magnetic anomaly regions were also described to be a felsic granitic intrusion. The intermediate and low magnetic signature region was also correlated to the Bimbila

Formation which is made up of grey–green mudstones and siltstones. It is seen that the contact zone of structures is being delineated and will be enhanced by subsequent filters. The RTP (Fig. 5.6) was compared with both the CBA map (Fig. 5.2) and Residual map (Fig. 5.3) which indicated high magnetic and gravity signatures at the south of the study area representing rock units which were magnetic and dense or a shallow basin. To the north, there was an indication of low magnetic and gravity signatures representing less magnetic and less dense rock units or a deep basin.

### 5.3.3 Analytic Signal Map

At low magnetic latitudes, It is very difficult to interpret magnetic field data due to the vector nature of the magnetic field which increases the complexity of anomalies from magnetic rocks. Maxima over magnetic contacts are produced by the magnitude of the analytic signal of the total magnetic field, regardless of the direction of magnetisation and is always positive.

The magnetic contacts could result from differences in magnetic susceptibility between an intrusive rock and a country rock between geologic contacts and across a fractured zone due to the oxidation of the magnetite or infilling of the fractured zone by magma thus forming intrusive bodies whose magnetic susceptibility is different from the host rock or in geothermal area the fractured zone is filled with geothermal fluid.

The analytic signal amplitude does not depend on the direction of the magnetisation of the source but is dependent to the amplitude of magnetisation (Nabighian, 1972; Roest and Pilkington, 1993). This implies that all structures with the same geometry possess the same

analytic signal. In addition to this, analytic signal transformations are not subjected to the instability that occurs in reduced-to-pole from low magnetic latitudes. This analytic signal maps also define source positions regardless of any remanence in the sources (MacLeod et al., 1993).

From the analytic signal map in figure 5.7, it was evident that the high magnetic intensity regions and the low magnetic intensity regions were clearly delineated as compared to the TMI map (Fig. 5.5) and the RTP map (Fig. 5.6).

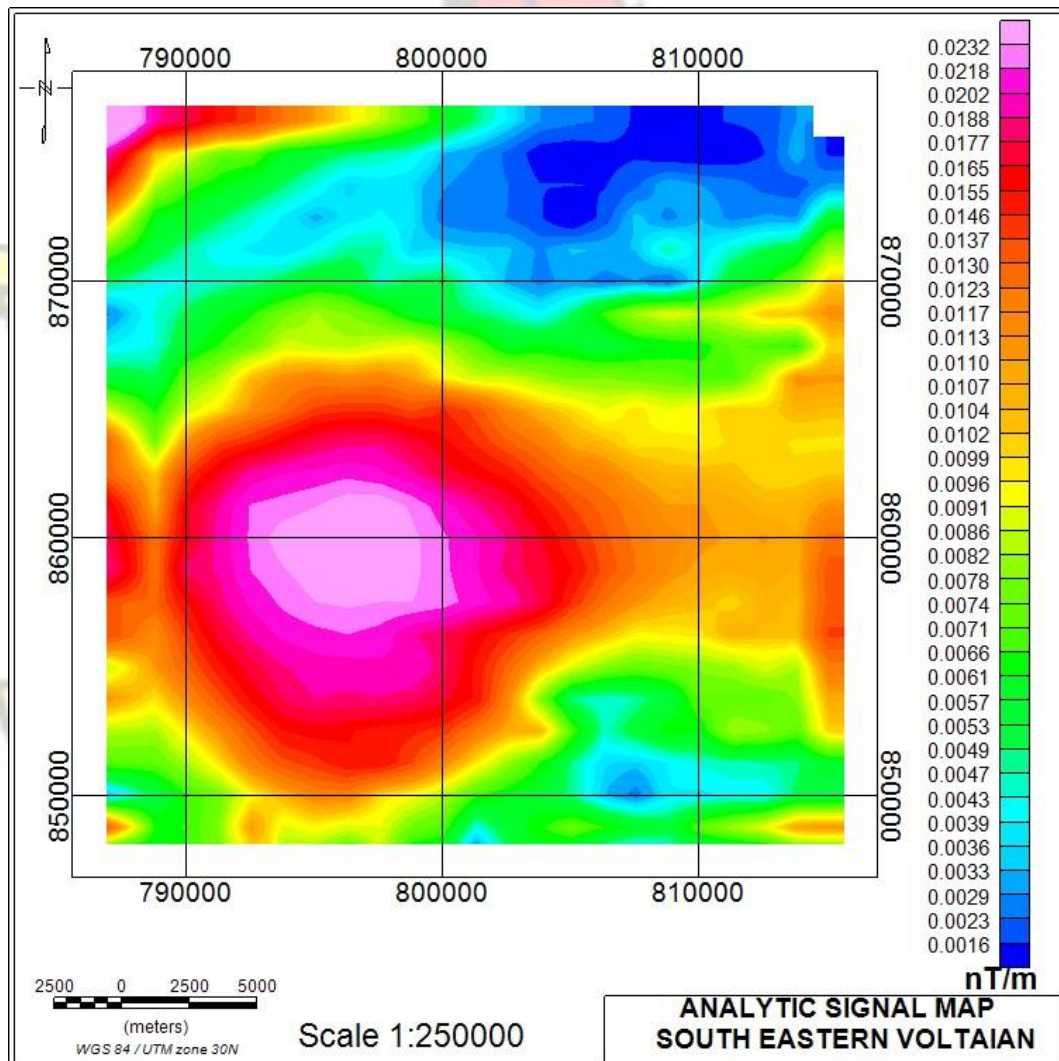


Figure 5.7: Analytic Signal Map of Study Area

The analytic signal map placed the anomalies directly over their source structures because the source positions of the anomalies are defined vertically over the source irrespective of any remanence in magnetisation. Furthermore, maximum anomaly was produced over the magnetic body irrespective of the direction of magnetisation. In totality, the boundaries that existed for different geological formations in the study area were well delineated by the application of the analytic signal filter.

#### 5.3.4 First Vertical Derivative (1VD) Map

The First Vertical derivative filter was applied on the RTP grid in order to observe the near-surface magnetic features that were correlated with geological structures. The colour vertical gradient images of the total magnetic intensity enhanced the image by displaying the dominant lithological and structural details which were masked in the TMI image (Fig. 5.5).

Computing the first vertical derivative in an airborne magnetic survey is similar to observing the vertical gradient directly with a magnetic gradiometer and has the same merits, which are to enhance shallow source, suppressing deeper sources, and producing better resolution of closely-spaced sources. Figure 5.8 is the first vertical derivative of the reduced-to-pole map in colour vertical gradient image showing near-surface magnetic source features that were related to geological structures. The 1VD operator aided the attenuation of broad, more regional anomalies and enhanced local, more subtle magnetic responses due to their sensitivity to shallow magnetic sources and contacts.

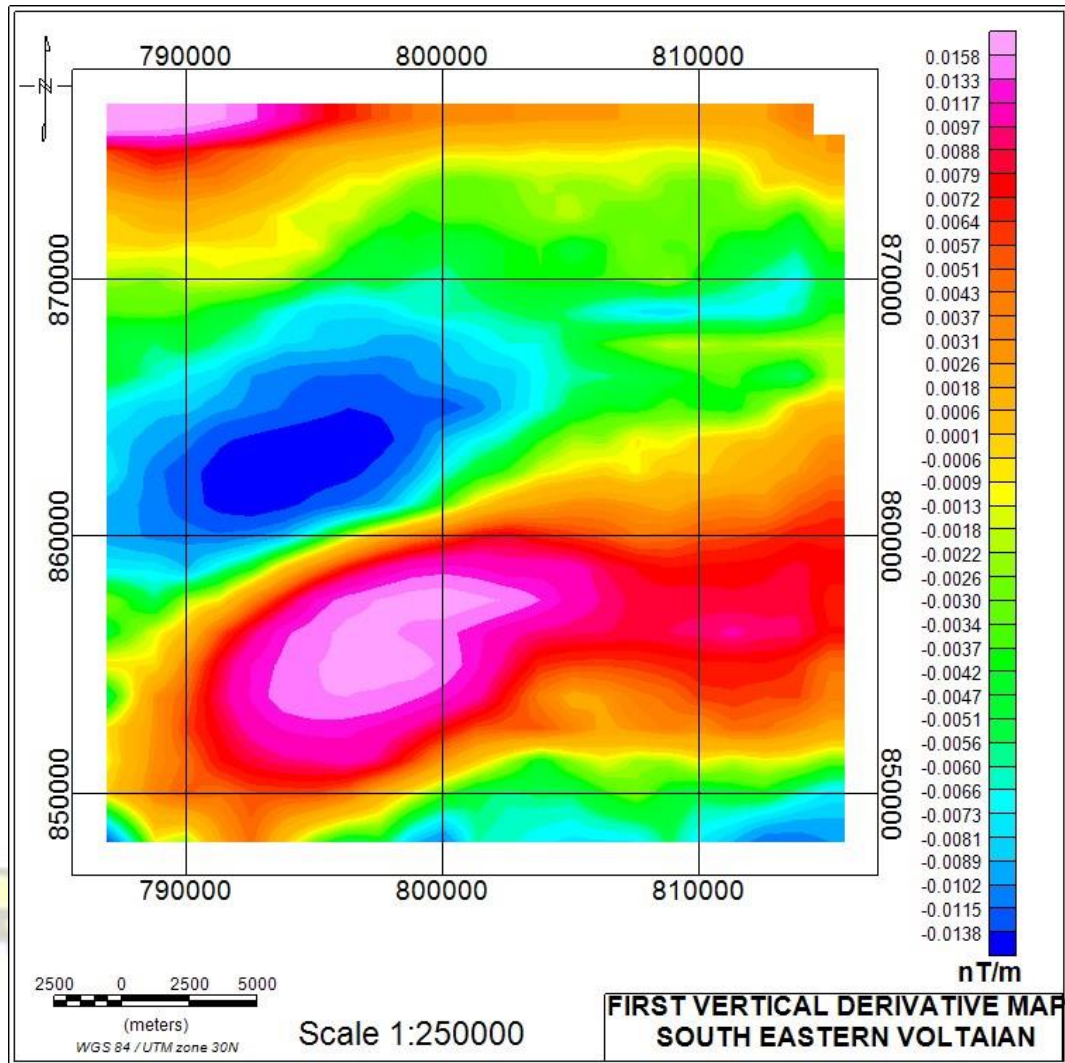


Figure 5.8: First Vertical Derivative of RTP Map of Study Area

The 1VD filter aided the decrease of broad and more regional anomalies and rather enhanced local magnetic responses which were interpreted as structures within the area. Lithological contacts were clearly delineated in figure 5.8. Majority of the structures that were delineated within the study area correlated with structures already delineated on the geological map of the area. Prominent among these structures delineated is the Pru fault at the central part of the study area and other brittle faults at the northern and southern part of the area. These faults correlated to the delineated faults which trended in the east–

west direction and defined in the magnetic data by a high frequency response. These brittle faults can also be inferred from the regional geological map of the area (GSD, 1988).

## 5.4 Summary

Interpretation of airborne gravity and magnetic (or any geophysical) data basically involves two exercises which are; firstly ascertaining the behaviour of the geophysical data and the physical nature of delineated anomalies and secondly, interpreting the geological significance of the geophysical indications (Murphy, 2007).

In an attempt to identify the geology and structures of the study area, distinguishable patterns from the TMI and enhanced maps were initially observed and correlations made to their possible physical causes. Moreover, the geophysical interpretations were accurately correlated with available geological publications, topography and geological data of the area to actually validate the interpreted geology. From the results of enhanced airborne gravity and magnetic maps, the gravity and magnetic signatures in the geology were distinguished due to the relative gravity values and the difference in magnetic susceptibilities respectively, structures and deformation styles of the gravity and magnetic units in the area. The area was divided into gravity and magnetic units based upon the density contrasts and magnetic intensities, structural styles and geological features. The boundaries of individual lithological regions coincide with the blunt changes in the gravity and magnetic intensities. The division was also based on the interpreted subsurface geology and structure, and circular features described in the previous sections (section 5.1 – 5.3).

Figure 5.9 is the interpreted geological map of the study area from the airborne magnetic data showing the various geological structures (faults, intrusives) and lithologies such as sandstone, mudstone, siltstone.

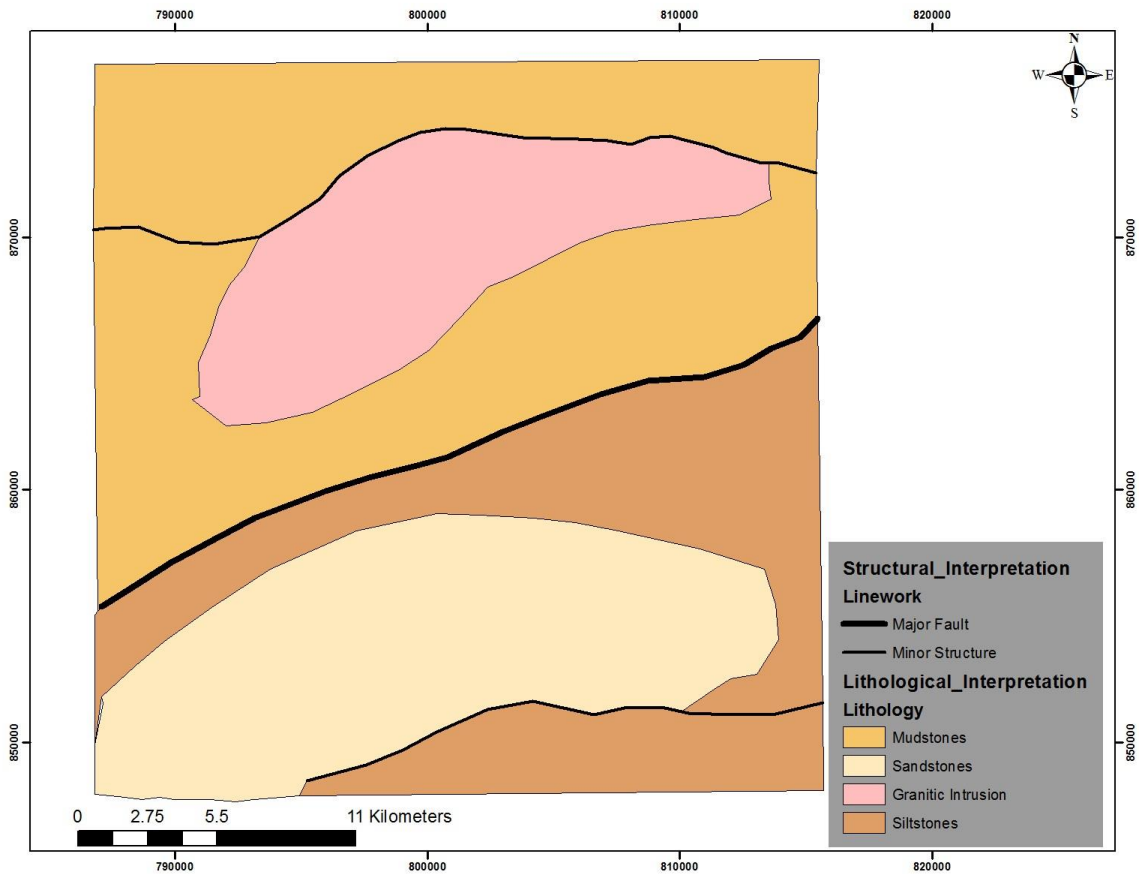
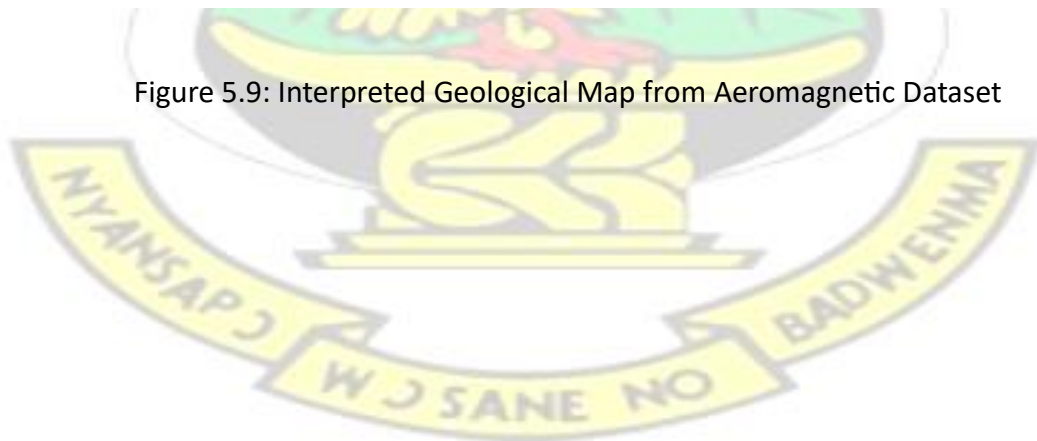
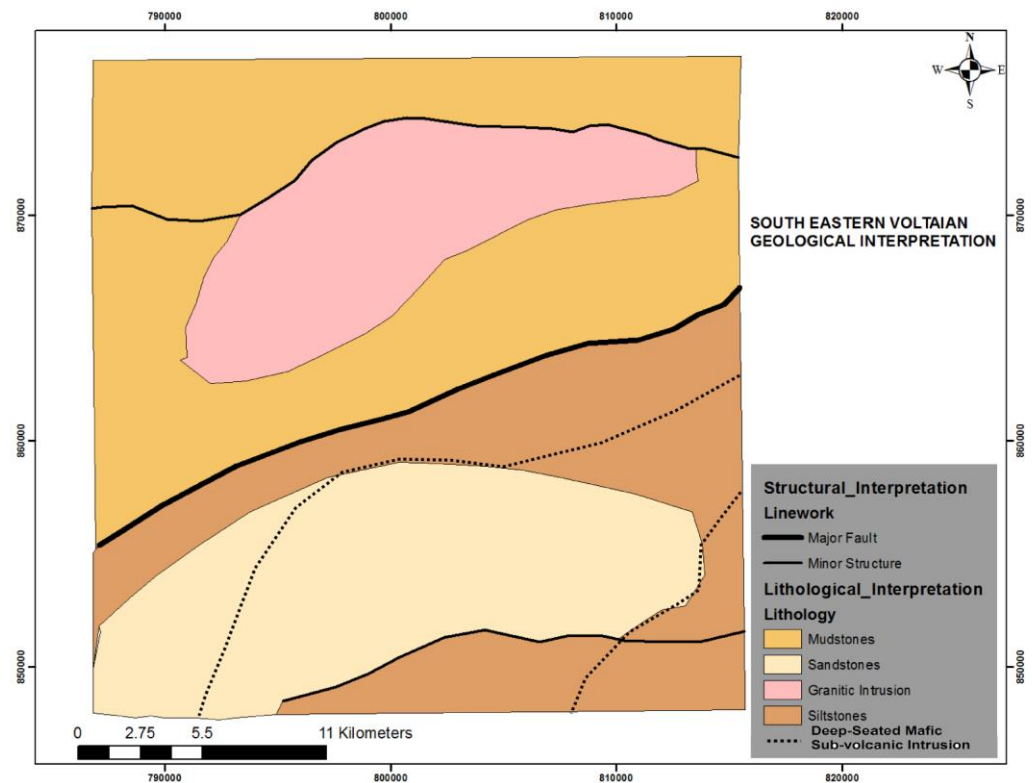


Figure 5.9: Interpreted Geological Map from Aeromagnetic Dataset



## 5.5 Proposed Geological Map of the Study Area from Airborne Gravity and Magnetic Datasets

From the analysis and interpretations drawn from airborne gravity dataset, aeromagnetic dataset and published literature of the study area a proposed regional geological map (Fig.



5.10) is presented which consists mainly of the Voltaian sediments of the Obosum Supergroup. The Obosum Supergroup is composed of shales and mudstones irregularly interbedded with subordinate siltstones and sandstones. The group is dominated by red, medium-to-coarse-grained highly immature lithic and feldspar-rich sandstones, with discontinuous lenses of poorly sorted pebble conglomerates.

Figure 5.10: Proposed Geological and Structural Map of the Study Area

The integrated geological map (Fig. 5.10) depicts several lithological units and the geological structures within the study area. It can be observed from the above map (Fig. 5.10) that a major fault divides two different rock units of the area. The southern part of the area is composed of the same rock unit (Densubon Sandstone Formation) with a structure going through it at the far southern side. There are mafic subvolcanic intrusives below the Voltaian which were the feeders for the Buem volcanics (Jones, 1990) and this is indicated at the south–eastern part of the study area. The northern part of the area is also composed of the rocks of the same unit (Mudstones) with a structure, possibly a fault, going through it. This correlate to the Bimbila Formation and at its central part has a different rock unit which is possibly a felsic granitic intrusion. The faults in the study area may have resulted from the reactivation of the Birimian and the Tarkwaian basement rocks and the Eburnean orogeny.

## 5.6 Proposed Geological Map compared with Existing Geological Map of the Study Area

Below are maps of the proposed geology of the study area (Fig. 5.10) and the existing geology of the study area (5.11). Both maps were compared to validate the methods used for this research.

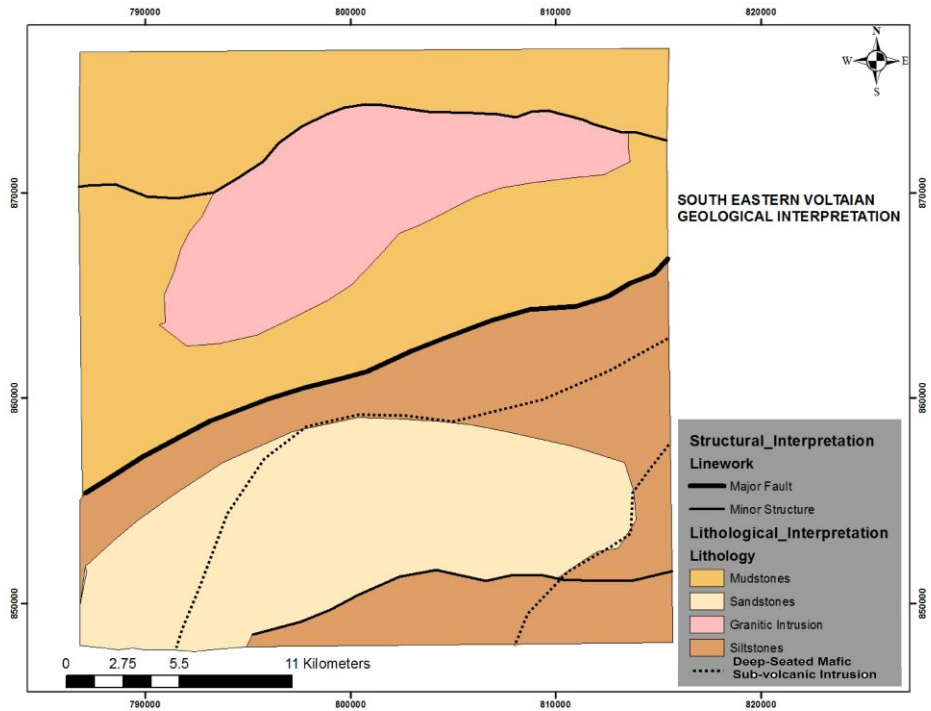


Figure 5.11: Proposed Geological Map of Study Area

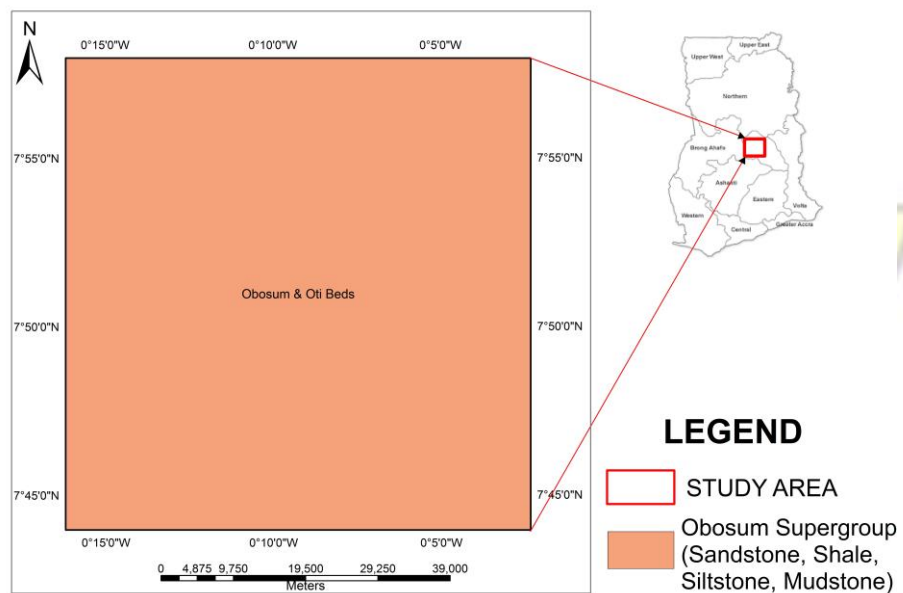


Figure 5.12: Existing Geological Map of the Study Area The research proposed a detailed geological map of the study area from airborne

gravity and magnetic datasets as compared with the existing geological map which provided a rather blurred geology of the study area. The existing geological map provided information about the type of formation within the study area, which is the obosum formation, made up of sandstones, mudstones and siltstones but did not delineate the composition of the obosum formation. The proposed geological map of the study area on the other hand, provided detailed information about the geology of study area and delineated the sandstone formations, the siltstones and mudstones as well as a major fault and some minor faults as seen in figure 5.11 above.



## CHAPTER 6

### CONCLUSION AND RECOMMENDATIONS

#### 6.1 Conclusion

The processed and enhanced airborne gravity and magnetic datasets showed that the study area is a sedimentary basin which constitutes some faults, some intrusive rocks and other Litho–magnetic rock units.

The research also delineated a massive sandstone at the southern part of the study area as well as some mudstones and siltstones. Some granitic intrusions in the study area were also identified and mapped out. The massive sandstone delineated, correlates to the Densubon Sandstone Formation which was permeated by a Mafic subvolcanic intrusion. The Densubon Sandstone of the Obosum supergroup overlies the larger causative bodies (Birimian rocks) within the Voltaian basin.

A major fault trending almost NE–SW was delineated at the central part of the study area, which separated two lithological units. Some minor faults trending almost E–W were also delineated at the northern and southern parts of the study area. The Voltaian basin in totality, rests unconformably on the lower Proterozoic Birimian Supergroup, which are very dense rock units and this, could be the reason for the high gravity signatures which resulted in the south eastern part as shown in figures 5.2 and 5.3. Jones (1990) also described the gravity highs in the study area to be due to mafic subvolcanic intrusives below the voltaian which were the feeders for the Buem volcanics. This conclusion is supported by the

presence of abundant volcanic rocks in the lower sandstones cut by the Premuase well as described by Watt (1977) and Anan-York and Cudjoe (1971).

The high-resolution airborne gravity and magnetic datasets have provided a synopsis of the regional geology (lithology) including further insight into structural controls of the study area. It also presents a detailed assessment of various lithologies.

## 6.2 Recommendations

Ground-based gravity and magnetic surveys should be carried out to ratify the findings of the airborne data since they have better depth and lateral resolutions.

Detailed geological and geophysical (deep 3D-seismic) studies should be carried out in the study area in order to compromise the information on the subsurface geological structures as this would guide in providing more detailed and in-depth information of the subsurface geology and economic geology of the study area.

More quantitative analyses of the aeromagnetic and gravity data will require two- and three- dimensional modeling. More detailed geophysical interpretations and modeling, especially depth-to-basement calculations using a 3-dimensional inversion of gravity data, should be carried out to ascertain the true nature of the basement topography.

The survey areas need to be extended in the NE-SW direction to cover larger area since it is seen from the geological map that, the faults are trending in the NE-SW and E-W direction beyond the area surveyed.

# References

1. Afenya, P. (1982). Ghana's mineral resources for small scale mining industries. *Strategies for small-scale mining and mineral industries, AGID Rep*, 8:24–28.
2. Affaton, P. (2008). Lithostratigraphy of the volta basin and related structural units. In *The Voltaian Basin, Ghana. Workshop and Excursion Report*, pages 13–17.
3. Affaton, P., Rahaman, M., Trompette, R., and Sougy, J. (1991). The dahomeyide orogen: tectonothermal evolution and relationships with the volta basin. In *The West African orogens and circum-Atlantic correlatives*, pages 107–122. Springer.
4. Airo, M. L. and Karell, F. (2001). Interpretation of airborne magnetic and gamma-ray spectrometric data related to Mammaslhti Cu-Zn-Au deposit in eastern Finland. *Special Paper 31*, pages 97–103.
5. Algermissen, S. T. (1961). Underground and surface gravity survey, leadwood, missouri. *Geophysics*, 26(2):158–168.
6. Anan-York, R. and Cudjoe, J. E. (1971). Geology of the Voltaian Basin (summary of current ideas). *Special Bulletin for Oil Exploration, Geological Survey Department, Accra, Ghana*, page 29.
7. Anderson, C., Dyke, A., Noble, M., and Raetz, M. (2006). The bhei falcon gravity survey and goldfinger bht project – exploration geophysics, geochemistry and geology integrated in 3d. In R. Korsch, and R. Barnes, comps., *Broken Hill Exploration Initiative: Abstracts for the September 2006 Conference: Geoscience Australia Record*, volume 21, pages 1–3.

8. Ansari, A. H. and Alamdar, K. (2009). Reduction to the pole of magnetic anomalies using analytic signal. *World Applied Sciences Journal*, 7(4):405–409.
9. Asadi, H. and Hale, M. (1999). Magmatic contribution to the carlin-type gold deposit at zarshuran, iran. In *Proceedings of the Fifth joint SGA-IAGOD International Meeting, Imperial College, London*, page 4.
10. Bandy, W. L., Gangi, A. F., and Morgan, F. D. (1978). Direct method for determining constant corrections to geophysical survey lines for reducing mis-ties. *Geophysics*, 43(6):1148–1156.
11. Barton, C., Lewis, A., and Kilgour, B. (1990). 2005. *Australian Geomagnetic Reference Field (2000 revision AGRF00)(National Geoscience Dataset)*. Geoscience, Australia.
12. Bayat, B. (2006). *Indirect Exploration for Ore Deposits in Weathered Terrains with Airborne Gravity Gradiometry*. PhD thesis, Curtin University of Technology.
13. Blakely, R. J. (1995). *Potential theory in gravity and magnetic applications* cambridge univ. Press, Cambridge.
14. Bozhko, N. (2008). Stratigraphy of the voltaian basin on evidence derived from borehole drillings. In *The Voltaian Basin, Ghana. Workshop and Excursion*, pages 7–12.
15. Briggs, I. C. (1974). Machine contouring using minimum curvature. *Geophysics*, 39(1):39–48.
16. Brown, J., Niebauer, T., Richter, B., Klopping, F., Valentine, J., and Buxton, W. (1999). Miniaturized gravimeter may greatly improve measurements. *Eos Trans. AGU*, 80:355.

17. Castro, D. D., Branco, R. M. G. C., Martins, G., and Castro, N. (2002). Radiometric, magnetic, and gravity study of the quixadá batholith, central ceará domain (ne-brazil): Evidence for an extension controlled emplacement related to the pan-african/brasiliano collage. *Journal of South American Earth Sciences*, 15(5):543–551.
18. Chandler, V. W. (1990). Geologic interpretation of gravity and magnetic data over the central part of the duluth complex, northeastern minnesota. *Economic Geology*, 85(4):816–829.
19. Christensen, A. N., Mahanta, A. M., Boggs, D. B., and Dransfield, M. H. (2001). Falcon airborne gravity gradiometer survey results over the cannington ag-pb-zn deposit. *ASEG Extended Abstracts*, 2001(1):1–4.
20. Clark, D. and Emerson, D. (1991). Notes on rock magnetization characteristics in applied Geophysical studies. *Exploration Geophysics*, 22(3):547–555.
21. Clark, D. A. (1999). Magnetic petrology of igneous intrusions: implications for exploration and magnetic interpretation. *Exploration Geophysics*, 30(1/2):5–26.
22. Cooley, J. W. and Tukey, J. W. (1965). An algorithm for the machine calculation of complex Fourier series. *Math. Comput.*, 19(90):297–301.
23. Craig, M. (1996). Analytic signals for multivariate data. *Mathematical Geology*, 28(3):315–329.
24. Crowe, W. and Jackson-Hicks, S. (2008). Intrabasin deformation of the volta basin. In *The Voltaian Basin, Ghana. Workshop and Excursion*, pages 31–38.

25. Dapaah-Siakwan, S. and Gyau-Boakye, P. (2000). Hydrogeologic framework and borehole yields in Ghana. *Hydrogeology Journal*, 8(4):405–416.
26. Davis, D. W., Hirdes, W., Schaltegger, U., and Nunoo, E. A. (1994). U-Pb age constraints on deposition and provenance of Birimian and gold bearing Tarkwaian sediments in Ghana, West Africa. *Precambrian Research*, 67:89–107.
27. Deynoux, M., Affaton, P., Trompette, R., and Villeneuve, M. (2006). Pan-african tectonic evolution and glacial events registered in neoproterozoic to cambrian cratonic and foreland basins of west africa. *Journal of African Earth Sciences*, 46(5):397–426.
28. Direen, N. G., Lyons, P., Korsch, R. J., and Glen, R. A. (2001). Integrated geophysical appraisal of crustal architecture in the eastern lachlan orogen. *Exploration Geophysics*, 32(3/4):252–262.
29. Dobrin, M. and Savit, C. (1988). Introduction to geophysical prospecting.
30. Eisenlohr, B. N. and Hirdes, W. (1992). The structural development of early Proterozoic Birimian and Tarkwaian rocks in southwest Ghana, West Africa. *Journal of African Earth Science*, 14(3):313–325.
31. Foss, C. (2011). Magnetic data enhancements and depth estimation. In *Encyclopedia of Solid Earth Geophysics*, pages 736–746. Springer.
32. Foster, M. R., Jines, W. R., and Weg, K. (1970). Statistical estimation of systematic errors at intersections of lines of aeromagnetic survey data. *Journal of Geophysical Research*, 75(8):1507–1511.
33. Ghana, Geological Survey (2009). *Geological map of Kumasi Metropolis*.

34. Grant, F. S. (1985). Aeromagnetic, geology of an ore environment, Magnetite in igneous, sedimentary and metamorphic rocks. *An overview of Geoexploration*, Vol. 23:303–33.
35. Griffis, R. J., Barning, K., Agezo, F. L., and Akosah, F. K. (2002). Gold deposits of Ghana. *Minerals Commission Report*, pages 7–12, 19–37, 163–169.
36. GSD (1988). Geology of the Ghana. *Geological Survey Department, Ghana*.
37. Gunn, P. J. (1978). Inversion of airborne radiometric data. *Geophysics*, 43:133–143.
38. Gunn, P. J., Minty, B. R. S., and Milligan, P. (1997). The airborne gamma-ray spectrometric response over arid Australian terranes. *Exploration*, 97:733–740.
39. Gupta, V. and Grant, F. (1985). Mineral-exploration aspects of gravity and aeromagnetic surveys in the Sudbury-cobalt area, Ontario. In *The Utility of Regional Gravity and Magnetic Anomaly Maps*, volume 20, pages 392–411. Society of Exploration Geophysicists Tulsa, Okla.,.
40. Hastings, D. A. (1983). On the tectonics and metallogenesis of Ghana. A model based on a new synthesis of geological and geophysical data. Unpublished report.
41. Herndon, J. M. (1996). Substructure of the inner core of the earth. *Proceedings of the National Academy of Sciences*, 93(2):646–648.
42. Hinze, W. J., Von Frese, R. R., and Saad, A. H. (2013). *Gravity and Magnetic Exploration: Principles, Practices, and Applications*. Cambridge University Press.
43. Hirdes, W. and Nunoo, B. (1994). The Proterozoic paleoplacers at the Tarkwa gold mine, SW - Ghana - sedimentology, mineralogy, and precise age dating of the main reef and west reef, and bearing of the investigations on source area aspects. In *Oberthür, T.*

(ed.), *Metallogensis of Selected Gold Deposits in Africa*, pages 247–298. Geologische Jahrbuch, Reihe D, Heft 100, Hannover.

44. Hirdes, W., Saager, R., and Leube, A. (1988). New structural, radiometric and mineralogical aspects of the Au-bearing Tarkwaian Group of Ghana. *Bicentennial Gold 88, Melbourne, Abstr.*, pages 146–148.
45. Hoffman, P. F. (1999). The break-up of rodinia, birth of gondwana, true polar wander and the snowball earth. *Journal of African Earth Sciences*, 28(1):17–33.
46. Holm, R. F. (1974). Petrology of alkalic gneiss in the dahomeyan of ghana. *Geological Society of America Bulletin*, 85(9):1441–1448.
47. Johnson, G. and Olhoeft, G. (1984). Density of rocks and minerals. *CRC Handbook of Physical Properties of Rocks*, 3:1–38.
48. Jones, W. B. (1990). The buem volcanic and associated sedimentary rocks, ghana: a field and geochemical investigation. *Journal of African Earth Sciences (and the Middle East)*, 11(3):373–383.
49. Junner, N. R. (1940). Geology of the Gold Coast and Western Togoland. *Geological Survey Bulletin No.1*.
50. Kalsbeek, F., Frei, D., and Affaton, P. (2008). Constraints on provenance, stratigraphic correlation and structural context of the volta basin, ghana, from detrital zircon geochronology: An amazonian connection? *Sedimentary Geology*, 212(1):86–95.
51. Keary, P. and Brooks, M. (1992). An introduction to exploration geophysics.

52. Keating, P. B. (1995). A simple technique to identify magnetic anomalies due to kimberlite pipes. *Exploration and Mining Geology*, 4(2):121–125.
53. Kennedy, W. (1964). The structural differentiation of africa in the pan- african ( $\pm 500$  my) tectonic episode. *Leeds Univ. Res. Inst. Afr. Geol. Annu. Rep*, 8:48–49.
54. Kesse, G. O. (1985). *The Mineral and Rock Resources of Ghana*.
55. Key, R. M. (1992). An introduction to the crystalline basement of africa. *Geological Society, London, Special Publications*, 1:29–57.
56. Koulomzine, T., Lamontagne, Y., and Nadeau, A. (1970). New methods for the direct interpretation of magnetic anomalies caused by inclined dikes of infinite length. *Geophysics*, 35(5):812–830.
57. LaFehr, T. R. (1991). An exact solution for the gravity curvature (Bullard B) correction. *Geophysics*, 56(8):1179–1184.
58. Lane, R. (2006). Investigations stemming from the 2003 broken hill airborne gravity gradiometer survey. In *Broken Hill exploration initiative 2006 conference abstracts, Geoscience Australia Record*, volume 21, pages 116–128.
59. Leube, A., Hirdes, W., Mauer, R., and Kesse, G. (1990). The early proterozoic birimian supergroup of ghana and some aspects of its associated gold mineralization. *Precambrian Research*, 46:139–165.
60. Li, X. (2008). Magnetic reduction-to-the-pole at low latitudes: Observations and considerations. *The leading edge*, 27(8):990–1002.
61. Luyendyk, A. P. J. (1997). Processing of airborne magnetic data. *AGSO Journal of Australian*

*Geology and Geophysics*, 17:31–38.

62. MacLeod, I. N., Jones, K., and Dai, T. F. (1993). 3-d analytic signal in the interpretation of total magnetic field data at low magnetic latitudes. *Exploration Geophysics*, 24(3/4):679–688.
63. Mahanta, A. and Billiton, B. (2003). Application of airborne gravity gradiometer technology in coal exploration. *ASEG Extended Abstracts*, (2):1–1.
64. Mani, R. (1978). The Geology of the Dahomeyan of Ghana; Geology of Ghana Project. In *Ghana Geological Survey Department Bulletin*, page 45.
65. Mairing, E., Beard, L. P., Kihle, O., and Smethurst, M. A. (2002). A comparison of aeromagnetic levelling techniques with an introduction to median levelling. *Geophysical Prospecting*, 50(1):43–54.
66. Mendonça, C. A. and Silva, J. B. C. (1993). A stable truncated series approximation of the reduction-to-the-pole operator. *Geophysics*, Vol. 58(No. 8).
67. Metelka, V. (2012). *Geophysical and remote sensing methodologies applied to the analysis of regolith and geology in Burkina Faso, West Africa*. PhD thesis, Citeseer.
68. Milligan, P. R. and Gunn, P. J. (1997). Enhancement and presentation of airborne geophysical data. *AGSO Journal of Australian Geology and Geophysics*, 17(2):64–774.
69. Milsom, J. (2003). *Field Geophysics*. John Wiley and Sons Ltd.
70. Moose, R. E. and Rockville, M. (1987). *The national geodetic survey gravity network*. Citeseer.

71. Morelli, C., Gantar, C., McConnell, R., Szabo, B., and Uotila, U. (1972). The international gravity standardization net 1971 (igs71). Technical report, DTIC Document.
72. Murphy, B. S. R. (2007). Airborne geophysics and the Indian scenario. *J. Ind. Geophysics Union*, 11(1):1–28.
73. Mussett, A. E. and Khan, M. A. (2000). *Looking into the earth: an introduction to geological geophysics*. Cambridge University Press.
74. Nabighian, M., Grauch, V., Hansen, R., LaFehr, T., Li, Y., Peirce, J., Phillips, J., and Ruder, M. (2005). The historical development of the magnetic method in exploration. *Geophysics*, 70(6):33ND–61ND.
75. Nabighian, M. N. (1972). The analytic signal of two-dimensional magnetic bodies with polygonal cross-section: its properties and use for automated anomaly interpretation. *Geophysics*, 37(3):507–517.
76. Nabighian, M. N. (1974). Additional comments on the analytic signal of two-dimensional magnetic bodies with polygonal cross-section. *Geophysics*, 39(1):85–92.
77. Nabighian, M. N. (1984). Toward a three-dimensional automatic interpretation of potential field data via generalized Hilbert transforms: Fundamental relations. *Geophysics*, 49(6):780–786.
78. Nagata, T. (1961). *Rock Magnetism*. Tokyo: Maruzen, 2nd edition.
79. Nelson, A., Holland, D., Heidorn, R., Leech, D., et al. (2004). Integrated use of seismic, ground and airborne gravity/gravity gradiometer, and ground geological mapping methods in the eastern Papua basin, PNG. *ASEG Extended Abstracts*, 2004(1):1–4.

80. Nettleton, L. L. (1976). *Gravity and magnetics in oil prospecting*. McGraw-Hill Companies.
81. Nicolet, J. P. and Erdi-Krausz, G. (2003). *Guidelines for radioelement mapping using gamma ray spectrometry data*. IAEA-TECDOC-1363. IAEA.
82. O'Brien, J., Rodriguez, A., Sixta, D., Davies, M. A., and Houghton, P. (2005). Resolving the k-2 salt structure in the gulf of mexico: An integrated approach using prestack depth imaging and full tensor gravity gradiometry. *The Leading Edge*, 24(4):404–409.
83. Opfer, R. P., Dark, J. A., et al. (1989). Application of gravstat to seismic statics and structural correction in nevada. In *1989 SEG Annual Meeting*. Society of Exploration Geophysicists.
84. Pesonen, L., Koeberl, C., and Hautaniemi, H. (2003). Airborne geophysical survey of the lake bosumtwi meteorite impact structure (southern ghana) – geophysical maps with descriptions. *Jahrbuch der Geologischen Bundesanstalt, Vienna (Yearbook of the Austrian Geological Survey)*, 143:581–604.
85. Petersen, N. (1990). Curie temperature. In *James, D. E. (ed.), The Encyclopedia of solid Earth Geophysics*, pages 166–173. New York: Van Nostrand Reinhold.
86. Phillips, J. D. (1998). *Potential-field Geophysical Software for the PC*. US Department of the Interior, US Geological Survey.
87. Plummer, C. C., McGeary, D., and Carlson, D. H. (2001). *Physical Geology*. New York: McGraw Hill, 8th edition.
88. Rajagopalan, S. (2003). *Exploration Geophysics*, Vol. 34(No. 4):257–262.
89. Reeves, C. V. (1989). Aeromagnetic interpretation and rock magnetism. *First Break*, Vol. 7:275–286.

90. Reynolds, J. M. (1997). *An introduction to Applied and Environmental Geophysics*. Wiley.
91. Roest, W. R. and Pilkington, M. (1993). Identifying remanent magnetization effects in magnetic data. *Geophysics*, 58:653–659.
92. Rose, M., Zeng, Y., and Dransfield, M. (2006). Applying falcon® gravity gradiometry to hydrocarbon exploration in the gippsland basin, victoria. *Exploration Geophysics*, 37(2):180–190.
93. Roy, A. (1966). The method of continuation in mining geophysical interpretation. *Geoexploration*, 4(2):65–83.
94. Sakuma, A. (1986). Second internal comparison of gravimeters. Technical report, Internal Report, Bureau International des Poids et Mesures.
95. Silva, A. M., Pires, A. C. B., McCafferty, A., Moraes, R. A. V., and Xia, H. (2003). Application of airborne geophysical data to mineral exploration in the uneven exposed terrains of the Rio Das Velhas greenstone belt. *Revista Brasileira de Geociências*, 33(2):17–28.
96. Swain, C. J. (1978). A fortran IV program for interpolating irregularly spaced data using the difference equations for minimum curvature. *Computer & Geosciences*, 4(2):209.
97. Telford, W. M. and Sheriff, R. E. (1990). *Applied geophysics*, volume 1. Cambridge university press.
98. Watt, D. S. (1977). Premuase–1 Well resume. Unpublished report of SHELL International, The Hague, Netherlands.

99. Wellman, P. and Hinze, W. (1985). Block structure of continental crust derived from gravity and magnetic maps, with australian examples. *The utility of regional gravity and magnetic anomaly maps*. Edited by WJ Hinze. Society of Exploration Geophysicists, pages 102–108.
100. Wemegah, D. D., Menyeh, A., and Danuor, S. K. (2009). Magnetic Susceptibility Characterization of mineralized and non mineralized rocks of the Subenso Concession of Newmont Ghana Gold Limited. In *Proc. of the 26th Biennial Conference of the Ghana Science Association*.
101. Whitham, K. (1960). Measurement of the geomagnetic elements. In *Methods and techniques in Geophysics*, volume Vol. 1, pages 134–48. S. K. Runcorn.
102. Woollard, G. and Rose, J. (1963). International gravity measurements. menasha, wisconsin, george banta company.
103. Wright, J. B. (1985). *Geology and Mineral Deposits of West Africa*. Allen and Unwin, London, 189 pp.
104. [www.earthsci.unimelb.edu.au/ES304/](http://www.earthsci.unimelb.edu.au/ES304/).
105. [www.geosoft.com](http://www.geosoft.com).
106. [www.sene.ghanadistricts.gov.gh](http://www.sene.ghanadistricts.gov.gh).
107. Yarger, H. L., Robertson, R. R., and Wentland, R. L. (1978). Diurnal drift removal from aeromagnetic data using least squares. *Geophysics*, 43(6):1148–1156.

## Appendix A

## A.1 Used Softwares

- L<sup>A</sup>T<sub>E</sub>X : typesetting and layout
- Geosoft Oasis Montaj: Data processing
- MapInfo 10.5: Data processing and enhancing
- ArcGIS 10: Data processing and enhancing

